



712
2017

Berichte

zur Polar- und Meeresforschung

Reports on Polar and Marine Research

The Expedition PS104 of the Research Vessel POLARSTERN to the Amundsen Sea in 2017

Edited by

Karsten Gohl

with contributions of the participants

Die Berichte zur Polar- und Meeresforschung werden vom Alfred-Wegener-Institut, Helmholtz-Zentrum für Polar- und Meeresforschung (AWI) in Bremerhaven, Deutschland, in Fortsetzung der vormaligen Berichte zur Polarforschung herausgegeben. Sie erscheinen in unregelmäßiger Abfolge.

Die Berichte zur Polar- und Meeresforschung enthalten Darstellungen und Ergebnisse der vom AWI selbst oder mit seiner Unterstützung durchgeführten Forschungsarbeiten in den Polargebieten und in den Meeren.

Die Publikationen umfassen Expeditionsberichte der vom AWI betriebenen Schiffe, Flugzeuge und Stationen, Forschungsergebnisse (inkl. Dissertationen) des Instituts und des Archivs für deutsche Polarforschung, sowie Abstracts und Proceedings von nationalen und internationalen Tagungen und Workshops des AWI.

Die Beiträge geben nicht notwendigerweise die Auffassung des AWI wider.

Herausgeber

Dr. Horst Bornemann

Redaktionelle Bearbeitung und Layout

Birgit Reimann

Alfred-Wegener-Institut
Helmholtz-Zentrum für Polar- und Meeresforschung
Am Handeshafen 12
27570 Bremerhaven
Germany

www.awi.de
www.reports.awi.de

Der Erstautor bzw. herausgebende Autor eines Bandes der Berichte zur Polar- und Meeresforschung versichert, dass er über alle Rechte am Werk verfügt und überträgt sämtliche Rechte auch im Namen seiner Koautoren an das AWI. Ein einfaches Nutzungsrecht verbleibt, wenn nicht anders angegeben, beim Autor (bei den Autoren). Das AWI beansprucht die Publikation der eingereichten Manuskripte über sein Repository ePIC (electronic Publication Information Center, s. Innenseite am Rückdeckel) mit optionalem print-on-demand.

The Reports on Polar and Marine Research are issued by the Alfred Wegener Institute, Helmholtz Centre for Polar and Marine Research (AWI) in Bremerhaven, Germany, succeeding the former Reports on Polar Research. They are published at irregular intervals.

The Reports on Polar and Marine Research contain presentations and results of research activities in polar regions and in the seas either carried out by the AWI or with its support.

Publications comprise expedition reports of the ships, aircrafts, and stations operated by the AWI, research results (incl. dissertations) of the Institute and the Archiv für deutsche Polarforschung, as well as abstracts and proceedings of national and international conferences and workshops of the AWI.

The papers contained in the Reports do not necessarily reflect the opinion of the AWI.

Editor

Dr. Horst Bornemann

Editorial editing and layout

Birgit Reimann

Alfred-Wegener-Institut
Helmholtz-Zentrum für Polar- und Meeresforschung
Am Handeshafen 12
27570 Bremerhaven
Germany

www.awi.de
www.reports.awi.de

The first or editing author of an issue of Reports on Polar and Marine Research ensures that he possesses all rights of the opus, and transfers all rights to the AWI, including those associated with the co-authors. The non-exclusive right of use (einfaches Nutzungsrecht) remains with the author unless stated otherwise. The AWI reserves the right to publish the submitted articles in its repository ePIC (electronic Publication Information Center, see inside page of verso) with the option to "print-on-demand".

Titel: Das Meeresboden-Bohrgerät MeBo70 des MARUM Zentrums für Marine Umweltwissenschaften zwischen seinen Einsätzen (Foto von Karsten Gohl, Alfred-Wegener-Institut, 17. Februar 2017).

Cover: Title: The seabed drilling device MeBo70 of the MARUM Center for Marine Environmental Science in between deployments (picture taken by Karsten Gohl, Alfred Wegener Institut, 17 February 2017).

The Expedition PS104 of the Research Vessel POLARSTERN to the Amundsen Sea in 2017

Edited by

Karsten Gohl

with contributions of the participants

Please cite or link this publication using the identifiers

hdl:10013/epic.51875 or <http://hdl.handle.net/10013/epic.51875> and

https://doi.org/10.2312/BzPM_0712_2017

ISSN 1866-3192

PS104

6 February 2017 - 19 March 2017

Punta Arenas – Punta Arenas

**Chief scientists
Karsten Gohl**

**Coordinator
Rainer Knust**

Contents

1.	Zusammenfassung und Fahrtverlauf	2
	Summary and Itinerary	3
2.	Weather Conditions	10
3.	ICE Sheet Dynamics of the Amundsen Sea Embayment with Mebo Shallow Drilling	13
4.	Near and Far Field Effects of Antarctica's Quaternary Ice Sheet Dynamics from Sediment Coring	27
5.	Bathymetric Mapping and Sub-Bottom Profiling	42
6.	Seismic Imaging and Stratigraphy of the Shelf Sediments	47
7.	Geothermal Gradients and Heat Flux Estimates	62
8.	Exhumation and Deglaciation of the Amundsen Sea Region	66
9.	Repeated GNSS Measurements in the Amundsen Sea Region to Investigate Glacial Isostatic Adjustment and Ice-Shelf Dynamics	73
10.	Helicopter-Magnetic Surveying to Delineate Basement Tectonics	80
11.	Satellite Ice Reconnaissance by near Real-Time (Nrt) Service of Dlr	84

APPENDIX

A.1	Teilnehmende Institute / Participating Institutions	87
A.2	Fahrtteilnehmer / Cruise Participants	89
A.3	Schiffsbesatzung / Ship's Crew	91
A.4	Stationsliste / Station List PS104	93

1. ZUSAMMENFASSUNG UND FAHRTVERLAUF

Karsten Gohl

AWI

Zusammenfassung

Der westantarktische Eisschild (WAIS) hat in seiner Geschichte vermutlich eine sehr dynamische Aktivität erfahren, da ein Großteil seiner Basis unter dem Meeresspiegel aufliegt und daher empfindlich auf klimatische Änderungen reagiert. Ein vollständiges Abschmelzen des WAIS hätte einen globalen Meeresspiegelanstieg von 3-5 m zur Folge. Die Quantifizierung des Abschmelzens des WAIS in Warmzeiten der geologischen Vergangenheit in Kombination mit der Rekonstruktion der klimatischen Begleitumstände würde notwendige Parameter für Eisschildmodelle liefern, die sein zukünftiges Verhalten und seinen Beitrag zu Meeresspiegeländerungen prognostizieren sollen. Große Unsicherheiten bestehen bezüglich der räumlichen und zeitlichen Variabilitäten sowie der Geschwindigkeiten der vergangenen Vorschübe und Rückzüge des WAIS über die vorgelagerten kontinentalen Schelfe. Insbesondere die Region des Amundsenmeeresektors zeigt seit einigen Jahrzehnten einen beobachteten ungewöhnlich rapiden Eisschildrückzug, der als Vorläufer für das zukünftige Schicksal des gesamten WAIS vermutet wird.

Das Hauptforschungsprogramm der *Polarstern*-Expedition PS104 wurde darauf ausgerichtet, unter Nutzung des Meeresboden-Bohrgeräts MARUM-MeBo70 eine Serie von mehreren Dezimetern langen Sedimentkernen von den ältesten zu den jüngsten Sediment-Sequenzen auf dem Schelf des Amundsenmeeres zu erbohren, um Sedimentmaterial für Analysen zur Rekonstruktion der Entwicklungsgeschichte und vergangenen Dynamik des WAIS im Bereich des Amundsenmeeres zu erhalten. Die durchgeführten 10 Bohrungen an 9 Bohrstationen befinden sich in isolierten Sedimentbecken vor dem Pine-Insel-Gletscher der Pine-Insel-Bucht, entlang des zentralen glazialen Pine-Insel-Troges des mittleren Schelfes im östlichen Amundsenmeer, sowie auf der westlichen Flanke des Bear-Rückens auf dem mittleren Schelf der westlichen Amundsenmeer-Bucht. Insgesamt sind aus Bohrtiefen von wenigen Metern bis zu maximal 36 m unkonsolidierte bis konsolidierte Sedimente und stark verfestigte Sedimentgesteine erbohrt worden, die geologische Epochen von vermutlich der Spätkreide bis ins Holozän umfassen. Der erstmalige Einsatz des MeBo in der Antarktis liefert wertvolle Erfahrungen in der Optimierung von Bohrungen auf glazialen Schelfen.

Ergänzt wurden die MeBo-Bohrungen durch zahlreiche konventionelle Sedimentbeprobungen über Sedimentlote. Seismische Untersuchungen wurden im Zusammenhang mit den MeBo-Bohrstationen und dem bereits existierenden seismischen Profilnetz durchgeführt, um eine bessere flächenhafte Abbildung der erbohrten Sedimentsequenzen zu erhalten. Der Einsatz einer Temperaturgradientensonde an zahlreichen Stationen liefert wertvolle Daten zum geothermischen Wärmestrom der Region. Bathymetrische und sedimentechographische Kartierungen sind Fahrtrouten begleitend, aber auch gezielt in bisher unvermessenen Gebiete durchgeführt werden. Auf dem Festland und den Inseln im Bereich der Pine-Insel-Bucht sowie in küstennahen Aufschlüssen von Marie-Byrd-Land wurden Gesteinsproben für thermochronologische Untersuchungen zur Hebungsgeschichte der Erdkruste und für kosmogene Isotopenanalysen zur Eisrückzugsrekonstruktion gesammelt. Geodätische GPS-

Messungen zur Berechnung des glazial-isostatischen Ausgleichs der Region sind ebenfalls an zahlreichen Messpunkten des Festlandes und der Inseln realisiert worden. Beide Landprojekte sowie ein aeromagnetisches Vermessungsprojekt wurden mit Hilfe der Helikopter unterstützt.

Insgesamt hat diese Expedition den erfolgreich Einsatz des MeBo auf der *Polarstern* im engen Wechsel mit weiteren Beprobungsprogrammen und geophysikalischen Messungen gezeigt. Die nachfolgenden Analysen der zahlreich gewonnenen Proben und Daten lassen wesentliche neue Erkenntnisse über die Entwicklung des WAIS vom Beginn der glazialen Epochen bis ins Holozän erwarten.

SUMMARY AND ITINERARY

The West Antarctic Ice Sheet (WAIS) is likely to have been subject of a very dynamic activity during its history as most of its base is grounded below present sea level and, thus, is sensitive to climatic changes. Its collapse would result in a global sea-level rise of 3-5 m. The reconstruction and quantification of WAIS collapses in warm periods of the geological past will provide constraints required for ice sheet models predicting its future behaviour and resulting sea-level rise. Large uncertainties exist regarding the chronology, extent, rates and spatial and temporal variability of past advances and retreats of the WAIS across the continental shelves. The Amundsen Sea sector in particular has shown unusual rapid retreat and thinning of the ice sheet for the last decades, which has been suggested to be a pre-cursor to the fate of the entire WAIS.

The main research programme of the *Polarstern* expedition PS104 was aimed to use the MARUM-MeBo70 seabed drill device to drill a series of several decimetres long sediment cores from the oldest to the youngest sedimentary sequences of the Amundsen Sea Embayment shelf. These cores will provide material for analyses to help reconstruct the development and past dynamics of the WAIS in the Amundsen Sea sector. The 10 boreholes on 9 different sites are located in isolated sedimentary basins off the Pine Island Glacier in southern Pine Island Bay, along the central glacial Pine Island Trough of the middle shelf in the eastern embayment, and on the western flank of the Bear Ridge on the middle shelf in the western embayment. Unconsolidated to consolidated sediments and very solid sedimentary rocks were drilled from drill depths of a few metres to a maximum of 36 m. They cover geological periods from presumably Late Cretaceous to Holocene. This first deployment of the MeBo drill device in Antarctica provides valuable experience in optimising drilling operations on glacial continental shelves.

In addition to MeBo drilling, numerous marine sediment samples were collected using various coring devices. Seismic surveying in connection to MeBo drill sites added profiles to the pre-existing network of seismic lines in order to improve regional imaging of the drilled sedimentary sequences. The deployment of a temperature-gradient probe at numerous sites provides valuable data to derive geothermal heat flux of the region. Bathymetric and sub-bottom profiler mapping was conducted along most of the ship track and in dedicated, previously unsurveyed areas. The land geology team collected rock samples from outcrops of the coastal mainland of Marie Byrd Land and on islands in Pine Island Bay to be used for thermochronological studies of crustal denudation and uplift processes and for cosmogenic isotope analyses to reconstruct glacial retreat. Geodetic GPS measurements were realised at numerous sites on the mainland and on islands to derive the regional glacial-isostatic adjustment. Both land operations and an aeromagnetic survey program were supported by helicopters.

In conclusion, the expedition demonstrated the successful operation of the MeBo drill device on *Polarstern* in alternation with the other comprehensive sampling and geophysical surveying programs. There is high expectation that the follow-up analyses of the numerous samples and data will contribute to a largely improved understanding of the development of the WAIS from early glaciation to the Holocene.

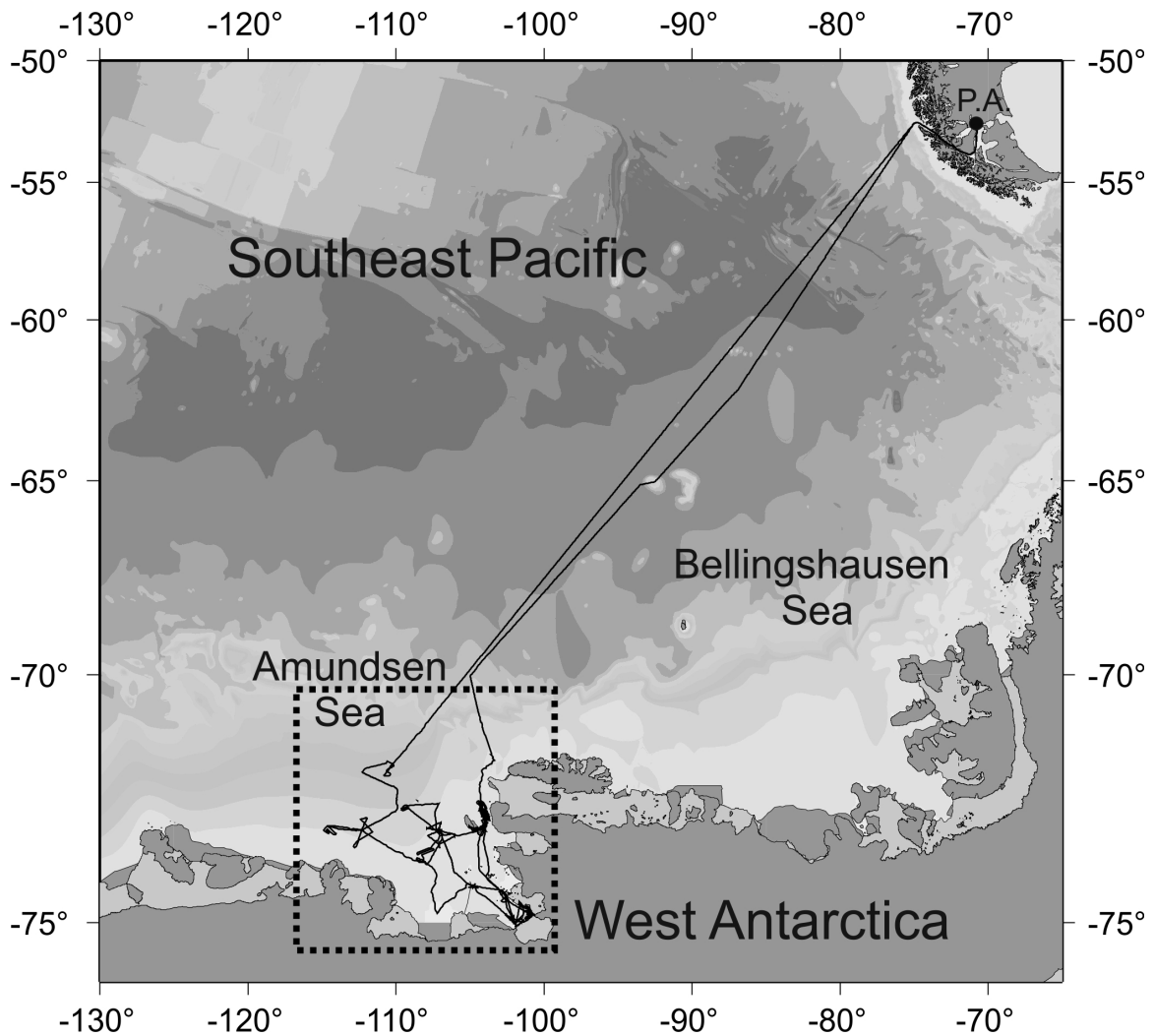


Fig. 1.1: Track of Polarstern during expedition PS104 from Punta Arenas (P.A.) to the Amundsen Sea and back to Punta Arenas. The dotted box indicates the working area in the Amundsen Sea Embayment (see Fig. 3.1).

Itinerary of science activities

Day	Date (2017)	Board time ca.	Science activities and events	Weather, seastate, ice
Sa	04.02.	(UTC-3h) 09:00 09:30	1-day Marine Mammal Observer (MMO) course for 15 participants in meeting room of hotel; Scientific advance team to ship; Beginning preparation for installation of seabed drill MeBo70 and other equipment;	fine, no wind
Su	05.02.	10:00	Embarkment of scientific participants; MeBo loading and installation; Loading and unpacking of equipment;	fine, no wind
Mo	06.02.	13:00	Continue MeBo loading and installation; Unpacking and assemblage of equipment; Departure from Mardones Pier and anchorage in bay;	partly cloudy, no to low winds
Tu	07.02.		Continue MeBo installation; Unpacking and assemblage of equipment;	cloudy, some showers, low winds
We	08.02.	08:45 13:30	MeBo water test (under observation by Port Authority); Departure from Punta Arenas , route through western Strait of Magellan;	partly cloudy, low winds, later some showers
Th	09.02.	03:00	Leaving Strait of Magellan and entering Pacific; Transit to Amundsen Sea Embayment;	cloudy, winds increasing 6-8 bf
Fr	10.02.	(UTC-4h)	Transit to Amundsen Sea Embayment;	sunny, winds decreasing
Sa	11.02.		Transit to Amundsen Sea Embayment;	cloudy, no winds
Su	12.02.	(UTC-5h)	Transit to Amundsen Sea Embayment;	cloudy, no winds
Mo	13.02.	10:00	Transit to Amundsen Sea Embayment; Recovery of unknown mooring component;	cloudy, low winds
Tu	14.02.	(UTC-6h) 11:30	Arrival at northern Amundsen Sea shelf; Station with multicorer and gravity corer; Land geology & geodesy by helicopter support; Transit to southern Pine Island Bay;	cloudy, low winds, low to medium ice coverage
We	15.02.	09:30 12:30 18:30	Arrival at southern Pine Island Bay; Deployment of hydroacoustic mooring; CTD, gravity corer u. multicorer; Deployment of seismic gear and start of seismic profiles AWI-20170001 to -07;	cloudy, low winds

Day	Date (2017)	Board time ca.	Science activities and events	Weather, seastate, ice
Th	16.02.	09:15 12:15 13:40	End seismic profile AWI-20170007; Land geology & geodesy by helicopter support; Gravity corer with temperature loggers at next MeBo site; MeBo drilling at site PIG-01-1 (test site);	cloudy, low to medium winds
Fr	17.02.	07:30 11:15 15:00	End MeBo drilling; Land geology & geodesy by helicopter support; MeBo back on deck; Bathymetry & Parasound survey along Pine Island Glacier front; CTD, box corer, gravity corer stations; Continue bathymetry & Parasound survey;	cloudy, low winds
Sa	18.02.	08:00 14:00	Gravity corer with temperature loggers; Land geology & geodesy by helicopter support; Geothermal heatflow probe stations; MeBo deployment at site PIG-02-1;	partly sunny, cloudy, low winds
Su	19.02.	01:45 02:30 08:30 09:40 23:00	MeBo tripping and hoisting due to iceberg; 2 nd MeBo deployment failed due to problem with flushwater pump; Box corer, gravity corer, multicorer stations; Land geology & geodesy by helicopter support; Bathymetric & Parasound surveying; Gravity corer, multicorer stations; Lifeboat drill of crew; Bathymetric & Parasound surveying; Box corer, gravity corer, multicorer stations; Geothermal heatflow probe station;	sunny, partly cloudy, low to no winds
Mo	20.02.	05:30 07:30 13:20 19:00 20:00	Geothermal heatflow probe station; Bathymetric & Parasound transit; Land geology & geodesy by helicopter support; Recovery of hydroacoustic mooring; CTD, multicorer and geothermal heatflow probe stations; Deployment of seismic gear and start of seismic profiles AWI-20170008 to -10;	cloudy, low to medium winds
Tu	21.02.	11:00 14:30 17:00 18:00	End seismic profile AWI-20170010; Land geology & geodesy by helicopter support; Helicopter-magnetic survey; Parasound survey; Gravity corer at next MeBo drill site; MeBo drilling at site PIT-03-1;	cloudy, medium winds
We	22.02.	15:00 20:00 22:30	Continue MeBo drilling at PIT-03-1; Land geology & geodesy by helicopter support; Helicopter-magnetic survey; End MeBo drilling due to iceberg approach; Gravity corer on last MeBo site; Bathymetric & Parasound survey;	cloudy, medium winds

Day	Date (2017)	Board time ca.	Science activities and events	Weather, seastate, ice
Th	23.02.	10:00 14:30 15:45	Continue bathymetric & Parasound survey; Helicopter-magnetic survey; Gravity corer on next MeBo site; MeBo drilling at site PIT-04-1;	partly cloudy to sunny, medium to low winds
Fr	24.02.	00:30 02:30 14:30 20:30	End MeBo drilling due to technical problem and iceberg approach; Bathymetric & Parasound survey; CTD, gravity corer, box corer station on grounding zone wedge (GZW4); 2 nd MeBo drilling at site PIT-04-2;	partly cloudy to sunny, medium winds
Sa	25.02.	09:30 13:00 14:15 14:30	Continue MeBo drilling at PIT-04-2; Land geology & geodesy by helicopter support; End MeBo drilling due to technical problem; Deployment of seismic gear and start of seismic profiles AWI-20170011 to -16; Helicopter-magnetic survey;	cloudy, low winds
Su	26.02.	16:00	Continue seismic profiling; End seismic profile AWI-20170016; Bathymetric & Parasound transect to Cosgrove-Abbot Trough and survey there; Land geology & geodesy by helicopter support; Helicopter-magnetic survey;	cloudy, medium winds
Mo	27.02.	10:00 11:00 14:00 15:00	Gravity corer on next MeBo site; Land geology & geodesy by helicopter support; MeBo drilling at site CAT-01; Helicopter-magnetic survey; End MeBo drilling due to technical problems; Gravity corer stations; Bathymetric & Parasound survey;	partly cloudy, medium winds
Tu	28.02.	08:15	Deployment of seismic gear and start of seismic profiles AWI-20170017 to -26; Land geology & geodesy by helicopter support; Helicopter-magnetic survey;	cloudy, low to medium winds
We	01.03.	02:20 08:30 09:30	End seismic profile AWI-20170026; Bathymetric & Parasound survey; Geothermal heatflow probe station; MeBo deployment not possible due to strong winds and sea-ice approaching; Helicopter ice reconnaissance flight; Bathymetric & Parasound transect to southern Pine Island Bay;	cloudy, strong winds increasing
Th	02.03.	00:30 02:00 09:30 11:00	Gravity corer station; Geothermal heatflow probe stations; Land geology by helicopter support; Gravity and box corer stations; MeBo deployment not possible due to strong winds; Transit to south-central Pine Island Bay;	cloudy, strong winds

Day	Date (2017)	Board time ca.	Science activities and events	Weather, seastate, ice
Fr	03.03.	00:30 06:30	Geothermal heatflow probe stations; MeBo drilling at site PIB-06; Helicopter-magnetic survey;	cloudy, medium to low winds
Sa	04.03.	16:00 16:30 19:00	Continue MeBo drilling at PIB-06; Helicopter-magnetic survey; End MeBo drilling; Geothermal heatflow probe and gravity corer station at MeBo site; Deployment of seismic gear and start of seismic profiles AWI-20170027 to -29;	cloudy, low winds
Su	05.03.	00:15 09:30	End seismic profile AWI-20170029; Bathymetric & Parasound transect to western Amundsen Sea Embayment shelf and survey in Dotson-Getz Trough; Helicopter-magnetic surveys;	cloudy, low winds
Mo	06.03.	10:30 13:40 19:00 22:30	Planned MeBo site in central Dotson-Getz-Trough cancelled due to ice and unfavourable site conditions; Bathymetric & Parasound transect; Land geology by helicopter support; Gravity corer at next MeBo site; MeBo drilling at site BEAR-07a; End MeBo drilling due to technical problem; Bathymetric & Parasound transect; MeBo drilling at site BEAR-08;	cloudy, strong winds
Tu	07.03.	08:30 13:30	End MeBo drilling due to technical problem; Bathymetric & Parasound transect; MeBo drilling at site BEAR-09;	cloudy, low winds
We	08.03.	08:00 13:30 14:15	End MeBo drilling, no further penetration; Bathymetric & Parasound survey; Gravity corer near next MeBo site; 2 nd MeBo drilling at site BEAR-07b; Helicopter-magnetic survey;	cloudy, low winds
Th	09.03.	17:00 19:00 21:00	Continue MeBo drilling; End MeBo drilling; CTD, box corer, geothermal heatflow station; Deployment of seismic gear and start of seismic profiles AWI-20170030 to -33;	cloudy, low winds
Fr	10.03.	20:30	Continue seismic profiling; End seismic profile AWI-20170033; Bathymetric & Parasound survey;	cloudy, low winds
Sa	11.03.	00:30 06:00	Gravity corer station; Bathymetric & Parasound survey; Departure from outer shelf of western Amundsen Sea Embayment shelf and beginning of transit to Punta Arenas; Disassembling and packing of equipment;	cloudy, low to medium winds

Day	Date (2017)	Board time ca.	Science activities and events	Weather, seastate, ice
Su	12.03.		Transit to Punta Arenas; Disassembling and packing of equipment;	cloudy, medium winds
Mo	13.03.	(UTC-5h)	Transit to Punta Arenas; Disassembling and packing of equipment;	partly cloudy, medium winds
Tu	14.03.		Transit to Punta Arenas; Disassembling and packing of equipment;	partly cloudy, medium winds
We	15.03.	(UTC-4h)	Transit to Punta Arenas;	cloudy, medium to strong winds
Th	16.03.		Transit to Punta Arenas;	cloudy, strong winds
Fr	17.03.	(UTC-3h)	Transit to Punta Arenas;	cloudy, strong to medium winds
Sa	18.03.	12:00	Arrival in Punta Arenas , bunker pier;	partly sunny, medium winds
Su	19.03.	08:30	Disembarkment of scientific participants;	

2. WEATHER CONDITIONS

Max Miller, Juliane Hempelt

DWD

On early Wednesday afternoon, February 08 2017, 13:40 pm, *Polarstern* left Punta Arenas for the campaign PS104. Fresh north-westerly winds, 14°C and partly cloudy skies were observed.

A low north of Bellingshausen Sea was weakening but a new storm approaching from west. Therefore *Polarstern* operated at the east side of this system at north-westerly winds. Steaming the Strait of Magellan we could observe the well-known large differences caused by the topography. At the western, funnel-shaped exit, winds freshened up to 8 Bft due to a jet effect. Reaching "open" waters on Thursday morning (Feb. 09) we measured only 6 to 7 Bft. But until evening north-westerly winds increased again up to 8 Bft and abated gradually during the night to Friday. The sea state peaked at 5 m. At the weekend we crossed the centre area of the low at often only light and variable winds. The low headed towards Drake Passage and winds veered south at 5 Bft on Monday (Feb. 13) while *Polarstern* was approaching Pine Island Bay (PIB).

On Tuesday (Feb. 14) a ridge crossed PIB. A storm off Ross Sea moved slowly east and became stationary north of PIB. After midweek we got at its south side and winds veered east. But we operated at the sheltered south-eastern end of the bay and wind force didn't exceed 4 Bft.

Only from Tuesday (Feb. 21) on, as *Polarstern* arrived at the centre area of PIB, easterly winds increased: at first up to 7 Bft and from Thursday (Feb. 23) on around 5 Bft.

During the following days the pressure gradient over PIB increased a bit. From Tuesday (Feb. 28) on we operated at the eastern edge of the bay and Föhn-like effects became a feature. Steaming zigzag along the coast line we often observed very large differences of wind speed and direction. Abrupt changes between nearly calm and 8 Bft were not unusual. Only from Friday (Mar. 03) on pressure gradient weakened.

On Saturday (Mar. 04) a new low over Ross Sea moved east. From Sunday on easterly winds increased and peaked at 7 Bft on Monday (Mar. 06). But the low split into several centres. During the second half of the week wind force did not exceed 5 Bft and wind direction changed often.

Saturday morning (Mar. 11) we headed back to Chile. A low north of PIB moved towards Bellingshausen Sea. *Polarstern* got at its west side at Bft 7 from southwest on Sunday (Mar. 12). During the night to Monday a small ridge caused temporarily abating winds. Northeast of Ross Sea a storm had formed and followed us. From Tuesday (Mar. 14) on we steamed at its east side. North to north-westerly winds increased and peaked at Bft 8 during the night to Thursday (Mar. 16) causing a sea state of 5 m.

Friday morning (Mar. 17) we entered the Strait of Magellan and observed sudden changes of wind speed due to the topography again.

On Saturday morning, March 18· 2017, *Polarstern* reached Punta Arenas at strong and gusty winds from west to northwest, isolated showers and 10°C.

For further statistics see attached Figs 2.1 to 2.5.

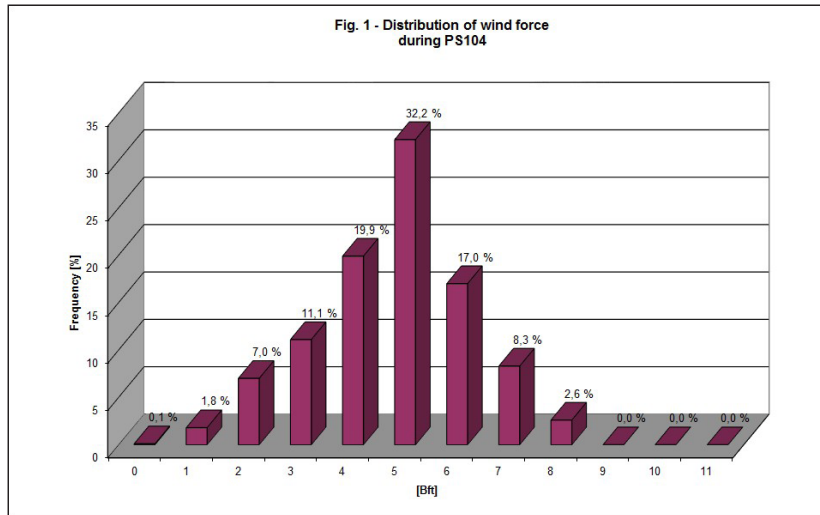


Fig. 2.1: Distribution of wind force

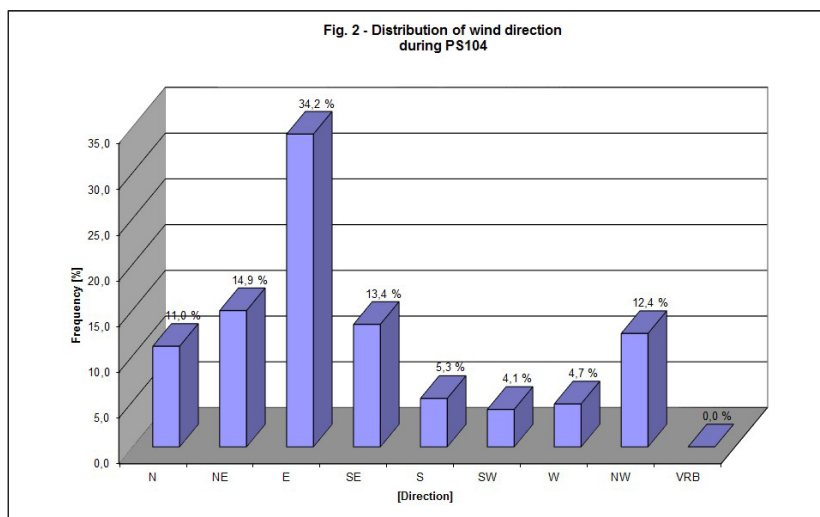


Fig. 2.2: Distribution of wind direction

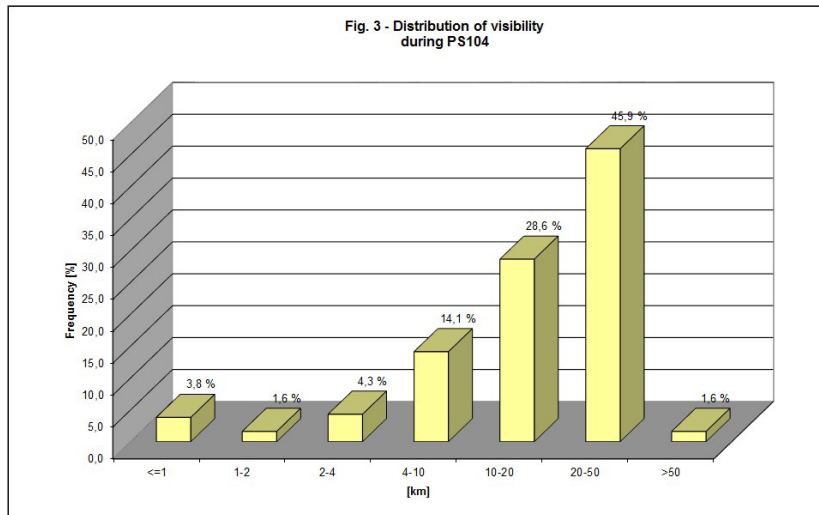


Fig. 2.3: Distribution of visibilit

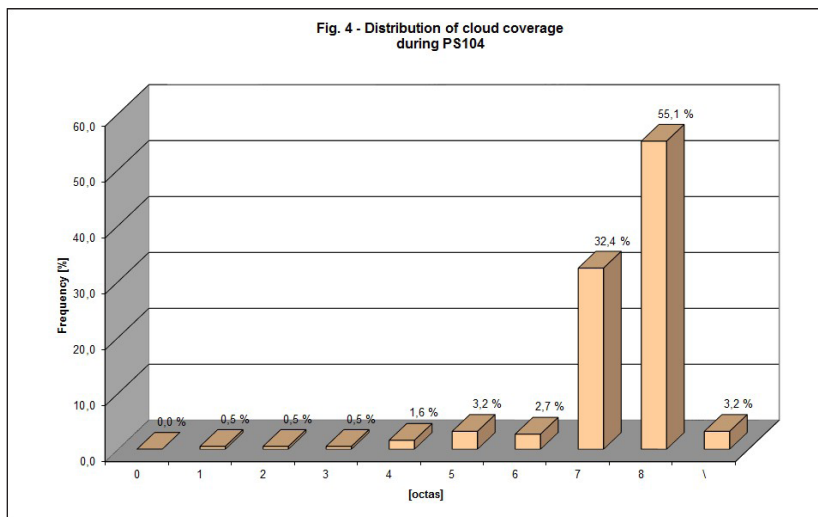


Fig. 2.4: Distribution of cloud coverage

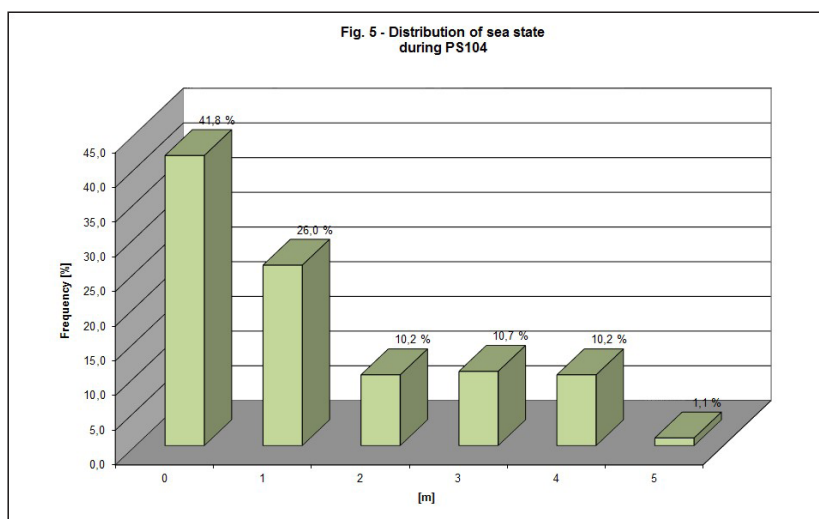


Fig. 2.5: Distribution of sea state

3. ICE SHEET DYNAMICS OF THE AMUNDSEN SEA EMBAYMENT WITH MEBO SHALLOW DRILLING

Karsten Gohl¹, Tim Freudenthal², Johann Klages¹,
Claus-Dieter Hillenbrand³, Marcelo Arevalo¹,
Markus Bergenthal², Torsten Bickert³, Thomas
Börner⁴, Steve Bohaty⁵, Ralf Düßmann², Ricarda
Dziadek¹, Werner Ehrmann⁶, Oliver Esper¹,
Thomas Frederichs³, Siefke Fröhlich², Arne
Kausche², Thorsten Klein², Kevin Küssner¹,
Robert Larter³, Norbert Lensch¹, Yanina Najman⁷,
Cornelius Noorlander², Heiko Pälike³, Michael
Reuter², Thomas Ronge¹, Jan Schüürman¹,
Patric Simoes Pereira⁸, James Smith³, Gabriele
Uenzelmann-Neben¹, Tina van de Flierdt⁸, Max
Zundel⁹, Gerhard Kuhn¹ (not on board)

¹AWI
²MARUM
³BAS
⁴Bauer
⁵U Southampton
⁶U Leipzig
⁷Lancaster U
⁸Imperial
⁹U Bremen

Grant-No. AWI_PS104_01

Objectives

The behaviour of the West Antarctic Ice Sheet (WAIS) in relation to climatic changes and its contribution to global sea-level change are poorly understood. The WAIS is suspected to be highly sensitive to changes in global sea level and regional oceanographic conditions as well as atmospheric conditions. Its collapse would result in a global sea-level rise of 3.3-4.3 m (e.g. Fretwell et al., 2013). Satellite observations in the last decades have shown that the Pine Island, Thwaites, Smith, Kohler, Haynes and Pope glacier systems of the Amundsen Sea Embayment (ASE) (Fig. 2) have thinned at an alarming rate, while flow speed of some of them has dramatically increased (e.g. Joughin et al., 2011, 2012). It is unclear, however, if the current fast retreat represents a phase of ongoing ice retreat since the Last Glacial Maximum (LGM) (e.g. Hillenbrand et al., 2013), or if it is triggered by recent climatic or oceanographic changes. Significant sub-ice shelf melting by relatively warm Circumpolar Deep Water (CDW) that spreads across the shelf through deep palaeo-ice stream troughs towards the grounding zone of the WAIS has been suggested as a possible cause (e.g. Joughin et al., 2012; Favier et al., 2014). Has the WAIS undergone similar thinning and retreat in warm climates of the past? What are the factors driving these retreats?

The main scientific questions and objectives addressed by this shallow seabed drilling project include:

1) What is the contribution of the West Antarctic Ice-Sheet to past sea level changes in terms of rate and magnitude? Have sectors of the marine-based WAIS experienced “runaway collapses” as a result of climate warming and/or changes in ocean circulation?

Marine sediment cores from the West Antarctic continental shelf have the potential to provide datable records of the glacial history of the WAIS, including phases characterised by major reductions in ice-sheet size. Changes in the geochemical provenance of ice-rafted debris (IRD) deposited on the ASE shelf will allow to recognize not only complete WAIS collapses

associated with the opening of Trans-Antarctic seaways, but also partial collapses of individual WAIS drainage basins along the Pacific margin. In addition, reconstructions of palaeo-seawater temperatures from micro-palaeontological (e.g. microfossil assemblages) and chemical proxies (biomarker, stable isotopes) will help to evaluate whether oceanic melting was the main driver of past WAIS collapses as modelling suggests.

2) How did the WAIS respond the last time when Earth's atmosphere contained more than 400 ppm CO₂?

The middle Pliocene represents the last time when Earth's atmospheric temperature was as high as it is predicted for the year 2100 (~3-4°C warmer than present). However, this warmth was achieved when the atmospheric pCO₂ concentration was just ca. 365-415 ppm and other climatic boundary conditions (e.g. plate-tectonic configuration) were the same. The ANDRILL AND-1B core provides a record of the variability of the East and West Antarctic ice sheets in the western Ross Sea during the Neogene. It has provided some critical insights into the dynamic behaviour of the WAIS and suggested WAIS collapses during past warmer-than-present interglacials, especially during the Pliocene. This conclusion, however, needs confirmation with an additional, less ambiguous WAIS-proximal record, and such a record can be acquired in the ASE.

3) How does the ice-sheet dynamics correlate with records of deep-ocean oxygen isotopes, atmospheric and oceanic temperatures and eustatic sea level?

Throughout most of the Cenozoic era, there are obvious but still unexplained discrepancies between Earth's temperature and global ice volume reconstructed from proxies in deep-sea sediments (such as stable oxygen isotope and Mg/Ca-derived temperature records from benthic foraminifera) or climate models, global sea-level estimates, and proximal evidence from Antarctica. The drill cores from the ASE are expected to characterise the climatic conditions during glacial and interglacial periods of the last 5 Ma, and to determine, whether major deglaciation had affected Antarctica during that time. Moreover, the study of the drill cores from the ASE will decipher, if the WAIS responded directly to the orbitally-paced climatic cycles of the Pliocene and Quaternary, or if it varied at periods determined by its internal dynamics.

4) How does the Antarctic Circumpolar Current (ACC) and Circumpolar Deep Water (CDW) incursions onto the continental shelf control the stability of marine ice-sheet margins?

Incursions of relatively warm CDW onto the West Antarctic continental shelf have been implicated in regulating WAIS behaviour on orbital and shorter timescales. Therefore, palaeo-records of CDW-pumping onto the West Antarctic shelf are urgently needed to understand the relationship between ice sheet variability and ocean circulation. Producing proxy records of past CDW incursions from marine sediment cores is still a challenge. With recent observations of present deep water incursions into the deep palaeo-ice stream troughs of the ASE shelf, shallow drilling in this area is expected to recover the sample material required for testing and improving proxies for CDW upwelling onto the shelf and its effect on WAIS dynamics.

5) How did processes operating at the base of the ice sheet enable streaming flow at the Last Glacial Maximum, and how did they affect the post-LGM retreat?

Does the sediment infill of deep subglacial meltwater channels and basins characterising the inner ASE shelf consist of sorted and graded coarse material indicating that the channels were active meltwater conduits during the last glaciation? How are grounding zone wedges constructed, how quickly did they form, and what are the implications for their potential to stabilise retreating grounding lines? What are the implications for subglacial processes operating at the ice sheet base during the LGM?

6) When did the WAIS first expand onto the ASE continental shelf and was ice sheet expansion related to uplift in neighbouring Marie Byrd Land? Does the denudation history of Marie Byrd Land recorded in ASE sediments indicate changes in the dynamic behaviour of the WAIS through time?

The beginning of major ice sheet build-up in West Antarctica is still unknown because of sparse drill sites with datable material. Ice sheet models have reconstructed an early ice-sheet nucleus on the top of elevated Marie Byrd Land, the Ellsworth Mts and parts of the southern Antarctic Peninsula mountain chain. The exhumation and erosion history of Marie Byrd Land, and particularly that of the Marie Byrd Land Dome, is particularly relevant for the interrelations between ice sheet and lithosphere dynamics. As subglacial erosion is a very effective mechanism, the onset of glaciation and changes in the style of glaciation will directly change erosion rates, and, due to isostatic adjustment, also exhumation rates. This objective will be addressed in collaboration with the fission-track analysis and provenance research program at the University of Bremen.

7) What were the environmental and climatic conditions of West Antarctica in the Cretaceous to Eocene greenhouse period?

Although the atmospheric $p\text{CO}_2$ concentration in the Cretaceous exceeded twice the present level, fossil dinocyst data give evidence for the presence of sea-ice, suggesting that glaciers and ice caps existed in areas of high elevation in Antarctica. The current horizon-stratigraphic model for the ASE (Gohl et al., 2013) indicates that Cretaceous sediments crop out at the seafloor of the inner shelf, which makes this a unique opportunity for collecting such rare samples from the Pacific margin of central West Antarctica.

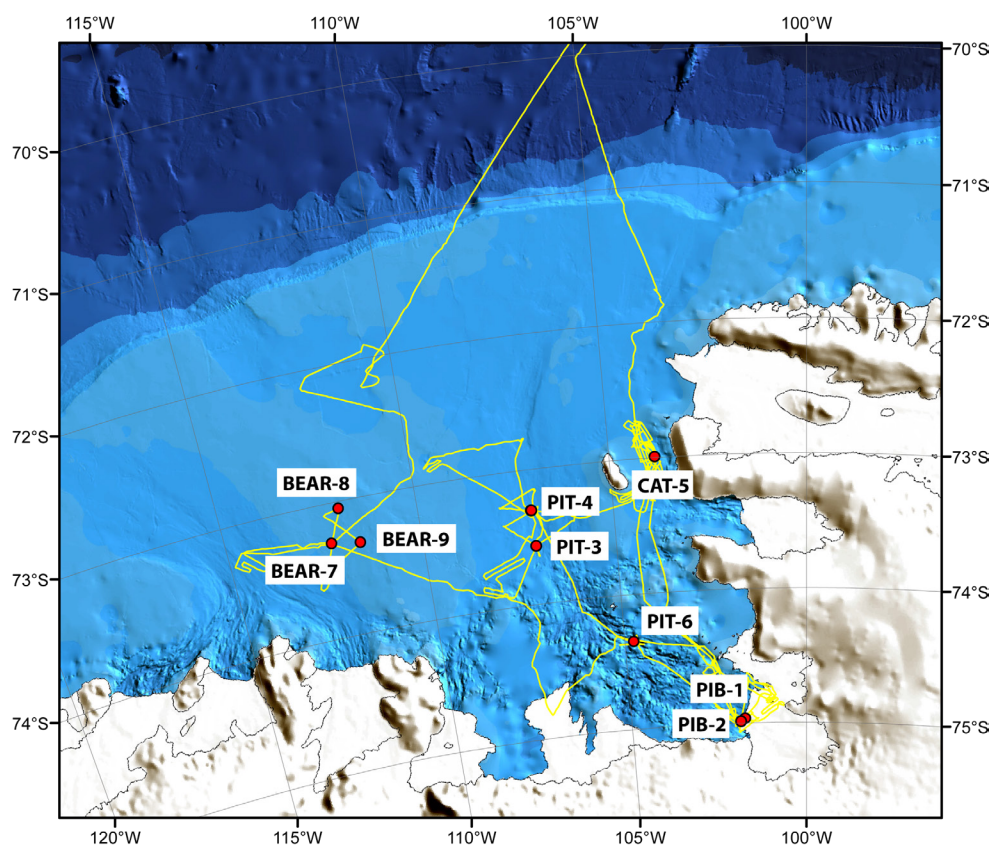


Fig. 3.1: Bathymetric map of the Amundsen Sea Embayment shelf (marked area in Fig. 1.1) with the ship track and MARUM-MeBo70 drill sites (yellow dots).

Work at sea

MeBo operation

The seafloor drill rig MARUM-MeBo70 (Fig. 3.2) was used for drilling long sediment cores. This device is a robotic drill that is deployed on the seabed and remotely controlled from the vessel (Freudenthal and Wefer, 2013). The complete MeBo70 system, which includes drill, winch, launch and recovery system, control unit, as well as workshop and spare drill tools, is shipped in seven 20' containers. A steel armoured umbilical with a diameter of 32 mm is used to lower the 10-tons heavy device to the sea bed where four legs are being armed out in order to increase the stability of the rig. Copper wires and fibre optic cables within the umbilical are used for energy supply from the vessel and for communication between the MeBo and the control unit on the deck of the vessel. The maximum deployment depth in the current configuration is 2000 m.

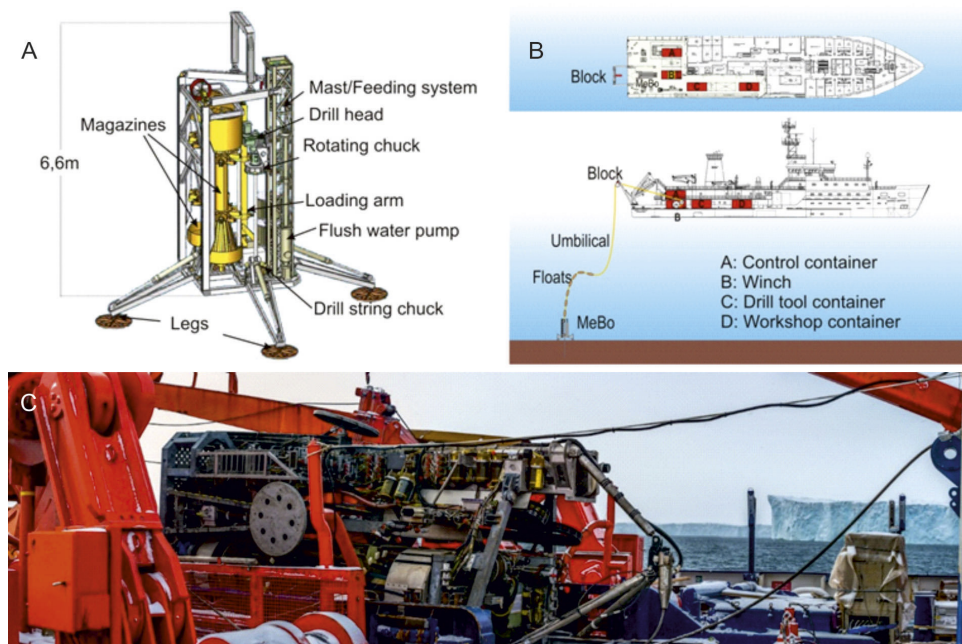


Fig. 3.2: (A) Schematic overview on the MARUM-MeBo70 seabed drill rig and (B) its deployment from a research vessel. (C) MeBo70 on Polarstern (photo: T. Klein).

The mast with the feeding system forms the central part of the drill rig. The drill head provides the required torque and rotary speed for rock drilling and is mounted on a guide carriage that moves up and down the mast with a maximum push force of 4 tons. A water pump provides sea water for flushing the drill string for cooling of the drill bit and for removing the drill cuttings. Core barrels and rods are stored on two magazines on the drill rig. We used wire-line core barrels (HQ) and hard metal drill bits as well as diamond bits (Fig. 3.3). The bits were used in combination with pilot core lifter cases for soft sediments (push coring, 55 m core diameter) and hard rock core lifter cases (rotary drilling, 63 mm core diameter). The stroke length was 2.35 m. With complete loading of the magazines, a maximum coring depth of more than 70 m can be reached. Station time can exceed 24 hrs per deployment.

A spectral gamma ray (SGR) probe was used for borehole logging. The probe is equipped with a 25 cm long scintillation crystal combined with a photo-multiplier. Light impulses that are generated by gamma ray collisions with the scintillation crystal are counted and analysed concerning the energy spectrum. The three naturally occurring gamma ray emitters – potassium,

uranium and thorium – generate different energy spectra. A GeoBase software package is used to calculate a best fit of the spectra. By combining the results of the spectrum fit with the gamma ray counts, the concentrations of K, U, and Th are calculated.



Fig. 3.3: MeBo70 drill bits used during PS104: (A) two step tungsten carbide bit; (B) conical tungsten carbide bit; (C) Diamond impregnated bit; (D) surface set diamond bit.

The SGR-Memory is an autonomous tool that is used with the MeBo drilling system. When the maximum coring depth is reached, the inner core barrel is replaced by the probe. The gravity point of the sensor is located about 60 cm above the drill bit and measures through the drill pipe. The probe is hooked up the borehole together with the drill pipe during recovery of the drill string (logging while tripping). Tripping speed was about 0.6 m per minute.

A newly developed autonomous acoustic borehole logging tool was tested with MeBo. The probe is equipped with a transmitter and two receiver located 90 cm and 100 cm below the receiver, respectively. The tool is deployed similar like the SGR-tool during trip out of the drill string. The sensor part is located about 1 m below the drill bit while logging the p-wave velocity of the formation.

A temperature probe was used for measuring formation temperature at different sediment depths. The probe consists of a probe that replaces an inner core barrel for conducting temperature measurements at discrete depths. The lower end of the probe is located below the drill bit at the base of the drill string is equipped with a miniaturized temperature data logger (MTL) with a 95 mm long tip. The temperature range of the MTL is -5 to 50°C with a resolution of about 1 mK. The absolute accuracy is about ± 0.1 K. The probe is pushed together with the drill string by 15 cm into the sediment. After 10 minutes measuring time, the temperature probe is hooked up out of the drill string using the wire line technique and core drilling can proceed. The MeBo70 was deployed 11 times at 9 sites to sample long cores from the Amundsen Sea Embayment shelf (Fig. 3.1). The total MeBo deployment was 193 hrs with 162 m drilled. In total, 150 m were cored with 56.91 m recovered, giving an average recovery rate of 38%. Altogether 8 temperature measurements at 2 stations were conducted. Borehole logging with the SGR logging probe and the acoustic logging probe was conducted at one station, respectively. Detailed information on the deployment of MeBo and recovery of sediments is summarized in Table 3.1.

MeBo drill sites

Seven boreholes were drilled on the eastern Amundsen Sea Embayment shelf:

Site PIB-1 (PS104/006-2): The drill rig was deployed for ca. 21.5 hrs in a deep sedimentary basin in the inner Pine Island Bay. Drill depth was 23.95 m, cored length (10 push cores) 23.75 m and recovery was 7.78 m of brown and olive mud and grey olive diamictons. A two-step tungsten carbide bit was used in combination with pilot core lifter cases (push coring technique). A spectrum gamma ray probe was successfully used for borehole logging during trip out (20.8 – 0.0 m).

Site PIB-2 (PS104/009-2): At this site of the same basin, MeBo drilled 16.90 m deep and cored a length of 16.70 m (7 push cores) within ca. 11.25 hrs using again the two-step tungsten carbide bit in combination with pilot core lifter cases. The drill rig recovered 3.91 m of the same type of sediments. Drilling had to be interrupted because of an iceberg passing by close to the ship, and a second drilling attempt at the same site (PS104/009-3) had to be abandoned after ca. 4 hrs due to a failure of the flush water pump.

Site PIT-3 (PS104/020-2): This site targeted dipping sedimentary strata cropping out near the seafloor north of the acoustic basement-sedimentary strata boundary in southern Pine Island Trough. Drilling strategy was to flush through the overlying unconsolidated glacial marine sediments and start core drilling with a surface set diamond bit as soon as harder strata were reached at 9.8 m below the sea floor. The drill rig was deployed for ca. 28.25 hrs and drilled 30.80 m deep, thereby coring 23.55 m of rotary cores. 10 rotary cores filled with 5.89 m of grey muddy quartz sandstone and underlying carbonaceous mudstone were retrieved. The drill bit was completely worn at the end of the drilling.

Site PIT-4a (PS104/021-2): This site targeted dipping sedimentary strata located north of site PIT-3. We started with a two-step tungsten carbide bit in combination with rotary drilling core lifter cases. For the next barrels a new bottom-hole assembly (BHA) with a diamond-impregnated bit was used. The deployment time was ca. 10 hrs, during which a drill depth of 5.10 m with a cored length of 4.95 m was achieved. The three recovered rotary cores contained brown mud in the upper core and grey-olive stratified mudstone in the two lower cores, while very stiff dark diamicton and mudstone were observed in the core catchers.

Site PIT-4b (PS104/021-3): The second drilling attempt at the same site lasted for ca. 16.75 hrs. We drilled with a diamond-impregnated bit. A new BHA with a diamond-impregnated bit was deployed after the second core barrel (4.6 m drilling depth). Total drill depth was 9.80 m and cored length 9.65 m. Five rotary cores recovered 7.36 m of sedimentary rocks with a similar lithology as retrieved from the first hole.

Site CAT-5 (PS104/024-2): The deployment time at this site on top of a grounding-zone wedge (GZW) in the Cosgrove-Abbot Trough was only ca. 3.75 hrs. Drilling had to be cancelled due to a technical problem (glued thread connection within BHA opened). Thus, drill depth was only 2.75 m with a cored length of 2.60 m. The single recovered rotary core that was used in combination with a diamond-impregnated bit retrieved 0.18 m of olive-brown sandy gravelly mud.

Site PIT-6 (PS104/038-1): At his site, another deep basin on the inner shelf of the eastern Amundsen Sea Embayment was targeted. A maximum drill depth of 35.65 m was reached within 34.25 hrs using a two-step tungsten carbide bit. The cored length was 32.25 m, and 14 push and 2 rotary cores were used. A total of 15.65 m of brown, olive and grey muds, sandy muds, sands and diamictons were recovered. Temperature measurements were conducted at 5.25 m, 9.95 m, 14.65 m, 19.35 m, 24.05 m and 28.75 m. The five deeper measurements may be affected by a slight bending of the probe that occurred during storage in the magazine after the first measurement.

Four boreholes were drilled on the western flank of Bear Ridge in the western Amundsen Sea Embayment and targeted exclusively dipping sedimentary strata:

Site BEAR-7a (PS104/040-2): The drill rig was deployed on top of the older part of the dipping strata for ca. 7.25 hrs. Maximum drill depth was 5.35 m and 5.20 m were cored by rotary drilling, which retrieved 0.94 m of brown mud overlying dark olive grey diatom-rich mudstone. The first barrel was drilled with a diamond-impregnated bit down to 2.75 m. Due to a jammed inner core barrel the shear pin at the overshot had to be activated and only one stroke with a second BHA again with a diamond-impregnated bit down to 5.35 m was possible. Open hole deployment of the SGR tool and acoustic bore hole logging probes fixed by the rotating chuck in the upper 2 m were not successful due to failure of probe activation.

Site BEAR-7b (PS104/040-3): Redeployment at the same site lasted for ca. 27.25 hrs and reached a depth of 17.97 m. The drilled length was 17.72 m. This time a conical tungsten carbide bit was used in combination with rotary core lifter cases. The 8 rotary cores collected 8.82 m of olive mudstone which is underlain by very dark grey gravelly sandy mudstone. The bit was worn after the end of the drilling. Despite of the consolidation status of the sediments, temperature measurements were tried at 14.5 and 16.9 m depth. A newly developed acoustic borehole logging probe and the SGR tool were used for borehole logging during trip out (16.5 - 0.3 m). Activation of the SGR probe failed.

Site BEAR-8 (PS104/041-1): The MeBo deployment at this site drilled down to a maximum depth of 7.45 m over 10.5 hrs and cored 7.30 m (3 rotary cores) with a recovery of 0.89 m. The upper cores from the younger part of the dipping sedimentary strata outcropping at site BEAR-8 consist of olive diamicton, while the lower cores sampled dark grey diamicton. The first barrel was drilled with a diamond-impregnated bit down to 2.75 m. Due to indication of a jammed inner core barrel, a second BHA with a diamond-impregnated bit was used for the second core barrel down to 5.1 m. The shear pin at the overshot had to be activated due to a jammed inner core barrel, and only one stroke with a third BHA with a diamond-impregnated bit down to 7.45 m was possible. Open hole deployment of logging probes fixed by the rotating chuck in the upper 2.1 m (SGR) and 2.8 m (acoustic) were successfully conducted.

Site BEAR-9 (PS104/042-1): At this last site, the rig penetrated the seafloor down to a depth of 6.15 m within ca. 18.75 hrs. The target was the oldest part of the dipping sedimentary strata and cored length was 6.00 m. The six rotary cores and one push core collected 2.40 m of brown soft diamicton near the top and dark olive mudstone in the lower part of the retrieved sedimentary column. The first 3 barrels were drilled down to 4 m with a conical tungsten carbide bit. Afterwards a second BHA with conical tungsten carbide bit was deployed and drilled down to 6 m until no further progress was reached with this bit. A third BHA with tungsten carbide bit also did not achieve further progress.

Lab workflow of MeBo drill cores

The workflow of the drilled MeBo70 cores after receiving them from the MeBo operation team on deck was undertaken by three separate geology teams: the deck team, the core catcher team, and the liner team.

Directly after the inner core barrels were taken from the frame by the MeBo operation team, they were marked with clips indicating the respective barrel number. Afterwards they were handed over to the deck team and carried to the workspace just in front of the lab, where they were deposited on wooden blocks. Barrel by barrel was then put on the rig to be fastened and opened. Subsequently, the core catcher had to be screwed off from the respective inner barrels in order to label them with a clip for the correct number and to hand them over to the

core catcher team. Finally, a cap had to be put at the bottom of the liner together with a clip for the correct number, before it was handed over to the liner team in the lab. Then the outer core barrels were cleaned.

Before the core catchers for each core section were brought into the lab, the core catcher liners were already labelled with the correct number and orientation (top & bottom). The sediment inside the core catchers was then pushed into the liners with the help of a plunger before it was sealed and labelled (inset of Fig. 3.4). The correct sediment orientation inside the liners was repeatedly checked. As a final step all core catchers were cleaned before handing them back to the MeBo operation team.

Meanwhile, the liner team had to cut each liner directly above the sediment surface to put a cap on top of each section. Afterwards, the entire liner had to be labelled on both sides (core number, archive/work half). In case the cut liner was longer than 130 cm it had to be cut in two segments, each of which was labelled (Fig. 3.4) and sealed separately.

As a final step both the core catcher liners and the core liners were logged for their physical properties after 24 hours and were then stored at 4°C in a reefer container.

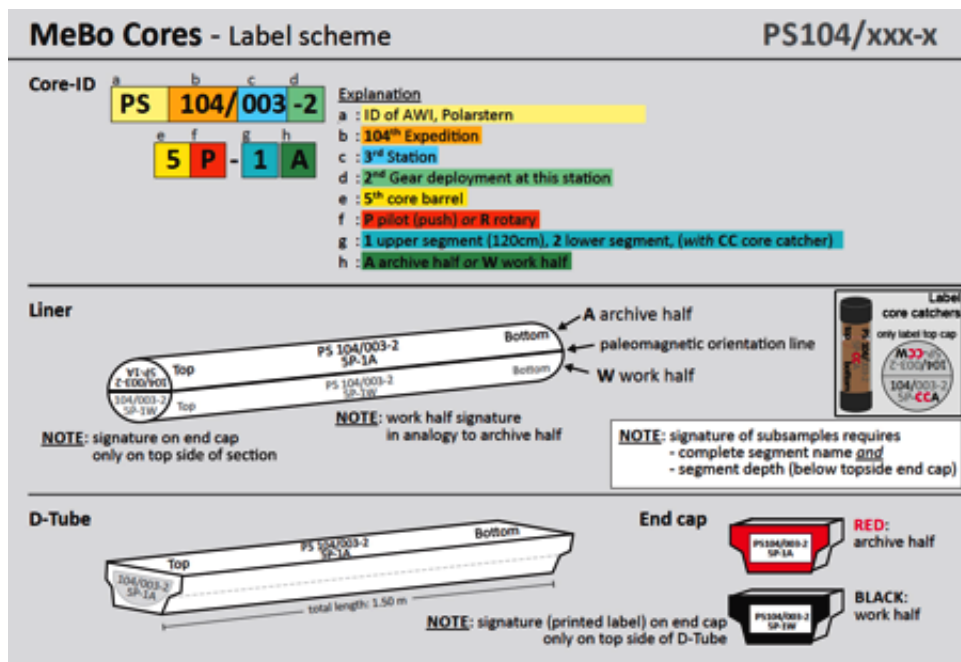


Fig. 3.4: Labelling scheme for MeBo cores during PS104 (modified after C. Wienberg, MARUM)

Preliminary results

Tables 3.1 and 3.2. summarise drill results and recovery of samples from MeBo70 drill sites.

Tab. 3.1: Summary of drill results from MeBo70 drill sites of PS104.

Drill site	Polarstern station no.	Coordinates [lat, lon]	Water depth [m]	Drill target(s)	Drilled depth / deployed cored length [m]	Drilled core [m]	Recovery	Recovered lithology	Remarks
PIB-1 (inner Pine Island Bay)	PS104/006-2	74°57.961' S 101°45.067' W	1051 (1050)	Quaternary/ Holocene	23.95 / 23.75	7.78	32.8 %	Very soft, fine to coarse grained glacial marine and pro-/subglacial sediments	Loading of only 20 m pipe for testing; drilling stopped due to iceberg approach
PIB-2 (inner Pine Island Bay)	PS104/009-2	74°59.201' S 101°52.325' W	989 (1017)	Quaternary/ Holocene	16.90 / 16.70	3.91	23.4 %	Very soft, fine to coarse grained glacial marine and pro-/subglacial sediments	Loading of 50 m pipe; drilling stopped due to iceberg approach, core 8 lost in drill hole; 2nd attempt failed due to flushwater pump failure;
PIT-3 (central Pine Island Trough)	PS104/020-2	73°34.095' S 107°05.626' W	946 (905)	Oldest dipping strata (near outcropping basement) (Cretaceous/ Paleogene ?)	30.80 / 23.55	5.89	25.0 %	Muddy grey sand (Qtz sand) in upper cores; carbonaceous mudstone at base of lowermost core (ca. 1.5 m), contains abundant microfossils, plant particles and pollen	Loading of 50 m pipe; uppermost 10 m flushed through; slow drilling progress of the last 3 m; drilling abandoned due to iceberg approach; complete loss of diamonds on surface set drill bit (abrasion by quartz grains);

Drill site	Polarstern station no.	Coordinates [lat, lon]	Water depth [m]	Drill target(s)	Drilled depth / deployed cored length [m]	Drilled core [m]	Recovery	Recovered lithology	Remarks
PIT-4a (central Pine Island Trough)	PS104/021-2	73°18.290' S 107°06.635' W	882 (844)	Dipping strata above seismic unconformity ASS-u2 (Oligocene to Miocene?)	5.10 / 4.95	3.09	62.4 %	Brown mud in upper core; grey-olive stratified mudstone in lower cores; very stiff dark grey diamicton and mudstone in core catchers; low diverse nanofossils in mudstone sample	Loading of 50 m pipe; problems in retrieval of uppermost core, then drilling continued; jammed inner barrel caused temporary halt of drilling; iceberg approach caused end of drilling;
PIT-4b (central Pine Island Trough)	PS104/021-3	73°18.327' S 107°06.550' W	882 (877)	(same as PIT-4a)	9.80 / 9.65	7.36	76.3 %	Brown mud in core 1; grey-olive stratified mudstone in cores 2-5; granite clast on top of upper section in core 3; rare, low diverse nanofossils of Miocene (?) age in mudstone	Loading of 20 m pipe; drilling stopped because drill head released barrel due to malfunction of releaser; granite clast possibly pushed down from core 2 into core 3.

3. ICE Sheet Dynamics of the Amundsen Sea Embayment with MeBo Shallow Drilling

Drill site	Polarstern station no.	Coordinates [lat, lon]	Water depth [m]	Drill target(s)	Drilled depth / deployed cored length [m]	Drilled core [m]	Recovery	Recovered lithology	Remarks
CAT-5 (Cosgrove-Abbott Trough)	PS104/024-2	72°59.713' S 103°50.347' W	520 (536)	Stacked grounding zone wedge (GZW); top of uppermost wedge	2.75 / 2.60	0.18	6.9 %	Olive-brown sandy gravelly mud	Drilling stopped after unwanted unscrewing (glued thread) of bottom-hole assembly part and failure to screw it back on. A damage of the umbilical (cable slipped from A-frame cable block) while MeBo was back on deck led to a time-consuming repair. After the umbilical repair, very strong and strengthening winds forced abandoning of site;
PIB-6 (south-central Pine Island Bay; deep basin in southern Pine Island Trough)	PS104/038-1	74°20.982' S 104°44.450' W	1453 (1430)	Deep basin in Pine Island Bay (paleo-subglacial lake deposits?)	35.65 / 32.25	15.65	48.5 %	Brown, olive and grey muds, sandy muds, sands and diamictons	Loading of 50 m pipe; uppermost 10 m flushed through; drilling stopped because of sediment ingress into drill string causing problems with retrieving lowermost inner core barrel (successfully retrieved); jammed drill string thread during trip out;
BEAR-7a (western Bear Ridge flank)	PS104/040-2	73°17.826' S 112°19.400' W	483 (454)	Older part of dipping strata on western flank of Bear Ridge	5.35 / 5.20	0.94	18.1 %	Brown mud on top, dark olive grey diatom-rich mudstone below	Loading of 50 m pipe; drilling stopped due to blocked inner core barrel caused breaking overshot shear pin (cores and barrels successfully retrieved);

Drill site	Polarstern station no.	Coordinates [lat, lon]	Water depth [m]	Drill target(s)	Drilled depth / deployed cored length [m]	Drilled core [m]	Recovery	Recovered lithology	Remarks
BEAR-7b (western Bear Ridge flank)	PS104/040-3	73°17.832' S 112°19.395' W	483 (454)	Older part of dipping strata on western flank of Bear Ridge (same as BEAR-7a)	17.97 / 17.72	8.82	49.8 %	Olive mudstone in upper part of core, very dark grey gravelly sandy mudstone in lower part of core (transition in core R4); some cores with isolated pebbles on top (washed through?)	Loading of 50 m pipe; drilling stopped because of loss of flush water;
BEAR-8 (western Bear Ridge flank)	PS104/041-1	73°03.188' S 111°58.025' W	415 (424)	Younger part of dipping strata on western flank of Bear Ridge	7.45 / 7.30	0.89	12.2 %	Olive diamicton in upper part, dark grey diamicton below	Loading of 50 m pipe; drilling stopped due to blocked inner core barrel caused breaking overshot shear pin (cores and barrels successfully retrieved);
BEAR-9 (western Bear Ridge flank)	PS104/042-1	73°19.875' S 111°34.827' W	356 (354)	Older part of dipping strata on western flank of Bear Ridge	6.15 / 6.00	2.40	40.0 %	Brown soft diamicton on top, dark olive mudstone in lower part of core, pebbles at base (pebbles probably downhole contamination)	Loading of 50 m pipe; drilling stopped because 3 drill bits worn out during drilling and very slow drilling progress;

3. ICE Sheet Dynamics of the Amundsen Sea Embayment with Mebo Shallow Drilling

Tab. 3.2: Recovery and samples of the MeBo70 drill sites (P: push core; R: rotary core; CC: core catcher)

MeBo site	Station	Recov. [m]	Samples
PIB-1	PS104/006-2	7.78	10 push cores (core P1: 21 cm +8 cm CC; core P2: 10 cm +13 cm CC; core P3: 43 cm +14 cm CC; core P4: 71 cm +13 cm CC; core P5: 59 cm + 3 cm CC; core P6: 9 cm +9 cm CC; core P7: 122 cm +15 cm CC; core P8: 88 cm + 11 cm CC; core P9: 131 cm +17 cm CC; core P10: 108 cm + 13 cm CC)
PIB-2	PS104/009-2	3.91	7 push cores (core P1: 62 cm +13 cm CC; core P2: 36 cm +14 cm CC; core P3: 22 cm +11 cm CC; core P4: 6 cm +6 cm CC; core P5: 105 cm +15 cm CC; core P6: 9 cm +8 cm CC; core P7: 76 cm +8 cm CC)
PIB-2	PS104/009-3	-	-
PIT-3	PS104/020-2	5.89	10 rotary cores (core R1: 92 cm +5 cm CC; core R2: 38 cm; core R3: 32 cm +4 cm CC; core R4: [liner sample in bag] [+CC bag sample]; core R5: [liner sample in bag] [+ CC bag sample]; core R6: 20 cm [+CC bag sample]; core R7: 120 cm +44 cm +5 cm CC; core R8: 14 cm +0 cm CC; core R9: 90 cm; core R10: 125 cm)
PIT-4a	PS104/021-2	3.09	3 rotary cores (core R1: 102 cm +13 cm CC [+CC bag sample]; core R2: 49 cm +12 cm CC [+CC bag sample]; core R3: pebbles [on top; in kautex bottle] +133 cm [incl. CC] [+CC bag sample])
PIT-4b	PS104/021-3	7.36	5 rotary cores (core R1: 35 cm +11 cm CC [+CC bag sample]; core R2: 137 cm +15 cm CC [+CC bag sample]; core R3: 47 cm +17 cm CC; core R4: 121 cm +96 cm +3 cm CC [+CC bag sample]; core R5: 120 cm +125 cm +9 cm CC)
CAT-5	PS104/024-2	0.18	1 rotary core (core R1: 12 cm +6 cm CC)
PIT-6	PS104/038-1	15.65	14 push cores, 2 rotary cores (core P1: 2 cm [in Kautex bottle] +10 cm CC; core P3: [sample in Kautex bottle] +12 cm CC; core P4: 87 cm +10 cm CC; core P6: 120 cm +85 cm +13 cm CC; core P7: 120 cm +53 cm +14 cm CC; core P9: 120 cm +24 cm +9 cm CC [+CC sample in bag]; core P10: 92 cm +14 cm CC [+CC sample in bag]; core P12: 131 cm +11 cm CC; core P13: 120 cm +36 cm +12 cm CC; core P15: 81 cm +13 cm CC; core P16: 80 cm +12 cm CC; core P17: 4 cm; core P19: 70 cm [+13 cm CC sample stored in bag]; core R20: 9 cm [+ 12 cm CC samples stored in bags]; core P21: 114 cm [including CC pushed back into liner]; core R22: 56 cm +6 cm CC [+CC sample in bag])
BEAR-7a	PS104/040-2	0.94	2 rotary cores (core R1: 40 cm +10 cm CC; core R2: 36 cm [+liner sample in bag] +8 cm CC [+CC sample in bag])
BEAR-7b	PS104/040-3	8.82	8 rotary cores (core R1: 37 cm +7 cm CC [+CC sample in bag]; core R2: 120 cm +37 cm +6 cm CC [+ CC sample in bag]; core R3: 107 cm +7 cm CC [+CC sample in bag]; core R4: 118 cm +9 cm CC [+CC sample in bag]; core R5: 121 cm +23cm +8 cm CC [+CC sample in bag]; core R6: 89 cm +6 cm CC [+CC sample in bag]; core R8: 85 cm +9 cm CC; core R9: 93 cm)
BEAR-8	PS104/041-1	0.89	3 rotary cores (core R1: 21 cm +12 cm CC [+CC sample in bag]; core R2: 19 cm +10 cm CC [+2 CC samples in bags]; core R3: 14 cm +13 cm CC [+CC sample in bag])
BEAR-9	PS104/042-1	2.40	6 rotary cores, 1 push core (core R1: 26 cm +9 cm CC [+CC sample in bag]; core R3: 45 cm [+ CC sample in bag]; core R4: [liner sample in bag] +7 cm CC [+CC sample in bag]; core R5: 65 cm +7 cm CC [+CC sample in bag]; core R6: 71 cm +10 cm CC [+CC sample in bag]; core R7: [liner sample comprising 3 pebbles in bag])

Smear slide methods of MeBo drill cores

Smear slides were prepared from all MeBo core catchers and section breaks for lithological and micro-palaeontological analysis. For these preparations, small sediment samples were disaggregated with a toothpick in de-ionized water on 22x50 mm (lithology) or 13 mm round (microfossils) cover slips and mounted on glass slides using Norland Optical Adhesive No. 61 (refractive index = 1.56). Selected samples for microfossil analysis were also sieved at 10 microns using nylon screens; the sieved fractions were transferred to vials and pipetted/dried on 22x50 mm cover slips as strewn mounts. The slides were examined for microfossil content on a Zeiss Axioplan II microscope at 400x and 1,000x, with initial characterization of siliceous microfossil (diatoms, silicoflagellates, radiolarians), calcareous nannofossil, pollen/spore, and juvenile foraminiferal abundance. Photomicrographs of selected microfossils were taken using a ProgRes C5 digital camera and software from Jenoptics. Lithological assessments of smear slides were made on a petrographic microscope at 100x and 200x.

Data management

All data and associated metadata will be stored in the Data Publisher for Earth & Environmental Science PANGAEA (www.pangaea.de).

References

- Favier L, Durand G, Cornford SL, Gudmundsson GH, Gagliardini O, Gillet-Chaulet F, Zwinger T, Payne AJ, Le Brocq AM (2014) Retreat of Pine Island Glacier controlled by marine ice-sheet instability. *Nature Climate Change*, 4, 117-121.
- Fretwell P and 59 co-authors (2013) Bedmap2: improved ice bed, surface and thickness datasets for Antarctica. *The Cryosphere*, 7, 375-393.
- Freudenthal T, Wefer G (2013). Drilling cores on the sea floor with the remote-controlled sea floor drilling rig MeBo. *Geoscientific Instrumentation, Methods and Data Systems*, 2(2), 329-337, doi:10.5194/gi-2-329-2013.
- Gohl K, Uenzelmann-Neben G, Larter RD, Hillenbrand CD, Hochmuth K, Kalberg T, Weigelt E, Davy B., Kuhn G, Nitsche FO (2013) Seismic stratigraphic record of the Amundsen Sea Embayment shelf from pre-glacial to recent times: Evidence for a dynamic West Antarctic ice sheet. *Marine Geology*, 344, 115-131, doi:10.1016/j.margeo.2013.06.011.
- Hillenbrand CD, Kuhn G, Smith JA, Gohl K, Graham AGC, Larter RD, Klages JP, Downey R, Moreton SG, Forwick M, Vaughan DG (2013). Grounding-line retreat of the West Antarctic Ice Sheet from inner Pine Island Bay. *Geology*, 41, 35-38, doi:10.1130/G33469.1.
- Joughin I, Alley RB (2011) Stability of the West Antarctic ice sheet in a warming world. *Nature Geoscience*, 4, 506-513.
- Joughin I, Alley RB, Holland DM (2012) Ice-sheet response to oceanic forcing. *Science*, 338, 1172-1176.
- Nitsche FO, Jacobs SS, Larter RD, Gohl K (2007) Bathymetry of the Amundsen Sea continental shelf: Implications for geology, oceanography, and glaciology. *Geochemistry Geophysics Geosystems*, 8, Q10009, doi:10.1029/2007GC001694.
- Nitsche FO, Gohl K, Larter RD, Hillenbrand CD, Kuhn G, Smith JA, Jacobs S, Anderson JB, Jakobsson M (2013) Paleo ice flow and subglacial meltwater dynamics in Pine Island Bay, West Antarctica. *The Cryosphere*, 7, 249-262.

4. NEAR AND FAR FIELD EFFECTS OF ANTARCTICA'S QUATERNARY ICE SHEET DYNAMICS FROM SEDIMENT CORING

Claus-Dieter Hillenbrand¹, Johann Klages²,
Torsten Bickert³, Thomas Frederichs³,
Norbert Lensch², Marcelo Arevalo², Steve
Bohaty⁴, Werner Ehrmann⁵, Oliver Esper²,
Catalina Gebhardt², Kevin Küssner², Heiko
Pälike³, Thomas Ronge², Jan Schüürman²,
Patric Simões Pereira⁶, James Smith¹, Tina
van de Flierdt⁶
not on board: Gerhard Kuhn², Edith Maier²,
Juliane Müller²

¹BAS
²AWI
³MARUM
⁴U Southampton
⁵U Leipzig
⁶Imperial College London

Grant-No. AWI_PS104_01

Objectives

Antarctica's ice sheet and sea-ice dynamics during the Quaternary glacial-interglacial climate cycles had a large effect on the frontal systems in the Southern Ocean and on related sedimentary records from the seafloor. Observations during the last few decades have shown that glaciers draining the West Antarctic Ice Sheet (WAIS) into the Amundsen Sea Embayment (ASE) have drastically thinned; the flow speed of some of them has dramatically increased, and numerical models indicate that ocean forcing has the potential to drive a future WAIS collapse (e.g. Pollard & DeConto, 2009; Joughin et al., 2014). It is unclear, however, whether the current fast retreat represents an episode of rapid grounding-line recession, which is characteristic for the long-term retreat from the outer and middle ASE shelf since the Last Glacial Maximum (LGM) (e.g. Larter et al., 2014; Smith et al., 2014; Klages et al. 2015), or whether it is triggered by recent climatic or oceanographic changes (Hillenbrand et al., 2013; Smith et al., 2017). Significant sub-ice shelf melting by relatively warm Circumpolar Deep Water (CDW) that spreads across the shelf through deep palaeo-ice stream troughs towards the grounding zone of the WAIS (e.g. Nakayama et al., 2013) has been suggested as a possible cause for the current mass loss (e.g. Joughin et al., 2012). Using conventional sediment coring tools in addition to the MeBo drilling system we recovered sediment core material in order to investigate the post-LGM deposits on the ASE shelf. We will utilize the collected sediment samples to answer our main geoscientific questions addressed by MeBo drilling: Has the WAIS undergone similar fast thinning and retreat during warmer early Holocene climate already? What were the factors driving the post-LGM retreat? Was the retreat of grounded ice from the inner shelf continuous or characterized by phases of fast retreat that alternated with phases of stabilization or even re-advances? What was the impact of ocean forcing compared to atmospheric or sea level forcing? What were the processes at the ice/subglacial substrate interface and how did the ice flow and subglacial hydrological system shape the seafloor as we see it today?

In addition to the collection of up to 10 m long sedimentary sequences a combined seawater and seafloor surface sediment sampling programme was carried out during cruise PS104. The data obtained from these samples will help to calibrate palaeo-proxies to be analysed on the long conventional and MeBo cores that recovered Quaternary sediments.

Work at sea

Work on conventional sediment cores

Conventional coring on expedition PS104 included deployments of gravity, box and multiple corers (Fig. 4.1, Table 4.1) that targeted predominantly five groups of sites: (1) Cores were recovered from MeBo drill sites in order to compensate for drilling disturbance/sediment loss due to flushing in the soft upper part of the sediment column drilled by MeBo (stations PS104/006, 009, 020, 021, 024, 038, 040); (2) cores were collected in front of and from the top of a stacked grounding-zone wedge (GZW) in Cosgrove-Abbot Trough (Klages et al., 2015) as well as from GZW 4 in Pine Island Trough (Larter et al., 2014) in order to reconstruct the post-LGM retreat history of the Cosgrove-Abbot palaeo-ice stream (stations PS104/001, 024 to 031) and the Pine Island-Thwaites palaeo-ice stream (station PS104/022) and to estimate fluxes of subglacial sediment transport under Antarctic ice streams; (3) cores were retrieved from deep sediment basins in Pine Island Bay (stations PS104/003, 006, 009, 017, 034, 036, 038) to test the hypothesis that subglacial lakes existed there during the last glacial period (Nitsche et al., 2013; Witus et al., 2014); (4) cores were recovered from subglacial bedforms visible in the multibeam bathymetry maps from Pine Island Bay, the western flank of Bear Ridge and the western branch of Pine Island Trough (stations PS104/008, 014, 043, 045) in order to investigate the sediment composition of these features; and (5) cores were collected from sediment pockets carved into bedrock at relatively shallow water depths (i.e. ≤ 650 m) in Pine Island Bay (stations PS104/012, 013, 035, 036) in order to obtain sediments bearing abundant calcareous microfossils and thus material suitable for reliable AMS ^{14}C dating (e.g. Hillenbrand et al., 2013) and proxy applications that will help to reconstruct Holocene grounding-line retreat and decipher forcing mechanisms driving ice-stream retreat and thinning during the last few millennia and centuries.

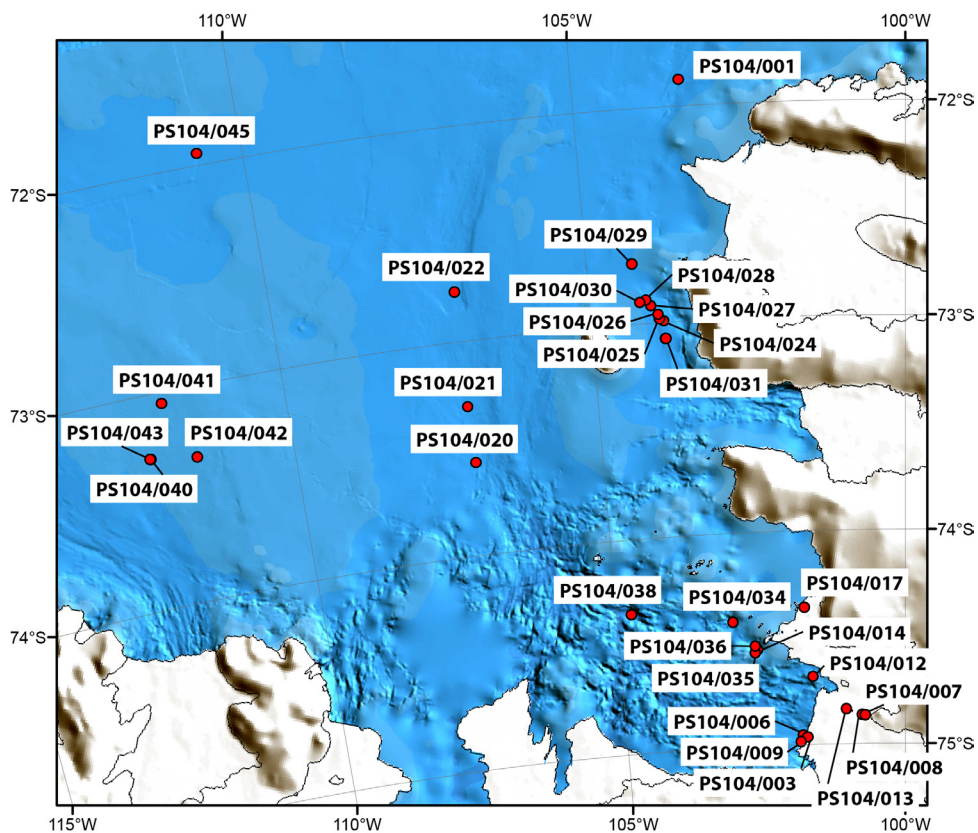


Fig. 4.1: Map of the study area with coring and CTD stations (for details see Table 4.1). Only the ID of one device is shown at stations where more than one geological device was deployed.

Deployed coring gear and sample distribution

In order to recover undisturbed surface sediments during cruise PS104 a giant box corer (GBC) (50 x 50 x 60 cm) was used at eight sites, a multiple corer (MUC) with 12 tubes of 6.7 cm diameter was recovered from five sites, and a MUC with ten tubes of 10 cm diameter and equipped with a TV camera was deployed at two sites (Table 4.1). While three GBC deployments (PS104/007-2, 008-1, 012-1) and one MUC (\varnothing 6.7 cm) deployment (PS104/013-1) in inner Pine Island Bay were unsuccessful because the presence of very soft fine-grained muds at the seafloor led to overpenetration of the GBC and MUC, respectively, all other GBC and MUC deployments were successful. The TV MUC (\varnothing 10 cm) retrieved four and nine tubes of sediment from sites PS104/001-1 and 003-3, respectively, while twelve sediment-filled tubes were collected at all MUC (\varnothing 6.7 cm) stations except from site PS104/013-1. Depending on the availability of recovered MUC tubes and the undisturbed surface area in a GBC, respectively, the samples were taken for the investigation of bulk sedimentology (either surface sediment samples or subcores cut into 1-cm slices, filled into pre-weighed whirlpak bags and stored at +4°C or whole subcores stored at +4°C), grain size and clay mineralogy (either surface sediment samples or subcores cut into 1-cm slices, filled into whirlpak bags and stored at +4°C or whole subcores stored at +4°C), benthic foraminiferal assemblages (either surface sediment samples or subcores cut into 1-cm slices with samples from the upper 10 cm mixed with a bengal rose-ethanol solution and stored in kautex bottles/whirlpak bags at +4°C or whole frozen subcores stored at -20°C), siliceous microfossils (either surface sediment samples or subcores cut into 1-cm slices, filled into whirlpak bags and stored at +4°C or whole frozen subcores stored at -20°C), opal isotopes (either subcores cut into 1-cm slices, filled into whirlpak bags and stored at +4°C or whole frozen subcores stored at -20°C), trace metals on calcareous foraminifera (either subcores cut into 1-cm slices, filled into whirlpak bags and stored at -20°C or whole frozen subcores stored at -20°C) and biomarkers (either subcores cut into 1-cm half slices, filled into petri dishes, wrapped in aluminum foil and stored at -20°C or whole frozen subcores wrapped in aluminum foil and stored at -20°C), and samples for archiving (either surface sediment samples or subcores cut into 1-cm slices and stored at +4°C or stored as whole subcores at +4°C and -20°C, respectively). Nitrile gloves were worn during the handling of samples for biomarker analysis.

A total of 30 gravity corers (GC) with a total core barrel length of 209 metres was deployed to recover long sedimentary sequences. The deployment of the gear types and the length of the coring devices were chosen based on (sub-)seafloor information derived from sediment acoustic profiles provided by the PARASOUND echosounding system. The GC was deployed with barrel configurations of 3, 5, 8, 10, 13 and 15 m length. With the exception of two unsuccessful GC deployments with negligible recovery (sites PS104/012-3, 040-1), where the GC apparently fell over due to the outcropping of consolidated sedimentary rocks or crystalline basement rocks at the seabed, all deployments were successful. Total conventional core recovery on expedition PS104 was 118.16 metres.

Analysis, splitting, documentation and, sampling of gravity cores

All GC cores were cut on board RV *Polarstern* into ≤ 1 m-long sections, and smear slide samples for lithological and micropalaeontological analyses were taken routinely from the tops of the GC sections and the core catchers (for smear slide methods see chapter 3). Physical properties of the recovered sediments were measured on the whole core sections of all collected GC cores and some of the GBC subcores with three differently equipped GEOTEK multi-sensor core loggers (MSCL) provided by AWI and the Faculty 5 Geosciences of the University of Bremen (GeoB). The AWI MSCL device (MSCL#25) was used for continuous whole core measurements of gamma-ray attenuation, P-wave velocity, magnetic susceptibility (Bartington Instruments loop sensor) and electrical resistivity at 1 cm resolution. In addition, the AWI MSCL

measured the core diameter and core temperature for the calculation of these values. The parameters listed in the logger settings of the MSCL software (version 6.2) and given in Table 4.2 were used for calibration. The second AWI MSCL (MSCL#50) was used for measurements of magnetic susceptibility on split core sections using a spot sensor (Bartington Instruments F-probe) in order to receive logs of magnetic susceptibility with higher spatial resolution. The GeoB MSCL was exclusively used for digital line scanning of split core sections (Imaging software version 2.4) providing bitmap images of the sediment surface at a resolution of 10 pixel per mm core depth, from which values of the colours red, green and blue were calculated. All physical property data were graphically corrected, and faulty values, e.g. at section breaks, were deleted. GC sections and GBC subcores that were not opened on board were stored in a refrigerated container at a temperature of +4° C and transported to Bremerhaven.

Six GCs recovered during cruise PS104 (PS104/006-1, 009-1, 020-1, 021-1, 024-1 and 038-3) with a total length of 24.32 metres were opened and sub-sampled at sea during the expedition. After the sediment core sections were split with a vibration saw, the working and archive halves were photographed. A description of the lithology and sedimentary structures of the cores was carried out on the archive halves. Microscope analysis of smear slides was also used to classify the main lithologies in the cores. Sediment colours were determined visually using a "Munsell Soil Color Chart", and visual colour reflectance from 400 to 700 nm (10 nm channels) and derived L*, a*, b* values were measured with a hand held Minolta CM2002 spectrophotometer. In addition, magnetic susceptibility was measured with an F-sensor at 1-cm intervals on the surfaces of the archive halves of the split cores with the AWI MSCL#50, while the GeoB MSCL was used for scanning an image with a line scan camera (RGB values).

Sampling procedures on the working halves of the split cores followed standard methods at AWI. Sampling types and intervals (usually 5, 10, or 15 cm) were varied according to the identified lithologies of the recovered sediments. The general sampling plan included sampling of a 25x10x1 cm sediment slab for X-raying. Thereafter, the shear strength of the sediments was analysed with a hand held shear vane. Samples (10 cm³ in volume each) for the determination of bulk parameters (water content, density, CaCO₃, total organic carbon and opal content) and grain-size distribution (including clay mineral analysis) were taken with syringes and stored in whirlpak bags, which had been pre-weighed for bulk samples. 1-cm thick sediment slices (ca. 40 cm³ volume) for investigations on the coarse grained (>63 µm) fraction were sampled with a spatula and stored in whirlpak bags. At GC sites in Pine Island Bay, where subglacial lakes may have existed during the last glacial period, porewater samples using rhizomes were taken on the working halves (cores PS104/006-1, 009-1, 038-3) and the whole cores (cores PS104/034-10, 036-2), respectively. Further laboratory analyses on all cores (such as XRF scanning of archive halves, preparation and investigation of X-radiographs) and on discrete samples taken from the cores will be carried out at AWI and BAS.

Work on seawater samples

To gain insight into the hydrographic structure of the water column in the ASE, in situ measurements of hydrographic variables (temperature, salinity, oxygen concentration and particle density) were conducted with a Conductivity Temperature Depth (CTD) probe at 5 stations along a transect from south (75°S) to north (71°S) (Fig. 4.1, Tables 4.1, 4.3). Most stations were complemented by seafloor surface sediment coring (i.e., MUC or GBC deployments) in order to allow for calibration of sedimentary parameters and hydroacoustic instruments (i.e. to calculate sound velocity profiles). A few sites were deliberately selected close to hydrographic profiles recorded on RV *Polarstern* expedition PS75 (ANT-XXVI/3) in 2010 (Gohl, 2010; Nakayama et al., 2013), allowing the investigation of inter-annual variability of water column properties. Temperature, salinity, etc. measurements from the CTD probe were accompanied by simultaneous seawater sampling with a water collector (rosette) to measure

concentrations of dissolved nutrients, stable isotopes ($\delta^{18}\text{O}$, $\delta^{13}\text{C}$, $\delta^{30}\text{Si}$), and biomarkers (for palaeo-seawater temperatures and sea-ice cover). Seawater collected from the rosette bottles was filtered for opal isotope measurements ($\delta^{30}\text{Si}$), and to determine the particle density and particle composition (plankton census, biomarkers, melt-water outflow) of the filter residue at several water depths. The goal of the latter is to derive information on the autecology of planktic microorganisms, such as diatoms, radiolarians and foraminifera, in conjunction with hydrographic data from the CTD probe as well as the nutrient distribution profiles. As the hard parts of these microorganisms are preserved in the sediment record, the data collected from the water column provide important information for addressing palaeoceanographic questions.

CTD water column profiling

The hydrographic profiling used a Seabird 911+ CTD (SN 937) connected to a carousel with 24 12-litre water samplers (SBE 32). The CTD contained two sensor pairs of conductivity (SBE 4, SN 2618, 2325) and temperature (SBE 3, SN 2678, 5027), a high precision pressure sensor Digiquartz TC (SN 937), an oxygen sensor (SBE 43, SN 0743), a fluorometer (WetLabs ECO-AFL/FL, SN 1853), an transmissometer (WetLabs CStar, 25 cm, SN 1220) and a Benthos altimeter Model PSA 900D (SN 51533).

Conductivity and temperature sensor calibrations were performed before the cruise at Seabird Electronics. The accuracy of the temperature sensors is 2 mK and readings for the pressure sensors are better than 2 dbar. The conductivity was corrected with salinity measurements from 16 discrete water samples using IAPSO Standard Seawater from the batch P158 ($K_{15} = 0.9997$) and an Optimare Precision Salinometer. Salinity was measured to an accuracy of 0.007 PSU.

Rosette water sampling

Each rosette cast collected 24 x 12-litre bottles of seawater at depths decided upon after the downward cast to best capture the hydrographic structure of the water column (Table 4.3). Samples were collected and processed immediately after the rosette was on board. The sampled water was assigned to specific analytical programmes, covering stable isotope measurements and determination of nutrient and biomarker concentrations (Table 4.4).

- For the calibration of the CTD salinity sensor, two samples from two representative water masses were taken in 250 ml glass bottles at 4 stations, and measured on board according to the above given procedure.
- To measure the stable isotopes $\delta^{13}\text{C}$ and $\delta^{18}\text{O}$, 12 x 50 ml and 100 ml subsamples were taken at 12 depths at each station, stored in seawater-cleaned glass bottles, sealed with wax and kept at +4°C. In addition, the $\delta^{13}\text{C}$ samples were treated with saturated HgCl_2 solution.
- For nutrient concentrations (nitrate, phosphate, silicate), 12 x 50 ml samples of water were collected in sea water-cleaned plastic bottles and frozen at -20°C.
- For opal isotope ($\delta^{30}\text{Si}$) measurements, approximately 12 x ~10 litres of seawater were filtered over polycarbonate filters. The filtered water was distributed into 2-litre plastic bottles, pre-cleaned with HCl, and stored at +4°C. The filter residuals were frozen and stored at -20°C.
- For the determination of biomarker concentrations, three to five ~10 litre samples of seawater were filtered over glass-fibre filters, which were subsequently frozen and stored at -20°C.

At site PS104/007-1 a special water sampling programme was conducted to capture potential meltwater outflow from below the Pine Island Glacier ice shelf. At this station, opal isotope samples were substituted by collection of samples for dissolved Nd isotopes. Neodymium isotopes and concentrations have been successfully applied as a water mass tracer in the region, and will help to determine a potential chemical signature of meltwater plumes in the area. For this purpose, ~10 litres of seawater was filtered over polycarbonate filters. The filter residues were frozen and stored at -20°C in order to allow for analysis of the terrigenous material composition and grain size of suspended sediment.

Preliminary results

Sediment cores

The sediments collected in the vicinity of the ice shelf front of Pine Island Glacier contain up to several decimetres of a very soft, fine-grained mud near the core surface that probably results from the deposition of the suspended load of meltwater plumes emanating from the base of the ice shelf. Glacimarine sediments cored in sediment pockets on bedrock highs contain, at least in some intervals, calcareous foraminifera. The sediment cores from deep inner basins in Pine Island Bay retrieved predominantly glacimarine terrigenous muds, sandy muds and thin sand beds likely of Holocene age. At least one core (PS104/038-3) shows indication of reworking of sediments by gravitational down-slope processes from bedrock highs surrounding the basins, which is evident from normally graded sand beds (probably deposited as turbidites) and a slump fold. The sedimentary sequences recovered from the GZWs in Pine Island Trough and Cosgrove-Abbot Trough consist of glacimarine muds overlying soft to stiff diamictons that are assumed to have formed subglacially during the post-LGM retreat of the respective palaeo-ice streams. A similar stratigraphic succession was observed in core PS104/014-1 retrieved from a set of moraines or debris flow deposits in eastern Pine Island Bay, core PS104/045-1 collected from lineated seafloor in the area of the western branch of Pine Island Trough and core PS104/043-1 that was retrieved from mega-scale lineations on the western flank of Bear Ridge.

At all conventional coring sites of expedition PS104 significant amounts of diatoms were only found in sediments from near the core tops. Diamictons at the bases of GCs that were collected from MeBo drill sites targeting dipping sedimentary strata cropping out near the seafloor often contain a mix of modern and ancient microfossils, with the latter likely being reworked subglacially from the underlying Late Mesozoic-Early Cainozoic substratum (e.g. core PS104/021-1). A similar mixing of young and old sediments was observed at the base of core PS104/020-1 recovered at MeBo station PIT-3 in southern Pine Island Trough, where muddy sediments are intruded by lenses of a grey, quartz-rich sand that probably represent rip-up clasts reworked by grounded ice from an underlying sandstone drilled by MeBo at the same location.

The physical properties of GC PS104/020-1 are shown in Fig. 4.2 as an example for the results from measurements of P-wave velocity, gamma density, magnetic susceptibility, electrical resistivity and digital imaging. The data reflect lithological down-core changes from a moderately bioturbated diatomaceous mud near the core top to a slightly laminated mud in the upper part of the core, then to a moderately to strongly laminated and stratified mud in its middle part and to the mixture of mud and sandy rip-up clasts at its base. However, some of the variations seen in the physical properties data are artifacts, which result from a thickening of core sections by the end-caps. This may also partly originate from core voids at the section breaks. Incomplete sound velocity data are probably due to insufficient transmission of the sound signal, in particular in the mixture of sandy lenses and mud at the core base.

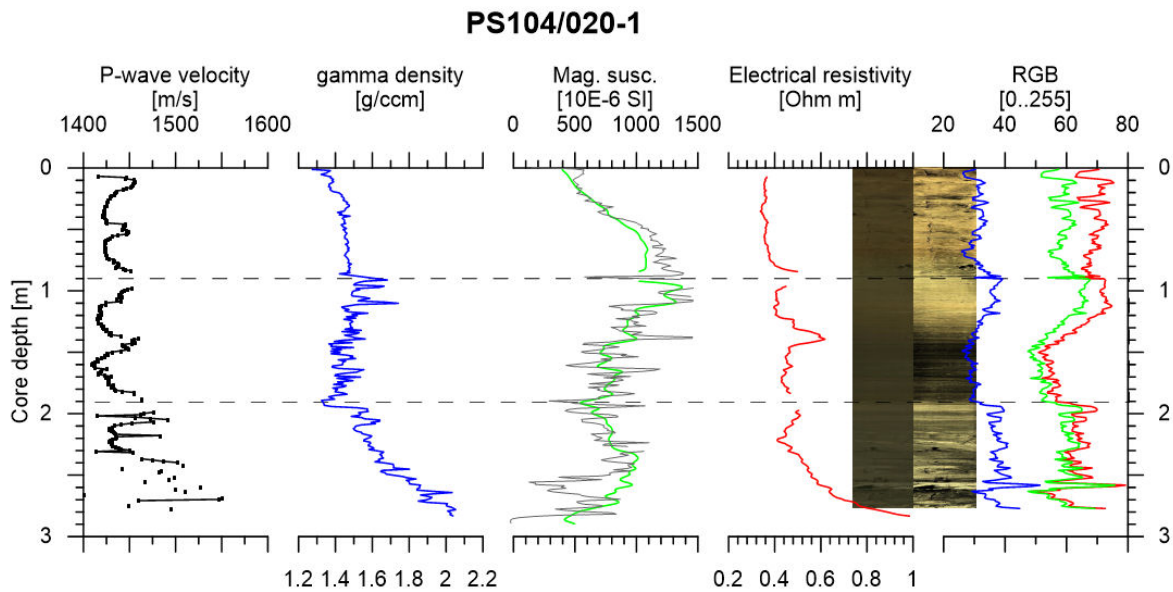


Fig. 4.2: Down-core changes in P-wave velocity, gamma density, magnetic susceptibility (measured with loop (green) and spot (grey) sensor), electrical resistivity and colour reflectance data of gravity core PS104/020-1. Dashed lines indicate section breaks. Colour images of the core show the realistic reflectance of the sediment surface on the left and a display of the data with enhanced brightness and contrast on the right.

CTD casts

The profiles in the eastern ASE show a distinctively warm water mass at water depths greater than 400 m, characterised by potential temperatures around +1.0°C (Fig. 4.3a). This water mass can be identified as Circumpolar Deep Water (CDW) and propagates from the outer shelf all the way along the shelf and into the Pine Island Glacier ice shelf cavity. It is the densest water mass on the ASE shelf due to its high salinity content of more than 34.70 psu (Fig. 4.3b). Compared to previous measurements during expedition PS75 (ANT-XXVI/3) in 2010 (Nakayama et al. 2013) this warm water is slightly cooler than observed seven years ago (ca. 1.3°C). The CDW is overlain by a mixture of meltwater and CDW, which forms the Winter Water (WW), characterized by a potential temperature minimum at 50-350 m water depth. The WW is covered by a well-oxygenated mixed layer from the sea surface down to the thermocline at ~50 m water depth. At site PS104/007-1 in the innermost Pine Island Bay, a meltwater plume is visible between 80 and 180 m water depth. Meltwater originating directly from the ice shelf front is identified by a discrete layer of intermediate temperatures of ca. -1.0°C (Fig. 4.3a) and low dissolved oxygen contents of ca. 5.5 ml/l (Fig. 4.3c).

Data management

Information regarding the shipboard data from the sediment cores (lithological descriptions, sample types and volumes) and CTD casts as well as the results of the various post-cruise analyses on the sediment and seawater samples will be made available in the PANGAEA database at AWI (<http://www.pangaea.de>).

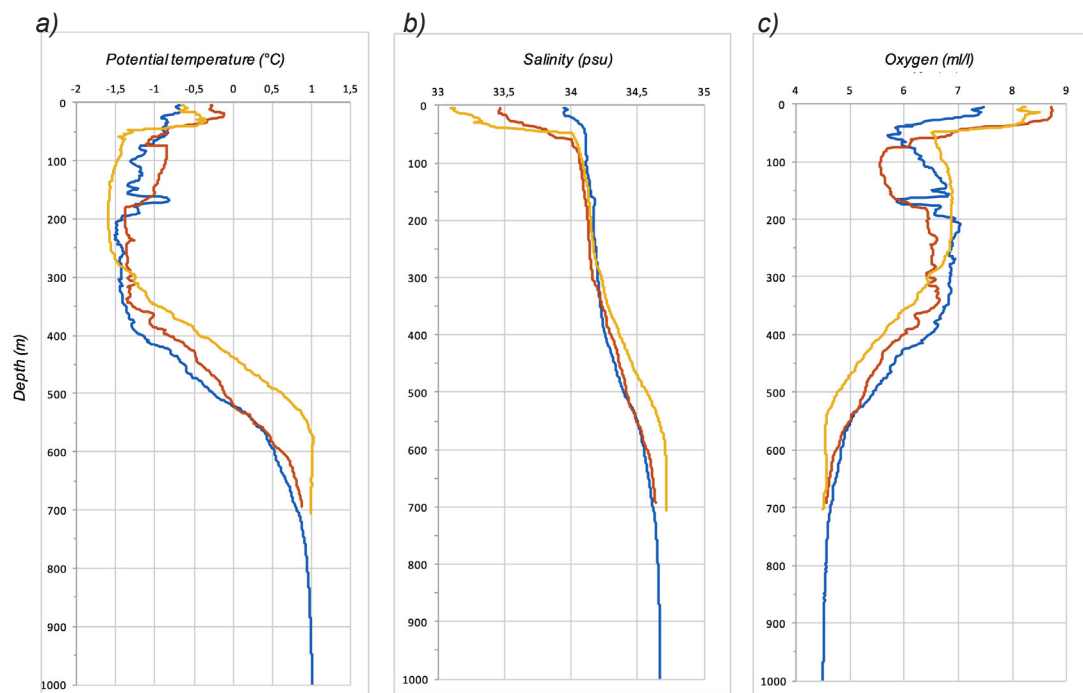


Fig. 4.3: Profiles of potential temperature (left), salinity (middle), and dissolved oxygen content (right) for CTD casts PS104/003-1 (blue), 007-1 (red), and 022-1 (yellow) in the eastern Amundsen Sea Embayment.

References

- Gohl K (Ed.) (2010) The expedition of the research vessel Polarstern to the Amundsen Sea, Antarctica, in 2010 (ANT-XXVI/3) Reports on Polar and Marine Research, 617, 173 pp.
- Hillenbrand C-D, Kuhn G, Smith JA, Gohl K, Graham AGC, Larter RD, Klages JP, Downey R, Moreton SG, Forwick M, Vaughan DG (2013) Grounding-line retreat of the West Antarctic Ice Sheet from inner Pine Island Bay. *Geology*, 41, 35-38.
- Joughin I, Alley RB, Holland DM (2012) Ice-sheet response to oceanic forcing. *Science*, 338, 1172-1176.
- Joughin I, Smith B, Medley B (2014) Marine ice sheet collapse potentially under way for the Thwaites Glacier basin, West Antarctica. *Science*, 344, 735-738.
- Klages JP, Kuhn G, Graham AGC, Hillenbrand C-D, Smith JA, Nitsche FO, Larter RD, Gohl K (2015) Palaeo-ice stream pathways and retreat style in the easternmost Amundsen Sea Embayment, West Antarctica, revealed by combined multibeam bathymetric and seismic data. *Geomorphology*, 245, 207-222.
- Larter RD, Anderson JB, Graham AGC, Gohl K, Hillenbrand C-D, Jakobsson M, Johnson JS, Kuhn G, Nitsche FO, Smith JA, Witus AE, Bentley MJ, Dowdeswell JA, Ehrmann W, Klages JP, Lindow J, Ó Cofaigh C, Spiegel C (2014) Reconstruction of changes in the Amundsen Sea and Bellingshausen Sea sector of the West Antarctic Ice Sheet since the Last Glacial Maximum. *Quaternary Science Reviews*, 100, 55-86.
- Nakayama, Y, Schröder, M, Hellmer, HH (2013) From Circumpolar Deep Water to the glacial meltwater plume on the eastern Amundsen Shelf. *Deep-Sea Research I*, 77, 50-62.

4. Near and Far Field Effects of Antarctica's Quaternary Ice Sheet Dynamics from Sediment Coring

- Nitsche FO, Gohl K, Larter RD, Hillenbrand C-D, Kuhn G, Smith JA, Jacobs S, Anderson JB, Jakobsson M (2013) Paleo-ice flow and subglacial meltwater dynamics in Pine Island Bay, West Antarctica. *The Cryosphere*, 7, 249-262.
- Pollard D, DeConto RM (2009) Modelling West Antarctic ice sheet growth and collapse through the past five million years. *Nature*, 458, 329-333.
- Smith JA, Hillenbrand C-D, Kuhn G, Klages JP, Graham AGC, Larter RD, Ehrmann W, Moreton SG, Wiers S, Frederichs T (2014) New constraints on the timing of West Antarctic Ice Sheet retreat in the eastern Amundsen Sea since the Last Glacial Maximum. *Global and Planetary Change*, 122, 224-237.
- Smith JA, Andersen TJ, Shortt M, Gaffney AM, Truffer M, Stanton TP, Bindschadler R, Dutrieux P, Jenkins A, Hillenbrand C-D, Ehrmann W, Corr HFJ, Farley N, Crowhurst S, Vaughan DG (2017) Sub-ice-shelf sediments record history of 20th Century retreat of Pine Island Glacier. *Nature*, 541, 77-80.
- Witus AE, Branecky CM, Anderson JB, Szczuciński W, Schroeder DM, Blankenship DD, Jakobsson, M (2014) Meltwater intensive glacial retreat in polar environments and investigation of associated sediments: example from Pine Island Bay, West Antarctica. *Quaternary Science Reviews*, 85, 99-118.

Table 4.1: Conventional coring and seawater sampling stations on cruise PS104. CTD: Conductivity-temperature-depth cast with rosette, GBC: giant box corer, GC: gravity corer, MUC: multiple corer (ø 6.7 cm), TV MUC: multiple corer (ø 10 cm) with TV camera.

Station	Gear	Area	Latitude	Longitude	Water depth [m]	Penetration depth/ deploy [m]	Core recovery [m]	Sediment description
PS104/001-1	TV MUC	Cosgrove-Abbot Trough	71° 52.744' S	103° 22.956' W	745	0.1/0.6	0.08	Brown sandy mud
PS104/001-2	GC	Cosgrove-Abbot Trough	71° 52.736' S	103° 23.007' W	745	6.5/8	3.76	Brown sandy mud on top, gravelly sand at base
PS104/003-1	CTD	Inner Pine Island Bay sedimentary basin	74° 57.475' S	101° 49.751' W	1041	n/a	n/a	n/a
PS104/003-2	GC	Inner Pine Island Bay sedimentary basin	74° 57.465' S	101° 49.713' W	1041	6/8	5.23	Brown sandy mud
PS104/003-3	TV MUC	Inner Pine Island Bay sedimentary basin	74° 57.484' S	101° 49.533' W	1041	0.6/0.5	0.56	Brown sandy mud; a few benthic and planktic foraminifera
PS104/006-1	GC	PIB-1: Inner Pine Island Bay sedimentary basin	74° 57.956' S	101° 44.914' W	1051	8/8	5.72	Brown sandy mud near top, greenish grey mud below
PS104/007-1	CTD	South Eastern Pine Island Ice Shelf front	74° 51.965' S	100° 45.607' W	698	n/a	n/a	n/a
PS104/007-2	GBC	South Eastern Pine Island Ice Shelf front	74° 51.984' S	100° 45.657' W	698	0.8/0.6	n/a	Very soft brown-olive mud
PS104/008-1	GBC	South Eastern Pine Island Ice Shelf front	74° 52.032' S	100° 42.658' W	698	0.8/0.6	n/a	Very soft brown-olive mud
PS104/008-2	GC	South Eastern Pine Island Ice Shelf front	74° 52.107' S	100° 42.689' W	698	11/10	7.59	Brown-olive mud
PS104/009-1	GC	PIB-2: Inner Pine Island Bay sedimentary basin	74° 59.213' S	101° 52.136' W	989	8.5/10	5.37	Brownish mud near top; greyish diamicton near base
PS104/012-1	GBC	Eastern Pine Island Bay	74° 41.030' S	101° 37.471' W	358	0.8/0.6	n/a	Very soft brown mud
PS104/012-2	GC	Eastern Pine Island Bay	74° 41.019' S	101° 37.321' W	358	5/10	3.31	Very soft brown mud on top, sandy mud at base

4. Near and Far Field Effects of Antarctica's Quaternary Ice Sheet Dynamics from Sediment Coring

Station	Gear	Area	Latitude	Longitude	Water depth [m]	Penetration depth/ deploy[m]	Core recovery [m]	Sediment description
PS104/012-3	GC	Eastern Pine Island Bay	74° 41.027' S	101° 37.494' W	358	0.5/5	n/a	Brown gravelly sand
PS104/012-4	MUC	Eastern Pine Island Bay	74° 41.013' S	101° 37.427' W	358	0.4/0.6	0.42	Very soft brown mud
PS104/013-1	MUC	Eastern Pine Island Bay	74° 50.281' S	101° 02.628' W	545	0.7/0.6	n/a	Very soft brown mud
PS104/013-2	GC	Eastern Pine Island Bay	74° 50.285' S	101° 02.622' W	545	8/10	6.25	Very soft brown mud
PS104/014-1	GC	Eastern Pine Island Bay	74° 32.939' S	102° 35.159' W	600	6/5	4.84	Brown mud on top, greyish foraminifera-bearing muddy gravelly sand at base
PS104/014-2	MUC	Eastern Pine Island Bay	74° 32.940' S	102° 35.141' W	600	0.4/0.6	0.40	Very soft brown mud
PS104/014-3	GC	Eastern Pine Island Bay	74° 32.937' S	102° 35.207' W	600	10/10	8.24	Brown mud on top, grey diamicton at base
PS104/017-1	CTD	Pine Island Bay sedimentary basin	74° 21.565' S	104° 44.841' W	1395	n/a	n/a	n/a
PS104/017-2	MUC	Pine Island Bay sedimentary basin	74° 21.559' S	104° 44.836' W	1395	0.3/0.6	0.25	Soft brown mud on top, more consolidated grey mud at base
PS104/020-1	GC	PIT-3: Southern Pine Island Trough	73° 34.088' S	107° 05.567' W	946	3/3	2.88	Brown mud on top, muddy grey sand (Qtz sand) at base
PS104/020-3	GC	PIT-3: Southern Pine Island Trough	73° 34.091' S	107° 05.620' W	947	3.5/5	3.30	Brown mud on top and base
PS104/021-1	GC	PIT-4a: Pine Island Trough	73° 18.290' S	107° 06.570' W	882	3.5/5	1.09	Brown mud on top, dark grey stiff diamicton (with till pellets and rare Early Cainozoic nanofossils) in core catcher
PS104/022-1	CTD	Pine Island Trough	72° 46.057' S	107° 05.576' W	733	n/a	n/a	n/a
PS104/022-2	GC	Pine Island Trough	72° 46.068' S	107° 05.545' W	733	3.5/5	1.76	Brown mud on top, dark grey diamicton in core catcher
PS104/022-3	GBC	Pine Island Trough	72° 46.076' S	107° 05.519' W	733	0.6/0.5	0.48	Brown mud
PS104/024-1	GC	CAT-5: GZW in Cosgrove-Abbot Trough	72° 59.708' S	103° 50.320' W	520	2/5	1.48	Brown mud on top, grey diamicton at base

Station	Gear	Area	Latitude	Longitude	Water depth [m]	Penetration depth/ deploy[m]	Core recovery [m]	Sediment description
PS104/025-1	GC	GZW in Cosgrove-Abbot Trough	72° 59.001' S	103° 54.438' W	530	2/5	1.48	Brown mud on top, greyish-olive soft diamicton at base; rock in core catcher
PS104/026-1	GC	GZW in Cosgrove-Abbot Trough	72° 57.377' S	103° 55.211' W	534	3/5	1.37	Brown mud on top, greyish-olive soft diamicton at base
PS104/027-1	GC	GZW in Cosgrove-Abbot Trough	72° 55.255' S	104° 01.802' W	515	2.5/5	2.12	Brown mud on top, greyish-olive soft diamicton at base
PS104/028-1	GC	GZW in Cosgrove-Abbot Trough	72° 53.498' S	104° 05.960' W	518	4/5	3.08	Brown mud on top, greyish-olive soft diamicton at base
PS104/029-1	GC	GZW in Cosgrove-Abbot Trough	72° 43.171' S	104° 17.059' W	535	2/5	1.88	Brown mud on top, greyish-olive soft diamicton at base
PS104/030-1	GC	GZW in Cosgrove-Abbot Trough	72° 54.134' S	104° 11.896' W	488	1/5	0.85	Brown mud on top, greyish-olive soft diamicton at base
PS104/031-1	GC	GZW in Cosgrove-Abbot Trough	73° 04.601' S	103° 49.750' W	577	3/5	1.61	Brown mud on top, greyish-olive soft diamicton at base
PS104/031-2	GBC	GZW in Cosgrove-Abbot Trough	73° 04.575' S	103° 49.618' W	577	0.6/0.6	0.43	Brown mud on top, pebbles & cobbles at base
PS104/034-1	GC	Basin in NE Pine Island Bay	74° 24.964' S	102° 59.473' W	769	10/15	6.82	Brown mud on top, olive-grey mud at base
PS104/034-10	GC	Basin in NE Pine Island Bay	74° 24.953' S	102° 59.471' W	769	14/13	8.93	Brown mud on top, olive-grey mud at base
PS104/035-1	GC	Shallow bedrock basin in NE Pine Island Bay	74° 33.834' S	102° 37.404' W	336	11/10	6.50	Brown mud on top and at base
PS104/035-2	GBC	Shallow bedrock basin in NE Pine Island Bay	74° 33.814' S	102° 37.402' W	336	0.5/0.6	0.49	Brown mud on top and at base
PS104/036-1	GBC	Bedrock basin in NE Pine Island Bay	74° 32.009' S	102° 37.120' W	618	0.5/0.6	0.46	Brown mud on top and at base
PS104/036-2	GC	Bedrock basin in NE Pine Island Bay	74° 31.984' S	102° 37.231' W	618	11/10	7.40	Brown mud on top and at base

4. Near and Far Field Effects of Antarctica's Quaternary Ice Sheet Dynamics from Sediment Coring

Station	Gear	Area	Latitude	Longitude	Water depth [m]	Penetration depth/ deploy[m]	Core recovery [m]	Sediment description
PS104/038-3	GC	PIT-6: Deep basin in Pine Island Bay	74° 20.955' S	104° 44.297' W	1453	11/10	7.78	Brown mud on top, olive sandy mud at base
PS104/040-1	GC	BEAR-7a: Western flank of Bear Ridge	73° 17.909' S	112° 19.366' W	482	0/3	n/a	Brown gravelly mud
PS104/043-1	GC	Western flank of Bear Ridge	73° 17.827' S	112° 19.892' W	481	3/3	2.78	Brown mud on top, dark olive grey soft diamicton at base
PS104/043-2	CTD	Western flank of Bear Ridge	73° 17.822' S	112° 19.708' W	482	n/a	n/a	n/a
PS104/043-3	GBC	Western flank of Bear Ridge	73° 17.830' S	112° 19.753' W	482	0.5/0.6	0.40	Brown mud on top; grey gravelly mud at base
PS104/045-1	GC	Western Pine Island Trough	71° 56.830' S	110° 40.581' W	559	1/3	0.77	Brown mud on top, brown stiff diamicton at base

Tab. 4.2: Sensors and parameter settings for measurements with the GEOTEK multi-sensor core logger during PS104

<p>P-wave velocity and core diameter plate-transducers diameter: 4 cm transmitter pulse frequency: 500 kHz gate: 2800 delay: 100 μs temperature = 20 °C, salinity = 35 psu, not corrected for water depth and <i>in-situ</i> temperature; calibrated with water core of known temperature and theoretical sound velocity</p>
<p>Temperature infrared thermometer type Micron M50-1C-06-L, calibrated by water of different known temperatures</p>
<p>Density gamma ray source: Cs-137; activity: 343 MBq; energy: 0.662 MeV aperture diameter: 5.0 mm (GC and GBC archive cores) gamma ray detector: Gammasearch2, Model SD302D, Ser. Nr. 3019, John Caunt Scientific Ltd.; count time 10 s</p>
<p>Fractional porosity mineral grain density = 2.7, water density = 1.026</p>
<p>Magnetic susceptibility coil sensor: BARTINGTON MS2C, S/N 208 nominal inner diameter: 14 cm true coil diameter: 14.8 cm alternating field frequency: 565 Hz, count time 10 s, precision $0.1 \cdot 10^{-5}$ (SI) magnetic field strength: ca. 80 A/m RMS Krel: (after MSCL manual from 2006, Figure 66): 1.84 (GC and GBC, 12 cm core-\emptyset) coil sensor correction factor: 7.18 for 10^{-6} (SI) spot sensor: BARTINGTON MS2F, S/N 507, spot sensor calibration factor 30 for 10^{-6} (SI)</p>
<p>Core thickness measurement Penny + Giles, Type HLP 190/3 calibrated with distance pieces</p>
<p>Electrical resistivity measurements GEOTEK inductive non-contact resistivity sensor (NCR), averaging over about 12 cm core length, calibrated with salt water solutions, porosity calculations after MSCL manual</p>
<p>Digital imaging on GeoB device GEOTEK line scan camera</p>

4. Near and Far Field Effects of Antarctica's Quaternary Ice Sheet Dynamics from Sediment Coring

Tab. 4.3: CTD/Rosette water sampling depths during PS104. *at station PS104/022-1 three bottles were taken each at 30 m and 10 m depth

Bottle	PS104/003-1	PS104/007-1	PS104/017-1	PS104/022-1	PS104/043-2
Latitude	74°57.475' S	74°51.965' S	74°21.565' S	72°46.057' S	73°17.822' S
Longitude	101°49.751' W	100°45.607' W	104°44.841' W	107°05.576' W	112°19.708' W
1, 2	998 m	685 m	1375 m	697 m	454 m
3, 4	900 m	450 m	1000 m	500 m	400 m
5, 6	500 m	320 m	500 m	300 m	300 m
7, 8	300 m	280 m	300 m	200 m	200 m
9, 10	180 m	240 m	200 m	150 m	150 m
11, 12	150 m	200 m	150 m	120 m	120 m
13, 14	120 m	120 m	120 m	90 m	90 m
15, 16	90 m	70 m	90 m	70 m	70 m
17, 18	70 m	50 m	70 m	50 m	50 m
19, 20	50 m	30 m	50 m	30 m*	30 m
21, 22	30 m	20 m	30 m	30 m, 10 m*	10 m
23, 24	10 m	10 m	10 m	10 m*	10 m

Tab. 4.4: CTD/Rosette water sample distribution during PS104. A: $\delta^{13}\text{C}$; B: $\delta^{18}\text{O}$; C: nutrients; D: biomarker; E: opal isotopes; F: Nd isotopes; G: particle filters

Bottle	PS104/003-1	PS104/007-1	PS104/017-1	PS104/022-1	PS104/043-2
1	A,B,C,D	A,B,C,D	A,B,C,D	A,B,C,D	A,B,C,D
2	E	F	E	E	E
3	A,B,C	A,B,C,F	A,B,C	A,B,C	A,B,C
4	E	F	E	E	E
5	A,B,C	A,B,C,G	A,B,C	A,B,C	A,B,C
6	E	G	E	E	E
7	A,B,C	A,B,C,G	A,B,C	A,B,C	A,B,C
8	E	F,G	E	E	E
9	A,B,C,D	A,B,C,D,G	A,B,C	A,B,C	A,B,C
10	E	F,G	E	E	E
11	A,B,C	A,B,C,G	A,B,C,D	A,B,C,D	A,B,C,D
12	E	G	E	E	E
13	A,B,C,D	A,B,C,D	A,B,C	A,B,C	A,B,C
14	E	F	E	E	E
15	A,B,C	A,B,C,G	A,B,C	A,B,C	A,B,C
16	E	F,G	E	E	E
17	A,B,C	A,B,C	A,B,C	A,B,C	A,B,C
18	E		E	E	E
19	A,B,C	A,B,C	A,B,C	A,B,C,D	A,B,C
20	E	F	E	E	E
21	A,B,C	A,B,C,D,G	A,B,C	D	A,B,C,D
22	E	G	E	D	E
23	A,B,C,D	A,B,C,G	A,B,C,D	A,B,C,D	D
24	E	F,G	E	E	

5. BATHYMETRIC MAPPING AND SUB-BOTTOM PROFILING

Catalina Gebhardt¹, Jan Erik Arndt¹, Anne Braakmann-Folgmann¹, Tobias Haupt¹, Victoria Afanasyeva¹, Ricarda Dziadek¹, Katharina Hochmuth¹, Robert Larter², Florian Riefstahl¹

¹AWI
²BAS

Grant-No. AWI_PS104_01

Objectives

Bathymetry

Despite swath bathymetric and single-beam echosounding of the Southern Ocean by several institutes in the last decades, the depths of a vast majority of its area remains unknown and needs to be interpolated or inferred from satellite altimetry data (Arndt et al., 2013). Nitsche et al. (2007) created the first bathymetric model of the Amundsen Sea Embayment and described cross-shelf troughs, once created by expanded ice sheets during glaciations and today serving as a pathway for warm water masses from the deep ocean onto the shelf and to the modern-day grounding line. The International Bathymetric Chart of the Southern Ocean (IBCSO) Version 1.0 (Arndt et al., 2013) incorporated additional bathymetric data collected during various expeditions taken place after 2007 and refined the shelf bathymetry. Nevertheless, also in this bathymetric compilation large data gaps exist (Fig.5.1).

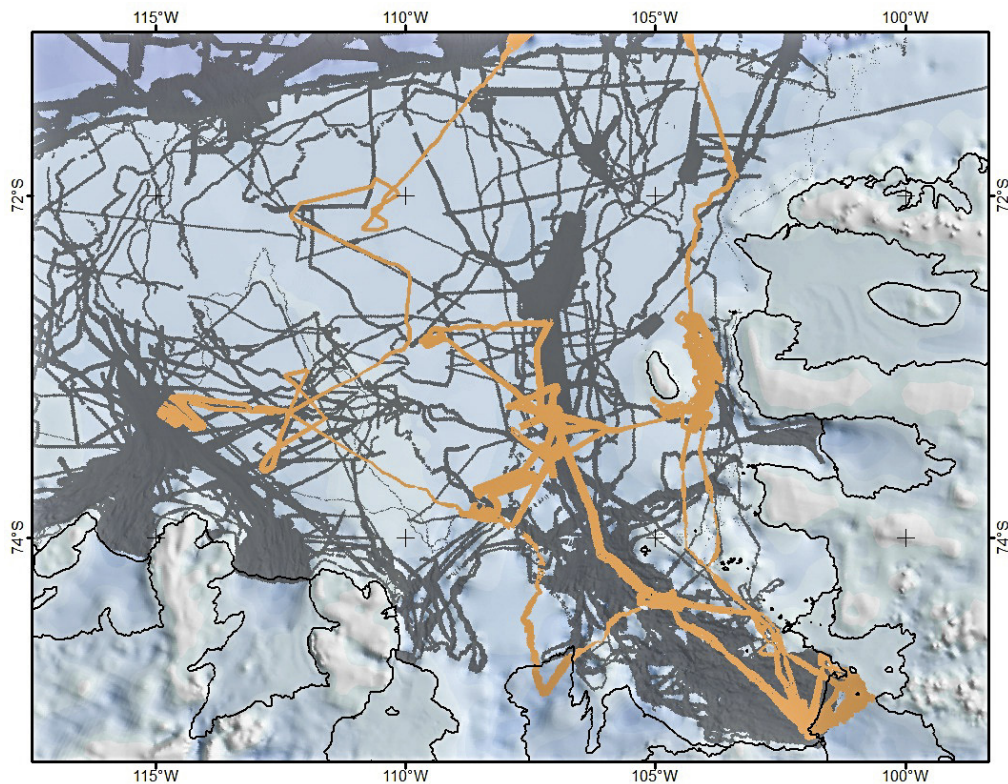


Fig. 5.1: Coverage of swath bathymetry data acquired during PS104 (orange) and coverage from IBCSO V1.0 (grey) (Arndt et al., 2013) in the Amundsen Sea Embayment

While these compilations provide coarsely resolved (500 m resolution) but comprehensive information on the seafloor morphology by interpolating between data gaps, high-resolution swath bathymetric data (~25 m resolution) provides information on small-scaled seafloor morphological features. In the Amundsen Sea Embayment these predominantly consist of glacially produced features, e.g. mega-scale glacial lineations, grounding zone wedges, drumlins, moraines, iceberg ploughmarks and meltwater channels, that provide important information on the setting and development of the expanded Antarctic Ice Sheet during and after glaciations (Klages et al., 2015; Nitsche et al., 2013; Jakobsson et al., 2012).

The swath bathymetric data acquired during PS104 is essential to improve our knowledge on glacial landform distribution and therefore the past ice sheet evolution and properties. Furthermore, the data will refine future regional compilations as the IBCSO and as being part of it also global bathymetric compilations like the General Bathymetric Chart of the Ocean (GEBCO) (Weatherall et al., 2015). In addition, the bathymetric data is essential for other working groups on board to plan the deployment of gear and later on to set punctual information into relation to its surrounding environment.

Parasound

High-resolution sediment echosounding of the upper tens of meters below the seabed provides insights into geological processes such as erosion, sediment transport, and deposition. Accurate knowledge of the geometries of the sampled seafloor is crucial for the interpretation of both short gravity and longer MeBo cores. For example, outcropping older strata, or areas with either reduced or enhanced sediment accumulation can easily be identified in sediment echosounding data and subsequently be sampled. In the Amundsen Sea Embayment where large areas are glacially overprinted, sediment echosounder data in concert with bathymetry data can be used to map the maximum extent, flow direction and retreat history of former ice streams (e.g., Klages et al., 2015; Nitsche et al., 2013; Jakobsson et al., 2012). Furthermore, sediment echosounder data help to identify small sedimentary basins that were potentially locations of subglacial lakes during the last deglaciation.

Work at sea

Bathymetry

The hull-mounted *Teledyne Reson Hydrosweep DS3* multibeam echosounding system has been used to collect swath bathymetric data during PS104. Data acquisition took place during all times of transit and was switched off during station time. The system was controlled using the program *Hydromap Control*. Live data visualisation was performed with the *Hypack 2016a* software package. The data was stored in ASD and HSX formats using the software *Parastore* and *Hypack 2016a*. Subsequent data processing and preliminary cleaning was performed in the *CARIS Hips and Sips* software. For further data visualisation and preparation of working maps we used *ESRI ArcGIS* and *QPS Fledermaus*.

Parasound

The *Teledyne Reson Parasound System DS3 (P70)* is a hull-mounted parametric echosounder. The transducer transmits signals to enable a maximum penetration depth of about 200 m in soft sediments. The system uses the parametric effect that occurs when very high (finite) amplitude sound waves are generated. If two waves of similar frequencies are generated simultaneously, interferences of the two primary frequencies are also emitted. The primary low frequency was set to 18 kHz during expedition PS104 and distributed energy within a beam of ~4.5°. The second primary frequency (Primary High Frequency, PHF) can be varied between 18.5 and 24 kHz, resulting in difference frequencies from 0.5 to 6.0 kHz. During PS104, the

Secondary Low Frequency (SLF) was set to 4 kHz, resulting in a PHF of ~22 kHz. The SLF signal travels within the narrow 18 kHz beam, which is much narrower than e.g. the 30° beam of a 4 kHz signal when emitted directly from the same transducer. Therefore, a higher lateral resolution can be achieved, and imaging of small-scale structures on the seafloor is superior to conventional systems.

Data acquisition took place from February 10, 2017, 21:20 UTC, to March 16, 2017, 08:00 UTC, in quasi-equidistant mode. The system was operated during all times of transit along with bathymetric data and was mostly switched off during station time. Only where exact positioning of either the MeBo or the gravity corer was required, the system was running during station work. The system was controlled using *Hydromap Control* and stored through *Parastore* software in ASD and PS3 format for both SLF and PHF signal. All data were subsequently converted to SGY format using the *ps32sgy* software (written by Hanno Keil, University of Bremen) and imported into *The Kingdom Software*® for visualization and quality control. Navigation was stored in UKOOA format using the *Postprocessor* Matlab script (written by Florian Riefstahl, AWI Bremerhaven).

Parasound data were used in concert with bathymetry and pre-existing seismic data to locate appropriate positions for MeBo and gravity coring sites.

Preliminary results

Bathymetry

During PS104, we covered an area of approximately 12,900 km² with swath bathymetric data on the shelf of the Amundsen Sea Embayment. Most of this area was previously not surveyed and provides first information on the ocean depths and on the structural composition of the seafloor (Fig.5.1). Preliminary investigation of the data shows that the seafloor basically consists of three different types: a) bedrock morphological features, e.g. knolls, gouges, meltwater channels, b) sedimentary morphological features, e.g. mega-scale glacial lineations, grounding zone wedges, iceberg ploughmarks, and c) a combination of both, e.g. drumlins (Fig. 5.2). Interpretation of these morphological features after the cruise will improve our understanding of past ice sheet dynamics and tectonic processes.

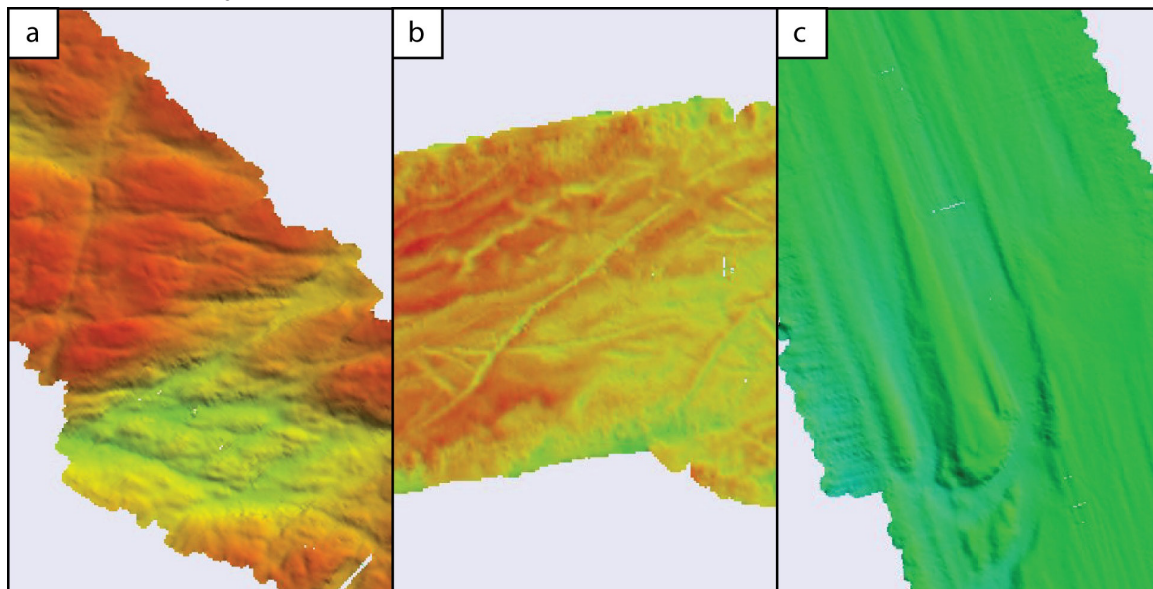


Fig. 5.2: Swath bathymetric data acquired during PS104 showing a) gouges in a bedrock environment, b) iceberg ploughmarks in sedimentary strata and c) a drumlin formed in a transition zone from bedrock to sedimentary strata

Parasound

During PS104, we acquired *Parasound* data along approximately 5,000 km on the shelf of the Amundsen Sea Embayment. Large parts of this area were previously not covered by *Parasound* surveys (cf. Fig.5.1) and hence provide a first insight into glacial dynamics of these areas. Mostly 3 different acoustic facies types were observed during PS104: Facies type I (Fig.5.3a) can be described as rough seafloor surface combined with little to no penetration of the *Parasound* signal, interpreted as glacially overprinted outcropping bedrock or glacial till with little to no cover of Quaternary sediments. Facies type II (Fig.5.3b) shows inclined reflectors truncated at or close to the seafloor with little to no cover of Quaternary sediments; the seafloor morphology encountered is mostly rather rough. Penetration into the dipping reflectors is up to 10-15 m in places. This second facies type can be interpreted as outcropping old sediment strata that were also known from previously acquired seismic profiles. The Quaternary cover of both facies types shows irregular incisions of variable size that could be identified as either iceberg scours or mega-scale glacial lineations using bathymetry data. Facies type III (Fig.5.3c) shows well-layered sediments with smooth seafloor surface and acoustic penetration of 20 m or more, interpreted as small sedimentary basins filled by postglacial and possible older sediments.

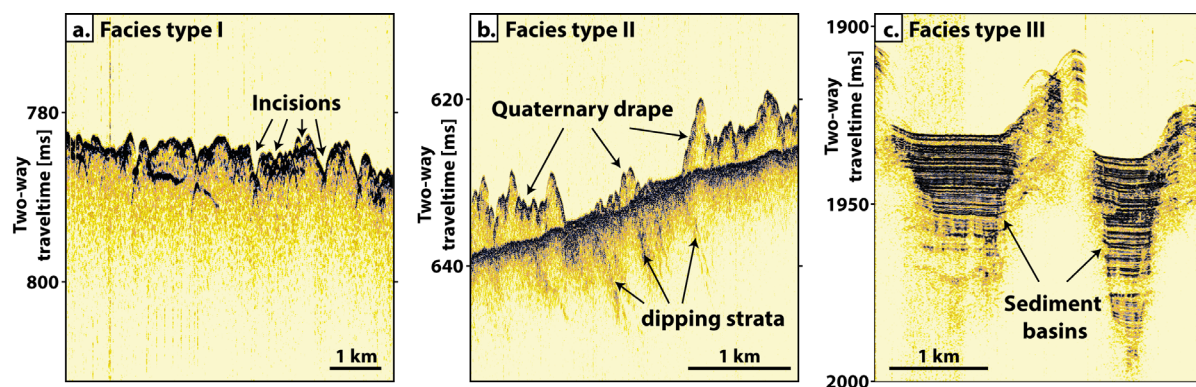


Fig. 5.3: *Parasound* data acquired during PS104 showing a) rough seafloor with little to no penetration, with irregular incisions interpreted as iceberg ploughmarks (Facies type I), b) dipping, truncated old strata partially covered by Quaternary sediments (Facies type II), and c) basins with well-layered sediments (Facies type III).

Furthermore, the newly acquired data will be used to improve upcoming regional and global bathymetric compilations. These are essential base information for a variety of scientific disciplines, e.g. geology, geophysics, oceanography, glaciology and biology.

Data management

The data will be archived in the PANGAEA database at AWI (<http://www.pangaea.de>).

References

- Arndt JE, Schenke HW, Jakobsson M, Nitsche FO, Buys G, Goleby B, Rebesco M, Bohoyo F, Hong J-K, Black J, Greku R, Udintsev G, Barrios F, Reynoso-Peralta W, Taisei M, Wigley R (2013) The International Bathymetric Chart of the Southern Ocean (IBCSO) Version 1.0 - A new bathymetric compilation covering circum-Antarctic waters. *Geophysical Research Letters* 40, 3111-3117, doi:10.1002/grl.50413.
- Jakobsson M, Anderson JB, Nitsche FO, Gyllencreutz R, Kirshner AE, Kirchner N, O'Regan M, Mohammad R, Eriksson B (2012) Ice sheet retreat dynamics inferred from glacial morphology of the central Pine Island Bay Trough, West Antarctica. *Quaternary Science Reviews*, doi:10.1016/j.quascirev.2011.12.017.
- Klages JP, Kuhn G, Graham AGC, Hillenbrand CD, Smith JA, Nitsche FO, Larter RD, Gohl K (2015) Palaeo-ice stream pathways and retreat style in the easternmost Amundsen Sea Embayment, West Antarctica, revealed by combined multibeam bathymetric and seismic data. *Geomorphology* 245, 207-222, doi:10.1016/j.geomorph.2015.05.020.
- Nitsche F, Gohl K, Larter RD, Hillenbrand CD, Kuhn G, Smith JA, Jacobs S, Anderson JB, Jakobsson M (2013) Paleo ice flow and subglacial meltwater dynamics in Pine Island Bay, West Antarctica. *The Cryosphere* 7, 249-262, doi:10.5194/tc-7-249-2013.
- Nitsche FO, Jacobs SS, Larter RD, Gohl K (2007) Bathymetry of the Amundsen Sea continental shelf: Implications for geology, oceanography, and glaciology. *Geochemistry Geophysics Geosystems* 8, Q10009, doi:10.1029/2007GC001694.
- Weatherall P, Marks KM, Jakobsson M, Schmitt T, Tani S, Arndt JE, Rovere M, Chayes D, Ferrini V, Wigley R (2015) A new digital bathymetric model of the world's oceans. *Earth and Space Science* 2, 2015EA000107, doi:10.1002/2015ea000107.

6. SEISMIC IMAGING AND STRATIGRAPHY OF THE SHELF SEDIMENTS

Gabriele Uenzelmann-Neben¹, Karsten Gohl¹,
Ricarda Dziadek¹, Thorsten Eggers¹, Catalina
Gebhardt¹, Katharina Hochmuth¹, Florian
Riefstahl¹, Robert Larter², Victoria Afanasyeva³,
Elke Burkhardt¹, Michael Flau¹, Alejandro
Cammareri⁴

¹AWI
²BAS
³VNII
⁴Marybio

Grant-No. AWI_PS104_01

Objectives

The Amundsen Sea Embayment forms the third-largest outflow area for the WAIS. The main ice streams in this embayment stem from the Pine Island, Thwaites and neighbouring glacier systems and have followed deeply eroded troughs on the inner to middle shelf. Most of the glacial-marine sediments have been transported onto the outer shelf of the Amundsen Sea Embayment and across the continental slope into the deep sea where they were redistributed by bottom currents. Seismic surveys of the sedimentary sequences and the underlying basement of the shelf, slope and rise along the continental margin of Marie Byrd Land, in the Amundsen Sea Embayment and in Pine Island Bay have allowed to decipher the main tectonic and sedimentary processes (e.g., Gohl et al., 2013; Lowe and Anderson, 2002; Uenzelmann-Neben and Gohl, 2014). However, stratigraphic ages have only been derived indirectly through 'jump' correlation with similar seismic characteristics observed from the Ross Sea shelf (Gohl et al., 2013).

The main aim of seismic surveys during this expedition is to link the *MeBo* drill sites with the existing seismic network on the shelf in order to establish a stratigraphic model that is age and process-constrained using results from the drill records. Cross-lines across the drill sites will enable three-dimensional images of the subsurface to better place the drill records into a regional deposition pattern.

Work at sea

The application of seismic methods was one of the operational objectives of PS104 in order to obtain information on the structure of sedimentary sequences in the Amundsen Sea Embayment and to extrapolate *MeBo* drilling results spatially. We used a standard multi-channel seismic reflection technique to image the outline and reflectivity characteristics of the sedimentary layers and the structure of the sub-sedimentary basement and lower crust by recording the returning near-vertical wave field. Fig.6.1 illustrates the principles of this technique.

Instruments

We used a cluster of 2 GI-Guns to resolve the sedimentary layers. A single GI-Gun™ is made up of two independent airguns within the same body. The first airgun ("Generator") produces the primary pulse, while the second airgun ("Injector") is used to control the oscillation of the bubble produced by the "Generator". We used the "Generator" with a volume of 0.72 litres

(45 in³) and triggered the “Injector” (1.68 litres = 105 in³) with a delay of 30 ms (33 ms). This led to an almost bubble-free signal. The guns were towed 20 m behind the vessel in 2 m depth and triggered every 10 s (~25 m shot interval) at a nominal pressure of 190 bar.

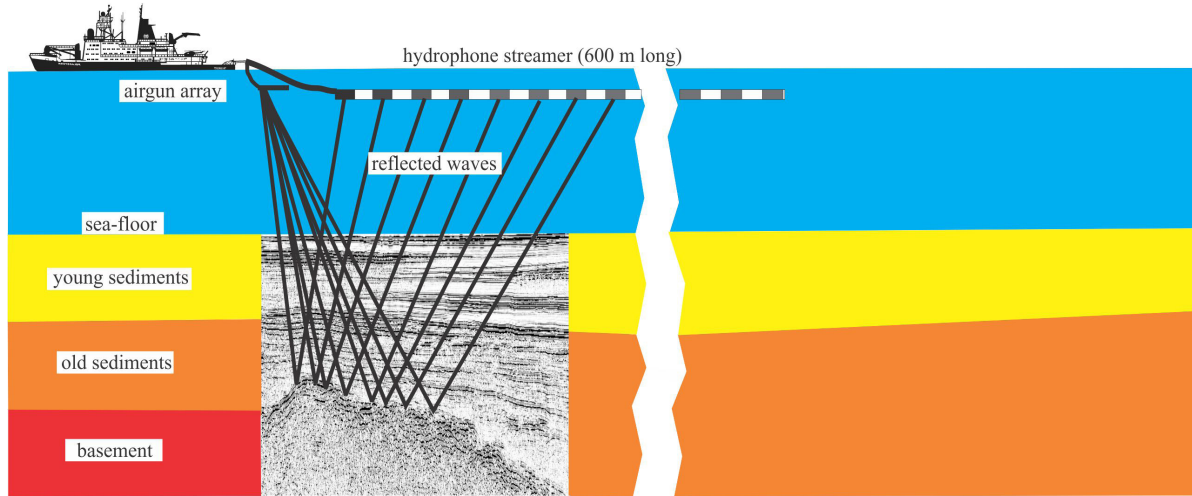


Fig. 6.1: Principle of marine seismic reflection surveying

Seismic data acquisition requires a very precise timing system, because seismic sources and recordings systems must be synchronised. A combined electric trigger-clock system was in operation in order (1) to provide the firing signal for the electric airgun valves, and (2) to provide the time-control of the seismic data recording. Due to the variable time difference in the NMEA format of the ship-provided clock and the DVS system, a separate Meinberg GPS clock was used with an antenna mounted on the upper deck. The clock provides UTC date and time (minute and second) pulses.

For multi-channel reflection data acquisition, we used a combined system of an analogue streamer and a set of multi-purpose seismic recorder. The in-sea equipment consists of a 96-channel analogue Streamer from PRAKLA-SEISMOS (Table 6.1, Fig. 6.2). This is coupled to the on board seismic recorder (Geode) from Geometrics. The analogue data collected by the hydrophone array is firstly submitted to a set of four GEODES (24-channel each) where the A/D conversion (24-bit result produced using Crystal Semiconductor sigma-delta converters and Geometrics proprietary over sampling) took place. The Geodes submitted the digitized data to the host computer via a standard Ethernet connection. The Geometrics Seismodule Controller Software stored the submitted data into SED-D files on the host computer hard drive (Fig.6.3). With a 12 s (5 s) shot interval the acquisition length was 5 s (1.3 s), limited by bandwidth of the data transmission (Geodes <-> host computer).

Tab. 6.1: Specification of PRAKLA-SEISMOS streamer

Active Streamer Section SHHP	
Length	50 m
Channels	8
Phones/group	8
1. Distance between Groups	6.25 m
2. Group length	4.86 m
3. Sensitivity	1.6 V/bar



Fig. 6.2: Winch with 600 m long analogue streamer



Fig. 6.3: Recording system used during PS104 seismic profiling.

A 150 m long, 24-channel streamer of type Geometric MicroEel was used parallel to the 96-channel streamer. This streamer was deployed on port side and floated at the sea surface. The data were stored via one Geode. The seismic acquisition parameters for all profiles can be found in Tables 6.2 (next page) and 6.3 (provided at the end of chapter 6).

Seismic profiling

A total of 397 nm of seismic reflection profiles (Figs 6.4 and 6.5, and Table 6.2) were recorded across a subglacial basin in front of Pine Island Glacier, in Pine Island Trough, east of Burke Island, and across Bear Ridge towards the outer shelf.

Technical problems of the seismic gear were almost negligible. However, a number of shutdowns of airgun operations, due to some whale (2) but mostly seal (24) occurrences close to the ship, caused partly large data gaps along some profiles. The data quality is generally at a high level due to relatively favourable weather conditions with calm seas.

Tab. 6.2: Brief description of seismic recording parameters

Profile Name	Active Length	Lead-in	Gun tow Distance	Record Length	Sample Rate
AWI-20170001 to AWI-20170010	600 m	144 m	20 m	4 s	1 ms
AWI-20170011 to AWI-20170026	600 m	144 m	20 m	5 s	1 ms
AWI-20170027 to AWI-20170029	600 m	144 m	20 m	1.3 s + 1s delay	1 ms
AWI-20170030 to AWI-20170033	600 m	144 m	20 m	4 s	1 ms
AWI-20171001 to AWI-20171026	150 m	30 m	20 m	7 s	1 ms
AWI-20171027 to AWI-20171033	150 m	30 m	20 m	4 s	1 ms

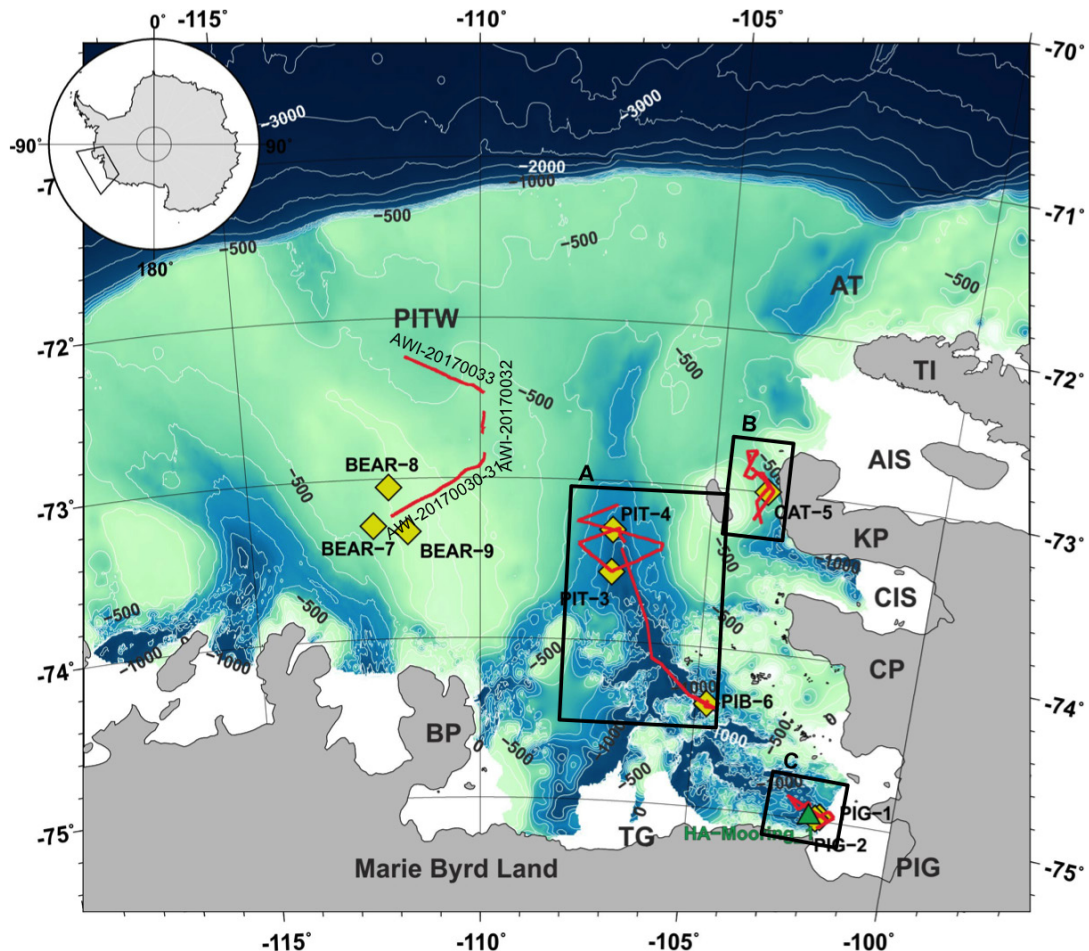


Fig. 6.4: Bathymetric map (Arndt et al., 2013) showing the location seismic reflection lines collected during the present cruise (red lines). Green triangle shows the location of the hydroacoustic mooring. Yellow diamonds show the locations of MeBo drill sites. AIS= Abbot Ice Shelf, AT= Abbot Trough, BP= Bear Peninsula, CIS= Cosgrove Ice Shelf, CP= Canisteo Peninsula, KP= King Peninsula, PIG= Pine Island Glacier, PITW= Pine Island Trough West, TG= Thwaites Glacier, TI= Thurston Island.

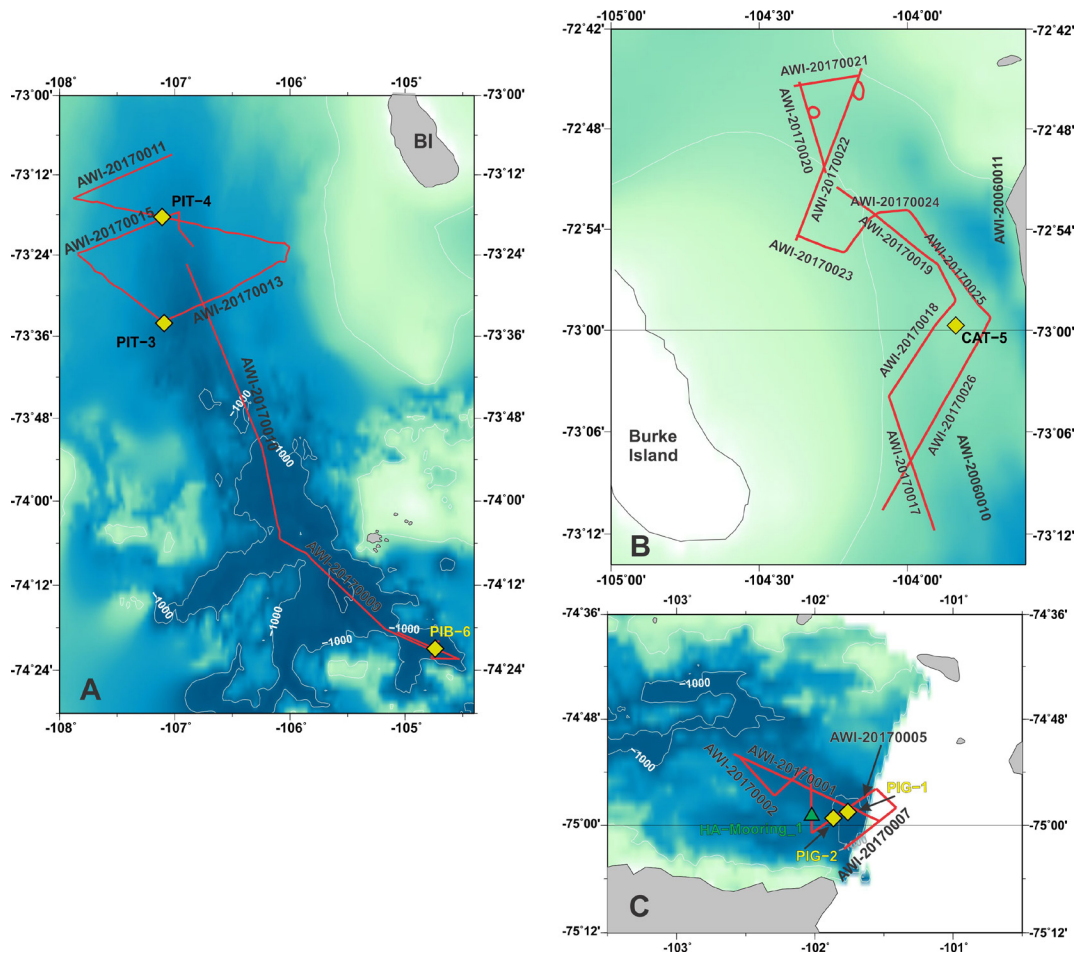


Fig. 6.5: Bathymetric maps (Arndt et al., 2013) showing the details of the smaller scaled seismic surveys (red lines). (A) Seismic survey along the Pine Island Trough with locations of MeBo sites PIT-03, PIT-04 and PIB-06 (yellow diamonds) west of Burke Island (BI). (B) Seismic survey east of Burke Island. Yellow diamond shows the location of MeBo site CAT-05. (C) Seismic survey in front of Pine Island Glacier. Yellow diamonds show the locations of MeBo sites PIT-01 and PIT-02; green triangle shows the location of the hydroacoustic mooring.

Mitigation for Marine Mammals

The mitigation regulations for seismic operations consisted of the deployment and recovery of a hydroacoustic mooring to achieve first insights of the natural and anthropogenically influenced soundscape of the southern Pine Island Bay area and visual observations for marine mammals within a predefined exclusion zone by marine mammal observers (MMOs). MMOs followed the mitigation protocol predefined by Umweltbundesamt (German environmental protection agency).

Hydroacoustic Mooring

A hydroacoustic mooring, containing two acoustic recorders at different water depths, was deployed on 15.02.2017 at 15:36 UTC and recovered on 20.02.2017 at 14:00 UTC in the southern Pine Island Bay (Fig. 6.5C). The recorders were set to record continuously at 32 kHz (Aural, MultiElectronique) and at 16 kHz (SonoVault, Develogic) respectively.

Tab. 6.4: Hydroacoustic mooring details

Mooring Name	Latitude / Longitude	Water Depth [m]	Recorder Type	Instrument Water Depth [m]
HA-Mooring 1	74°58.946' S 102°01.343' W	925	Aural Sn 086LF	120
			Sonovault Sn 1049	220

Marine mammal observations

During seismic operations, a constant visual watch for marine mammals was conducted by three marine mammal observers (herein MMOs) to prevent that marine mammals enter the predefined exclusion zone without being noticed. Therefore one observer was placed on the bridge observing the area ahead of the ship and two additional observers were located on portside and starboard side observing the respective sides as well as the back area around the seismic sources. The MMOs scanned the ship's perimeter with naked eye and 7x50 handheld binoculars. Observations started at least 60 minutes (so called pre-watch) before scheduled seismic operations were to begin to ensure that no marine mammal occurred within the mitigation zone when seismic operations were due to start. Clearance for soft-start procedure (a gradual increase of energy and number of the air pulsers) was given when the mitigation area was free of marine mammals. A summary of the mitigation effort during this cruise is given in Table 6.5. To ensure that most of the perimeter of the seismic sources is observed continuously, a thermal imaging sensor (FIRST Navy) was installed in the crow's nest of Polarstern (Zitterbart et al., 2013). The sensor constantly monitors its environment within a field of view of 360.0° horizontally by 28.8° vertically. The retrieved image data were processed by an automatic detection algorithm, which operated throughout the seismic reflection transects. The algorithm detects and processes thermographic signatures of marine mammals and provides the MMOs with detected cues onto a tablet computer to give further assistance to the observer in a probable shutdown situation. During hours of complete darkness the IR system was used only. The thermal imaging system worked during operation times without any flaws. Table 6.6 lists IR operation times.

During seismic operations, we recorded 112 detections of marine mammals, 100 visual sightings and 12 IR detection. 107 of these detections were pinnipeds, and 5 were cetaceans. In 103 of these encounters mitigation actions had to be conducted. Besides detections of animals in the water, we also recorded seals resting on ice floes (268 sightings with a total of 463 individuals). Species composition is given in Table 6.7.

The MMO watches were conducted by E. Burkhardt, A. Cammereri, M. Flau, J. Arndt, M. Arevalo, S. Bohaty, A. Braakmann-Folgmann, B. Ebermann, O. Esper, T. Haupt, K. Küssner, Y. Najman, T. Ronge, M. Scheinert, J. Schüürmann, P. Simoes Pereira, C. van de Flierdt and M. Zundel.

Tab. 6.5: Summary of MMO observation times during seismic operations

Date	Total hrs. Obs. [hh:mm]	Pre-watch [n]	Soft start [n]	Total sightings	Sightings visual [n]	Sightings IR [n]	Mitigation actions [n]	Shut down [n]	Delay [n]	Seals on ice [n]
15./16.02.2017	14:40	1	1	1	1	0	0	0	0	0
20./21.02.2017	15:29	1	1	1	0	1	0	0	0	0
25./26.02.2017	25:52	1	2	7	7	0	5	4	1	52
28.02./01.03.2017	18:22	1	1	3	3	0	3	3	0	33
04.03.2017	05:28	1	1	0	0	0	0	0	0	0
10.03.2017	22:44	1	5	100	89	11	95	19	76	378
Total	102:35	6	11	112	100	12	103	26	77	463

Tab. 6.6: Summary of operating times of AWI first Navy IR System during seismic operations

Sensor head No.	Date/Start time	Date/End Time	Total hours
01	15.02.2017 23:53	16.02.2017 15:17	15:24:06
	20.02.2017 22:28	21.02.2017 19:06	20:38:00
	25.02.2017 19:05	26.02.2017 22:00	26:54:55
	28.02.2017 13:31	01.03.2017 08:27	18:55:46
	05.03.2017 00:10	05.03.2017 06:22	06:12:20
	10.03.2017 00:11	11.03.2017 02:19	26:08:02
			114:13:09

Tab 6.7: Species Composition

CETACEANS	Species	Number of detections
	Minke whale	3
	whale spp.	2
	total	5
PINNIPEDS	Crabeater seal	42
	Leopard seal	1
	Seal spp.	64
	total	107

Preliminary results

A total of 397 nm of seismic reflection profiles (Figs 6.4 and 6.5, and Table 6.2) were recorded across a subglacial basin in front of Pine Island Glacier, in the Pine Island Trough, east of Burke Island, and across Bear Ridge towards the outer shelf. Due to problems with the processing system, only a quality control of the individual shot gathers could be carried out. Thus, no constant-offset plots could be generated for a preliminary interpretation. Processing of the data will be performed at AWI in Bremerhaven.

Data management

All seismic data will be uploaded to the SCAR Antarctic Seismic Data Library System (SDLS) 4 years after acquisition for restricted access and 8 years after acquisition for unrestricted access.

References

- Arndt JE, Schenke HW, Jakobsson M, Nitsche FO, Buys G, Goleby B, Rebesco M, Bohoyo F, Hong J, Black J, Greku R, Udintsev G, Barrios F, Reynoso-Peralta W, Taisei M, Wigley R (2013) The International Bathymetric Chart of the Southern Ocean (IBCSO) Version 1.0 – A new bathymetric compilation covering circum-Antarctic waters. *Geophysical Research Letters* 40, 3111-3117.
- Gohl K, Uenzelmann-Neben G, Larter RD, Hillenbrand C-D, Hochmuth K, Kalberg T, Weigelt E, Davy B, Kuhn G, Nitsche FO (2013) Seismic stratigraphic record of the Amundsen Sea Embayment shelf from pre-glacial to recent times: Evidence for a dynamic West Antarctic ice sheet. *Marine Geology* 344, 115-131.
- Lowe AJ, Anderson JB (2002) Reconstruction of the West Antarctic ice sheet in Pine Island Bay during the Last Glacial Maximum and its subsequent retreat history. *Quaternary Science Reviews* 21, 1879–1897.
- Uenzelmann-Neben G, Gohl K (2014) Early glaciation already during the Early Miocene in the Amundsen Sea, Southern Pacific: Indications from the distribution of sedimentary sequences. *Global and Planetary Change* 120, 92-104.
- Zitterbart DP, Kindermann L, Burkhardt E, Boebel O (2013) Automatic round-the-clock detection of whales for mitigation from underwater noise impacts. *PLoS ONE*, 8, e71217.

Tab. 6.3: Seismic profile summary (information in italics refers to recordings with 150 m long MicroEel streamer).

PROFILE NO.	Start / End	DATE [UTC]	TIME (UTC)	LATITUDE	LONGITUDE	FFIDs, NO. OF SHOTS	RECORD LENGTH [s]	SAMP. RATE [ms]	SHOT INTERVAL [s]	PROFILE LENGTH [nm]	STREAMER	GI-GUN CLUSTER		COMMENT
												Set-up	Total volume	
20170001 <i>(20171001)</i>	start end	16.02.17 16.02.17	02:31:00 06:07:00	-74.99214 -74.86551	-101.53341 -102.58550	10179- 11471, 1293 <i>(10163- 11468, 1305)</i>	4 <i>(7)</i>	1	10	17.5	PRAKLA 600 m <i>(MICROEEL 150 m)</i>	2 GI-guns, true GI mode (45+105 in ³), 30 ms delay	2 * 2.4 l	Start of ramp-up 01:53, full power 02:31
20170002 <i>(20171002)</i>	start end	16.02.17 16.02.17	06:23:00 07:33:00	-74.86841 -74.94156	-102.54579 -102.30299	11569- 11987, 419 <i>(11556- 11981, 426)</i>	4 <i>(7)</i>	1	10	5.7	PRAKLA 600 m <i>(MICROEEL 150 m)</i>	2 GI-guns, true GI mode (45+105 in ³), 30 ms delay	2 * 2.4 l	
20170003 <i>(20171003)</i>	start end	16.02.17 16.02.17	07:33:00 08:34:00	-74.94156 -74.88998	-102.30299 -102.06321	11988- 12352, 365 <i>(11982- 12347, 365)</i>	4 <i>(7)</i>	1	10	4.9	PRAKLA 600 m <i>(MICROEEL 150 m)</i>	2 GI-guns, true GI mode (45+105 in ³), 30 ms delay	2 * 2.4 l	
20170004 <i>(20171004)</i>	start end	16.02.17 16.02.17	08:43:00 10:09:00	-74.89320 -75.01497	-102.03080 -102.02154	12405- 12920, 516 <i>(12401- 12915, 515)</i>	4 <i>(7)</i>	1	10	7	PRAKLA 600 m <i>(MICROEEL 150 m)</i>	2 GI-guns, true GI mode (45+105 in ³), 30 ms delay	2 * 2.4 l	
20170005 <i>(20171005)</i>	start end	16.02.17 16.02.17	10:30:00 12:18:00	-75.01442 -74.93179	-102.02183 -101.56008	13050- 13702, 653 <i>(13041- 13693, 652)</i>	4 <i>(7)</i>	1	10	8.8	PRAKLA 600 m <i>(MICROEEL 150 m)</i>	2 GI-guns, true GI mode (45+105 in ³), 30 ms delay	2 * 2.4 l	
20170006 <i>(20171006)</i>	start end	16.02.17 16.02.17	12:44:00 13:21:00	-74.93179 -74.96753	-101.55372 -101.40987	13855- 14078, 244 <i>(13846- 14069, 223)</i>	4 <i>(7)</i>	1	10	3	PRAKLA 600 m <i>(MICROEEL 150 m)</i>	2 GI-guns, true GI mode (45+105 in ³), 30 ms delay	2 * 2.4 l	

PROFILE NO.	Start / End DATE [UTC]	TIME (UTC)	LATITUDE	LONGITUDE	FFIDs, NO. OF SHOTS	RECORD LENGTH [s]	SAMP. RATE [ms]	SHOT INTERVAL [s]	PROFILE LENGTH [nm]	STREAMER	GI-GUN CLUSTER		COMMENT
											Set-up	Total volume	
AWL-... 20170007 (20171007)	start end 16.02.17 16.02.17	13:44:00 15:07:00	-74.95726 -75.04366	-101.41303 -101.78682	14078- 14711, 633 (14202- 14711, 509)	4 (7)	1	10	6.8	PRAKLA 600 m (MICROEEL 150 m)	2 GI-guns, true GI mode (45+105 in ³), 30 ms delay	2 * 2.4 l	
20170008 (20171008)	start end 21.02.17 21.02.17	03:13:47 04:47:07	-74.35899 -74.30549	-104.71492 -105.15537	14972- 15592, 620 (14973- 15593, 620)	4 (7)	1	10	8.4	PRAKLA 600 m (MICROEEL 150 m)	2 GI-guns, true GI mode (45+105 in ³), 33 ms delay	2 * 2.4 l	Start of ramp-up 02:30:27, full power 03:01:07
20170009 (20171009)	start end 21.02.17 21.02.17	04:47:07 08:44:32	-74.30549 -74.09159	-105.15537 -106.07853	15593- 16956, 1363 (15594- 16957, 1363)	4 (7)	1	10	18.4	PRAKLA 600 m (MICROEEL 150 m)	2 GI-guns, true GI mode (45+105 in ³), 33 ms delay	2 * 2.4 l	
20170010 (20171010)	start end 21.02.17 21.02.17	08:44:32 16:59:47	-74.09159 -73.42261	-106.07853 -106.89624	16957- 19928, 2971 (16958- 19932, 2974)	4 (7)	1	10	40.1	PRAKLA 600 m (MICROEEL 150 m)	2 GI-guns, true GI mode (45+105 in ³), 33 ms delay	2 * 2.4 l	
20170011 (20171011)	start end 25.02.17 26.02.17	22:28:00 01:50:00	-73.14876 -73.25893	-107.02216 -107.87651	20189- 20991, 802 (20201- 21004, 803)	4 (7)	1	12	12.9	PRAKLA 600 m (MICROEEL 150 m)	2 GI-guns, true GI mode (45+105 in ³), 33 ms delay	2 * 2.4 l	Start of ramp-up 21:28:00, full power 21:58:00 Trigger off due to MM sighting 22:28:55-22:55:45 Start of ramp-up 22:55:45, full power 23:25:06 Trigger off due to MM sighting 00:01:18-00:15:30, 01:17:00-01:32:30,

6. Seismic Imaging and Stratigraphy of the Shelf Sediments

PROFILE NO.	Start / End DATE [UTC]	TIME (UTC)	LATITUDE	LONGITUDE	FFIDs, NO. OF SHOTS	RECORD LENGTH [s]	SAMP. RATE [ms]	SHOT INTERVAL [s]	PROFILE LENGTH [nm]	STREAMER	GI-GUN CLUSTER		COMMENT
											Set-up	Total volume	
AWL-... 20170012 (20171012)	start end 26.02.17 26.02.17	02:12:52 08:52:20	-73.25876 -73.37737	-107.87954 -106.01482	21105- 23102, 1997 (21118- 23115, 1997)	4 (7)	1	12	32.3	PRAKLA 600 m (MICROEEL 150 m)	2 GI-guns, true GI mode (45+105 in ³), 33 ms delay	2 * 2.4 l	
20170013 (20171013)	start end 26.02.17 26.02.17	08:52:42 13:31:14	-73.37766 -73.56729	-106.01372 -107.09591	23103- 24418, 1315 (23116- 24431, 1315)	4 (7)	1	12	21.3	PRAKLA 600 m (MICROEEL 150 m)	2 GI-guns, true GI mode (45+105 in ³), 33 ms delay	2 * 2.4 l	Trigger off due to MM sighting 11:23:17- 11:39:14
20170014 (20171014)	start end 26.02.17 26.02.17	13:31:26 16:37:50	-73.56715 -73.39976	-107.09687 -107.84150	24419- 25351, 932 (24432- 25370, 938)	4 (7)	1	12	15	PRAKLA 600 m (MICROEEL 150 m)	2 GI-guns, true GI mode (45+105 in ³), 33 ms delay	2 * 2.4 l	
20170015 (20171015)	start end 26.02.17 26.02.17	16:57:38 20:11:14	-73.39628 -73.29294	-107.84444 -106.96855	25450- 26418, 968 (25465- 26431, 966)	4 (7)	1	12	15.7	PRAKLA 600 m (MICROEEL 150 m)	2 GI-guns, true GI mode (45+105 in ³), 33 ms delay	2 * 2.4 l	
20170016 (20171016)	start end 26.02.17 26.02.17	20:39:24 21:51:50	-73.29177 -73.37904	-106.96315 -106.83854	26559- 26921, 362 (26572- 26934, 362)	4 (7)	1	12	5.7	PRAKLA 600 m (MICROEEL 150 m)	2 GI-guns, true GI mode (45+105 in ³), 33 ms delay	2 * 2.4 l	
20170017 (20171017)	start end 28.02.17 28.02.17	15:27:12 17:02:23	-73.19639 -73.06744	-103.90837 -104.05892	27016- 27531, 515 (27073- 27548, 475)	4 (7)	1	12	8.3	PRAKLA 600 m (MICROEEL 150 m)	2 GI-guns, true GI mode (45+105 in ³), 33 ms delay	2 * 2.4 l	Start of ramp-up 15:00:00, full power 15:30:12

PROFILE NO.	Start / End DATE [UTC]	TIME (UTC)	LATITUDE	LONGITUDE	FFIDs, NO. OF SHOTS	RECORD LENGTH [s]	SAMP. RATE [ms]	SHOT INTERVAL [s]	PROFILE LENGTH [nm]	STREAMER	GI-GUN CLUSTER		COMMENT	
											Set-up	Total volume		
AWL-... 20170018 (20171018)	start end	28.02.17 28.02.17	17:02:35 18:23:54	-73.06725 -72.97319	-104.06011 -104.84181	27532-27938, 406 (27549-27951, 402)	4 (7)	1	12	6.6	PRAKLA 600 m (MICROEEL 150 m)	2 GI-guns, true GI mode (45+105 in ³), 33 ms delay	2 * 2.4 l	
20170019 (20171019)	start end	28.02.17 28.02.17	18:24:06 20:29:39	-72.97300 -72.85826	-103.84138 -104.23726	27939-28566, 627 (27952-28579, 627)	4 (7)	1	12	10.2	PRAKLA 600 m (MICROEEL 150 m)	2 GI-guns, true GI mode (45+105 in ³), 33 ms delay	2 * 2.4 l	
20170020 (20171020)	start end	28.02.17 28.02.17	20:44:01 22:17:40	-72.84409 -72.75309	-104.27541 -104.36469	28568-28949, 381 (28580-28961, 381)	4 (7)	1	12	6.2	PRAKLA 600 m (MICROEEL 150 m)	2 GI-guns, true GI mode (45+105 in ³), 33 ms delay	2 * 2.4 l	Trigger off due to MM sighting 20:29:39-20:44:01, 22:03:48-22:20:52
20170021 (20171021)	start end	28.02.17 28.02.17	22:38:28 23:28:50	-72.75727 -72.74666	-104.38188 -104.16252	29055-29293, 238 (29068-29306, 238)	4 (7)	1	12	3.9	PRAKLA 600 m (MICROEEL 150 m)	2 GI-guns, true GI mode (45+105 in ³), 33 ms delay	2 * 2.4 l	Trigger off due to MM sighting 23:26:04-23:41-14
20170022 (20171022)	start end	28.02.17 01.03.17	23:45:50 02:27:14	-72.74001 -72.91079	-104.15446 -104.37570	29317-30124, 807 (29330-30137, 807)	4 (7)	1	12	13	PRAKLA 600 m (MICROEEL 150 m)	2 GI-guns, true GI mode (45+105 in ³), 33 ms delay	2 * 2.4 l	
20170023 (20171023)	start end	01.03.17 01.03.17	02:45:26 03:16:26	-72.90595 -72.92209	-104.37186 -104.2257	30215-30370, 155 (30228-30383, 155)	4 (7)	1	12	2.5	PRAKLA 600 m (MICROEEL 150 m)	2 GI-guns, true GI mode (45+105 in ³), 33 ms delay	2 * 2.4 l	

6. Seismic Imaging and Stratigraphy of the Shelf Sediments

PROFILE NO.	Start / End DATE [UTC]	TIME (UTC)	LATITUDE	LONGITUDE	FFIDs, NO. OF SHOTS	RECORD LENGTH [s]	SAMP. RATE [ms]	SHOT INTERVAL [s]	PROFILE LENGTH [nm]	STREAMER	GI-GUN CLUSTER		COMMENT
											Set-up	Total volume	
AWL-... 20170024 (20171024)	start end 01.03.17 01.03.17	03:16:38 04:15:38	-72.92218 -72.88129	-104.22459 -103.99894	30371- 30660, 289 (30384- 30679, 295)	4 (7)	1	12	4.7	PRAKLA 600 m (MICROEEL 150 m)	2 GI-guns, true GI mode (45+105 in ³), 33 ms delay	2 * 2.4 l	
20170025 (20171025)	start end 01.03.17 01.03.17	04:15:50 05:45:38	-72.88167 -72.98457	-103.99585 -103.72628	30661- 31116, 455 (30680- 31129, 449)	4 (7)	1	12	7.4	PRAKLA 600 m (MICROEEL 150 m)	2 GI-guns, true GI mode (45+105 in ³), 33 ms delay	2 * 2.4 l	
20170026 (20171026)	start end 01.03.17 01.03.17	05:45:50 08:21:38	-72.9855 -73.17549	-103.72364 -104.08296	31117- 31895, 778 (31130- 31909, 779)	14 (7)	1	12	12.6	PRAKLA 600 m (MICROEEL 150 m)	2 GI-guns, true GI mode (45+105 in ³), 33 ms delay	2 * 2.4 l	
20170027 (20171027)	start end 05.03.17 05.03.17	02:27:28 (02:15:28) 02:59:23	-74.34570 (-74.3144) -74.37192	-104.73319 (-104.68250) -104.77316	32240- 32523, 283 (32216- 32745, 529)	1 s delay + 1.3 (4)	1	5	1.9	PRAKLA 600 m (MICROEEL 150 m)	1 GI-gun, true GI mode (45+105 in ³), 33 ms delay	1 * 2.4 l	Start of ramp-up 01:50:33, full power 02:20:42
20170028 (20171028)	start end 05.03.17 05.03.17	03:19:53 04:06:33	-74.37223 -74.37300	-104.77447 -104.52645	32769- 33329, 560 (32994- 33548, 554)	1 s delay + 1.3 (4)	1	5	3.8	PRAKLA 600 m (MICROEEL 150 m)	1 GI-gun, true GI mode (45+105 in ³), 33 ms delay	1 * 2.4 l	
20170029 (20171029)	start end 05.03.17 05.03.17	04:26:33 06:18:08	-74.37500 -74.31035	-104.52771 -105.06713	33469- 34908, 1439 (33788- 35124, 1426)	1 s delay + 1.3 (4)	1	5	9.7	PRAKLA 600 m (MICROEEL 150 m)	1 GI-guns true GI mode (45+105 in ³), 33 ms delay	1 * 2.4 l	

PROFILE NO.	Start / End DATE [UTC]	TIME (UTC)	LATITUDE	LONGITUDE	FFIDs, NO. OF SHOTS	RECORD LENGTH [s]	SAMP. RATE [ms]	SHOT INTERVAL [s]	PROFILE LENGTH [nm]	STREAMER	GI-GUN CLUSTER		COMMENT
											Set-up	Total volume	
AWL-... 20170030 (20171030)	start end 10.03.17 10.03.17	04:31:40 09:57:12	-73.23639 -73.02876	-111.93491 -110.61263	34909- 35793, 884 (35128- 36009, 881)	4	1	12	26.4	PRAKLA 600 m (MICROEEL 150 m)	2 GI-guns, true GI mode (45+105 in ³), 33 ms delay	2 * 2.4 l	Start of ramp- up 04:31:20, full power at 05:36:30 Trigger off due to MM sighting 04:52:32- 05:07:42, 05:12:42- 05:32:43, 06:44:06- 07:00:48, 07:38:24- 08:29:13 Start of ramp- up 08:29:13, full power at 09:15:20 Trigger off due to MM sighting 08:44:38- 08:59:10, 09:19:30- 09:37:11, 09:38:19- 09:53:23
20170031 (20171031)	start end 10.03.17 10.03.17	09:57:24 13:17:46	-73.02911 -72.84493	-110.61246 -109.90172	35794- 36725, 931 (36010- 36941, 931)	4	1	12	16.2	PRAKLA 600 m (MICROEEL 150 m)	2 GI-guns, true GI mode (45+105 in ³), 33 ms delay	2 * 2.4 l	Trigger off due to MM sighting 12:54:36- 13:08:56, 13:17:46- 14:41:57
20170032 (20171032) Continued on next page	start end 10.03.17 10.03.17	14:41:57 16:21:52	-72.72502 -72.58949	-109.96192 -109.91863	36726- 37112, 386 (36942- 37328, 386)	4	1	12	8.1	PRAKLA 600 m (MICROEEL 150 m)	2-1 GI- guns, true GI mode (45+105 in ³), 33 ms delay	2 * 2.4 l (1 * 2.4 l)	Start of ramp- up 14:41:57, full power 15:11:09 Trigger off due to MM sighting 15:28:45-

7. GEOTHERMAL GRADIENTS AND HEAT FLUX ESTIMATES

Ricarda Dziadek¹, Katharina Hochmuth¹, Karsten Gohl¹, Norbert Kaul² (not on board)

¹AWI
²U Bremen

Grant-No. AWI_PS104_01

Objectives

Marine heat flow observations provide fundamental constraints on physical, chemical and biological processes occurring near and below the seafloor. Processes that influence and are influenced by heat transport within seafloor sediments and basement rocks include:

- (1) *the thermal evolution of the oceanic crust and lithosphere;*
- (2) *the geodynamics of plate boundaries and mantle convection;*
- (3) *fluid circulation and associated impacts on water-rock interactions, seismicity, tectonics, and magmatism.*

Understanding these processes involves the quantification of energy and fluid fluxes, requiring knowledge of the thermal state deduced from observations that include heat flow, sub-bottom temperature, and thermos-physical sediment properties.

The objective of our temperature measurements during *Polarstern* expedition PS104 was an assessment of the geothermal heat flux across the Amundsen Sea Embayment, which in general is poorly constrained by direct observations in all of Antarctica. These measurements are directly related to the helicopter-magnetic surveys (see Chapter 10), because the magnetic anomaly grids are used to derive geothermal heat flux from Curie depth estimates.

On a broader perspective, the break-up history of Gondwana's Pacific margin will be investigated. Therefore the results will be compared with the crustal thermal state of the conjugate continental margin located at the Chatham Rise of New Zealand, which has been constrained by temperature gradient measurements during the *Sonne* expedition SO246 in early 2016.

Work at sea

We used Miniaturized Temperature Loggers (MTL), which are autonomously operating precision thermometers for deep-sea applications. The housing is designed for an operation depth of up to 6,000 m and sediment penetration. The sampling rate can be adjusted between 1 s and several minutes, yielding a registration time of 1 hour to 6 months. The MTL are constructed for 0.001 K resolution and 0.1 K precision (Pfender and Villinger, 2002) and were equidistantly mounted on either a 4 m or 7 m sensor rod. Whenever applicable, MTLs were also mounted on a gravity corer (length: 5, 8, 10 m). The standard procedure includes a calibration deployment of the MTL mounted on a CTD at the beginning of the cruise to obtain absolute temperatures. Schematically represented in Fig. 7.1 are the MTLs details and the probe geometry, where six MTL are mounted below the weight with a fixed distance.

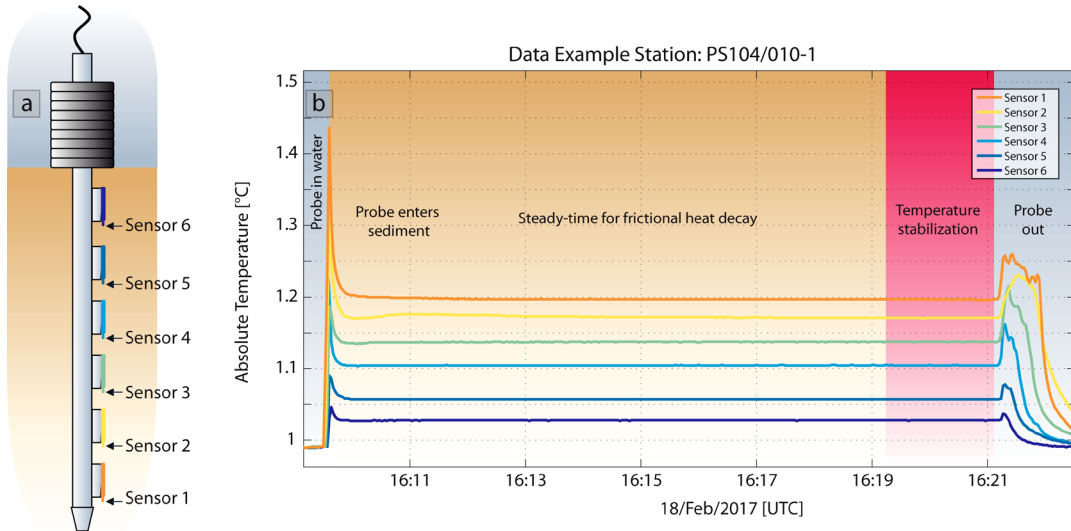


Fig. 7.1: a) Schematically representation of the sensor mounting on the gradient probe. b) Data example of station PS104/010-1. While entering the sediment frictional heat is generated which then decays, depending on the thermal conductivity of the sediment. After 8 minutes steady-time the temperature curves have stabilized and temperature gradients can be estimated.

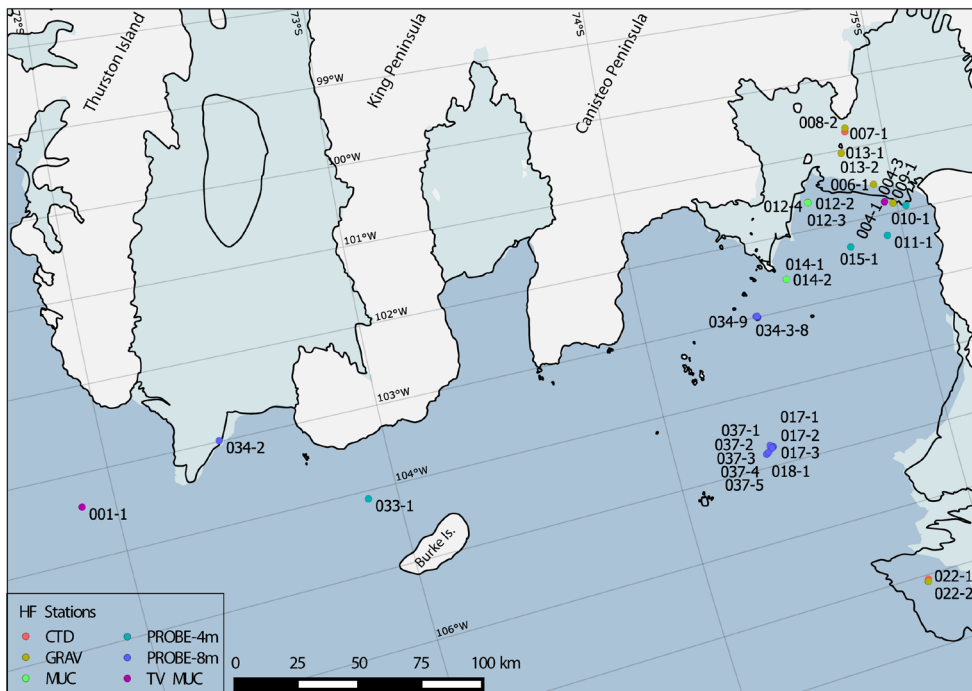


Fig. 7.2: Map shows deployment of Miniaturized Temperature Loggers (MTL) at selected sites in the Amundsen Sea Embayment. The different instruments are colour-coded. CTD stations were used for calibration purposes. At Video-MUC sites we monitored the temperature distribution of the water column while lowering the instrument. We mounted the MTLs at the gravity corer (GRAV) at selected stations and deployed gradient probes for sediment temperature measurements. See Table 7.1 for details of the stations.

The instrumented probe was lowered with 1.8 m/s to 50 m above the sea floor. Then winch speed is reduced to 0.8 m/s for the probe to penetrate the sediment supported by the force of its own weight. The probe typically sits in the sediment for 8-10 minutes (steady time) for any frictional heat to decay and to enable undisturbed measurements of *in-situ* sediment temperatures (Fig. 7.1 b). After recovery, the data are obtained via a readout unit without opening the loggers casing.

Tab. 7.1: Station protocol of MTL deployments during PS104. Comment section denotes the deployed instrument, where the MTL were mounted on: conductivity, temperature and depth (CTD), multicorer (MUC) with optional video signal (TV MUC), gravity corer (GRAV) and thermal gradient probe with different lengths in x metres (PROBE xm)

Date	Station	Latitude	Longitude	Depth [m]	Comments
14.02.17	PS104/001-1	71° 52.727' S	103° 22.984' W	754	TV MUC
15.02.17	PS104/004-1	74° 57.475' S	101° 49.751' W	1014	CTD
15.02.17	PS104/004-3	74° 57.484' S	101° 49.533' W	1016	TV MUC
16.02.17	PS104/006-1	74° 55.870' S	101° 33.380' W	883	GRAV
17.02.17	PS104/007-1	74° 51.934' S	100° 45.641' W	719	CTD
18.02.17	PS104/008-2	74° 52.106' S	100° 42.667' W	700	GRAV
18.02.17	PS104/009-1	74° 59.213' S	101° 52.134' W	980	GRAV
18.02.17	PS104/010-1	75° 01.855' S	101° 56.319' W	950	PROBE 4m
18.02.17	PS104/011-1	74° 56.548' S	102° 17.699' W	936	PROBE 4m
19.02.17	PS104/012-2	74° 41.020' S	101° 37.328' W	345	GRAV
19.02.17	PS104/012-3	74° 41.025' S	101° 37.484' W	340	GRAV
19.02.17	PS104/012-4	74° 41.013' S	101° 37.427' W	340	MUC
19.02.17	PS104/013-1	74° 50.281' S	101° 02.628' W	530	MUC
20.02.17	PS104/013-2	74° 50.285' S	101° 02.624' W	530	GRAV
20.02.17	PS104/014-1	74° 32.935' S	102° 35.160' W	600	GRAV
20.02.17	PS104/014-2	74° 32.940' S	102° 35.141' W	597	MUC
20.02.17	PS104/015-1	74° 48.181' S	102° 20.630' W	1000	PROBE 4m
20.02.17	PS104/017-1	74° 21.469' S	104° 44.829' W	1375	CTD
20.02.17	PS104/017-2	74° 21.556' S	104° 44.737' W	1375	MUC
20.02.17	PS104/017-3	74° 21.543' S	104° 44.817' W	1384	PROBE 7m
21.02.17	PS104/018-1	74° 21.309' S	104° 45.413' W	1387	PROBE 7m
24.02.17	PS104/022-1	74° 46.046' S	107° 05.589' W	707	CTD
24.02.17	PS104/022-2	74° 46.069' S	107° 05.544' W	707	GRAV
01.03.17	PS104/033-1	72° 53.473' S	104° 05.932' W	490	PROBE 4m
02.03.17	PS104/034-2	72° 24.931' S	102° 59.418' W	744	PROBE 7m
02.03.17	PS104/034-3	74° 25.035' S	103° 00.321' W	740	PROBE 7m
02.03.17	PS104/034-4	74° 24.953' S	103° 00.054' W	740	PROBE 7m
02.03.17	PS104/034-5	74° 24.899' S	102° 59.860' W	740	PROBE 7m
02.03.17	PS104/034-6	74° 24.839' S	102° 59.679' W	737	PROBE 7m
02.03.17	PS104/034-7	74° 24.783' S	102° 59.493' W	740	PROBE 7m
02.03.17	PS104/034-8	74° 24.729' S	102° 59.300' W	735	PROBE 7m
02.03.17	PS104/034-9	74° 24.965' S	102° 59.193' W	735	PROBE 7m
03.03.17	PS104/037-1	74° 19.798' S	104° 49.333' W	1400	PROBE 7m
03.03.17	PS104/037-2	74° 19.857' S	104° 49.177' W	1395	PROBE 7m
03.03.17	PS104/037-3	74° 20.339' S	104° 47.950' W	1388	PROBE 7m
03.03.17	PS104/037-4	74° 20.968' S	104° 43.276' W	1405	PROBE 7m
03.03.17	PS104/037-5	74° 21.278' S	104° 45.586' W	1385	PROBE 7m
10.03.17	PS104/043-4	73° 17.823' S	112° 19.809' W	466	PROBE 4m

Preliminary results

The on board data processing is exemplarily shown for station PS104/010-1 in Fig. 7.3. *In-situ* temperatures of all sensors are plotted in the graph on the left-hand side together with a close up of sensor 2. Considering the polynomial fit of the measurements and the $\pm 2\delta$ confidence interval (95 %) the temperatures were regarded as stabile. The mean of the stabilization temperatures was then used for plotting the temperature gradient. Assuming a steady-state, one-dimensional heat conduction, constant thermal conductivity ($k = 1$, applicable for soft, water saturated sediments) and the neglecting radioactive heat production, the geothermal heat flux (Q) can be calculated via the product of thermal conductivity and the temperature gradient.

$$Q = k \delta T \delta z^{-1} \text{ [mWm}^{-2}\text{]}$$

The preliminary geothermal heat flux approximation for station PS104/010-1 was 49 mWm⁻². Detailed data processing will be conducted after the expedition in Bremerhaven. The thermal conductivity will be further constrained by measuring the value directly on split gravity cores taken at or in the vicinity of the temperature sites.

Data management

All data will be uploaded on Pangaea after publication.

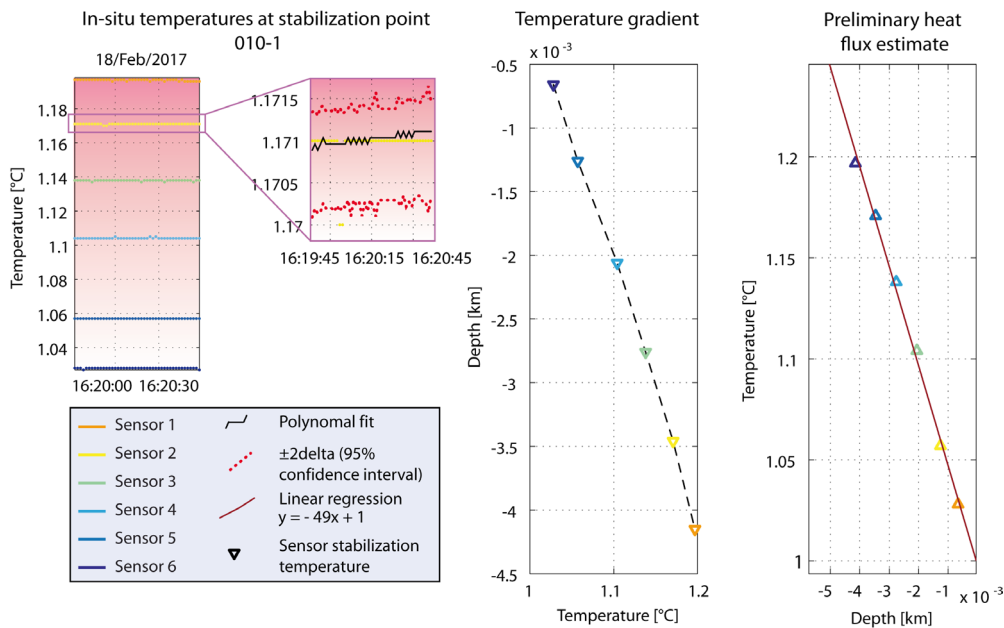


Fig. 7.3: Example of on-board data processing.

References

Pfender M, Villinger H (2002) Miniaturized data loggers for deep sea sediment temperature gradient measurements, *Marine Geology*, 186, 557–570.

8. EXHUMATION AND DEGLACIATION OF THE AMUNDSEN SEA REGION

Maximilian Zundel¹, Yani Najman²,
Cornelia Spiegel¹ (not on board), Frank Lisker¹
(not on board)

¹U Bremen
²Lancaster U

Grant-No. AWI_PS104_02

Objectives

1) Constraining the timing of establishment of modern ice sheet configuration, in particular investigating how rapidly the West Antarctic Ice Sheet adjusted to the changed environment following the Last Glacial Maximum (LGM).

This will be achieved through determination of the timing and rates of glacial retreat and thinning, using cosmogenic nuclide exposure dating. Main targets for sample collection are the small islands scattered across the Amundsen Sea Embayment. These are situated along the Pine Island Trough in front of the Pine Island and Thwaites Glacier and cover a north-south distance of nearly 150 km. Exposure ages from three islands already exist (Johnson et al., 2008; Lindow et al., 2014), which is, however, not sufficient for deriving retreat rates or a detailed retreat history including potential non-linear retreat. Glacial erratics from as many of these islands as possible will be sampled and used for cosmogenic ¹⁰Be exposure dating. Ideally, sampling will be of sufficient spatial extent to allow a transect to be constructed. This will provide a detailed picture of when these islands became free of ice and thus of the retreat history of Pine Island and Thwaites Glacier.

2) Constraining the timing of onset of glaciation in West Antarctica

There is mostly consensus that large-scale East Antarctic glaciation initiated around the Eocene-Oligocene boundary. However, direct evidence for the onset of continental glaciation in West Antarctica is absent. Various previous works propose onset at the Eocene-Oligocene boundary, Early Miocene or Late Miocene (e.g. Barker and Camerlenghi, 2002; Wilson et al. 2013). Thermochronology allows documentation of exhumation and by inference uplift, which is an important prerequisite for glaciation. Our thermochronology data suggest that Pine Island Bay region was of low relief during the Cenozoic (Lindow et al., 2016). Uplift is recorded from the Marie Byrd Land dome as only starting in the Early Miocene (Spiegel et al., 2016), yet based on limited data. We therefore propose to collect more samples from Martin and Bear Peninsula for low temperature thermochronology, to compare with data already published from adjacent areas (Lindow et al., 2016; Spiegel et al., 2016). Further sampling will also be undertaken for thermochronology in the Amundsen Sea Embayment, to increase the database, for locations where we are already being deployed for cosmogenic sampling (see objective 1).

Work on land

For both cosmogenic exposure dating and thermochronological analysis, the main priority was sampling along iso-altitude horizontal profiles, because it is possible to derive lateral glacial

retreat rates from them, and they reveal information on fault movements, crustal tilting, and paleotopography. For surface exposure dating, sampling of erratic boulders and/or glacially-eroded bedrock, (ideally striated) was carried out. Because surface exposure dating relies on the accumulation of ^{10}Be in quartz, quartz-bearing lithologies such as granites, granodiorites, and gneisses were collected. Most of ^{10}Be production occurs in the upper few cm of a rock and thus the surfaces of exposed rocks have been sampled. Since these are difficult to sample from unweathered, rounded bedrock or boulders, a rock saw was used to cut up to 5 cm deep grids into the rock's surface, for samples which were too big to sample the entire erratic. After sawing, the samples were removed from the surface with a hammer and chisel. Where entire erratics were collected, the upper side of the sample was noted on the rock. At each location where samples were collected for cosmogenic analysis, shielding measurements were taken at 30° increments through 360° .

For thermochronology, *in-situ* bedrock samples were collected. The applied thermochronological dating methods are based on the radioactive decay of U (and Th and Sm) in the mineral apatite; accordingly apatite bearing rocks were sampled, which involves essentially the same lithologies as required for surface exposure dating.

For samples taken for structural geological research, oriented samples were taken.

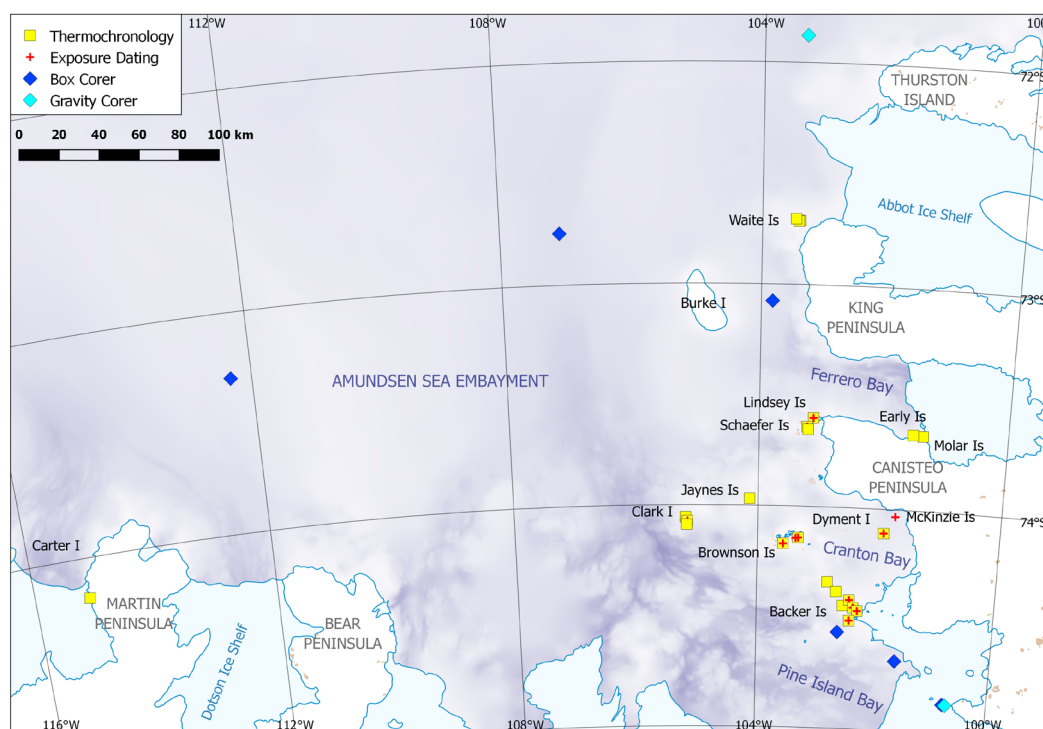


Fig. 8.1: Map showing the working area of the Amundsen Sea Embayment and the samples taken from onshore and offshore localities for thermochronology (including samples for structural and microscopical analyses) and cosmogenic exposure dating.

Work at sea

Marine-deposited clastic sediments derived from our onshore study areas complemented our sample set for thermochronology. Therefore, the coarse-grained detrital fraction from the upper ca. 1 m of ocean sediment was collected. This was recovered using a box-corer from the marine geology group (see chapter 4). At gravity corer sites, additional coarse-grained material was collected where it fell off the core. Dating of this ice-rafted debris yields averaged age

patterns that reflect the cooling and exhumation history integrated over the whole source area. The main priority was to target coring sites that can be related to well-defined glacial catchments. Information about box and gravity corer samples is provided in Fig. 8.1 and Table 8.1.

Preliminary results

A variety of locations on land were sampled in the Amundsen Sea Embayment (Fig. 8.1). In the Pine Island Bay region, the Backer Islands, Jaynes Islands, Brownson Islands and Clark Islands were sampled; in the King Peninsula region the Waite Islands were sampled; in the Cranton Bay area the McKinzie Islands and Dymont Islands were sampled; in the Canisteo Peninsula region the Lindsey Islands and Schaefer Islands were sampled; in the Ferrero Bay region the Molar Islands and Early Islands were sampled; and in the Martin Peninsula region the Siglin Rocks were sampled. Additionally, Webber Nunatak was visited but no rocks were collected due to the unsuitable lithology, a flight was made to Thurston Island but landing was not possible, and a flight was attempted to Bear Peninsula but poor weather conditions precluded us reaching the destination.

At all locations bar Martin Peninsula, the priority for sampling was the collection of felsic erratics (granites, granodiorites, gneisses) for cosmogenic exposure dating. Where such material was not available, or there was sufficient time for additional fieldwork and sampling (time on site was generally limited to 45 minutes due to helicopter regulations, except at a couple of sites where we were dropped off and collected later after a couple of hours), bedrock samples for thermochronological analysis, oriented samples for structural analysis, and structural data were collected. Apart from sample collection, observations on structural evolution, tectonic activity and glacial geomorphology were included in the fieldwork. At the Siglin Rocks on Martin Peninsula, sampling for thermochronological analysis was prioritised, and poor weather conditions permitted a stop of only 10 minutes on site. Tables 8.1 and 8.2 provide information on all samples collected at each location.

Islands in the Amundsen Sea Embayment

33 samples from 22 islands in the Amundsen Sea Embayment were taken for thermochronology and microscopical analysis (Fig. 8.1, Table 8.2). The islands mostly consist of coarse-grained granitic to granodioritic rocks which are thought to be Early to Late Cretaceous in age (Mukasa and Dalziel, 2000). According to textural and mineral assemblages, different granitic varieties were identified. Most varieties are characterized by a porphyritic texture and a mineral assemblage comprising quartz, plagioclase, K-feldspar and biotite. Hornblende-bearing varieties are also quite common and are indicative of an I-type setting. Most granitic varieties bear mafic microgranular enclaves ranging from a few cm to a couple of dm. Quartz-rich coarse-grained equigranular granites from the northern Backer and Brownson Islands also comprise red, euhedral garnet of 1-2 mm. On Waite Island hornblende- and biotite-bearing granodiorites show locally a weak magmatic foliation. Gabbroic rocks were only observed on the Brownson Islands where they form pyroxene-plagioclase-rich layers of different grain sizes. Felsic to mafic dikes frequently cross-cut the granitic to gabbroic basement (Fig. 8.2a); they occur in very high numbers on Lindsey and Schaefer Islands. Coarse-grained gneisses occur on the Early Islands as well as on Clark and Molar Islands. Pankhurst et al. (1998) constrained an Ordovician age for the gneisses on Clark Island. The gneisses mostly display a continuous gneissic foliation of alternating grey plagioclase-quartz-rich and black biotite-hornblende-rich bands (Fig. 8.2b). In addition, basaltic rocks with a black fine-grained groundmass and porphyritic plagioclase phenocrysts were observed on Clark Island, too.

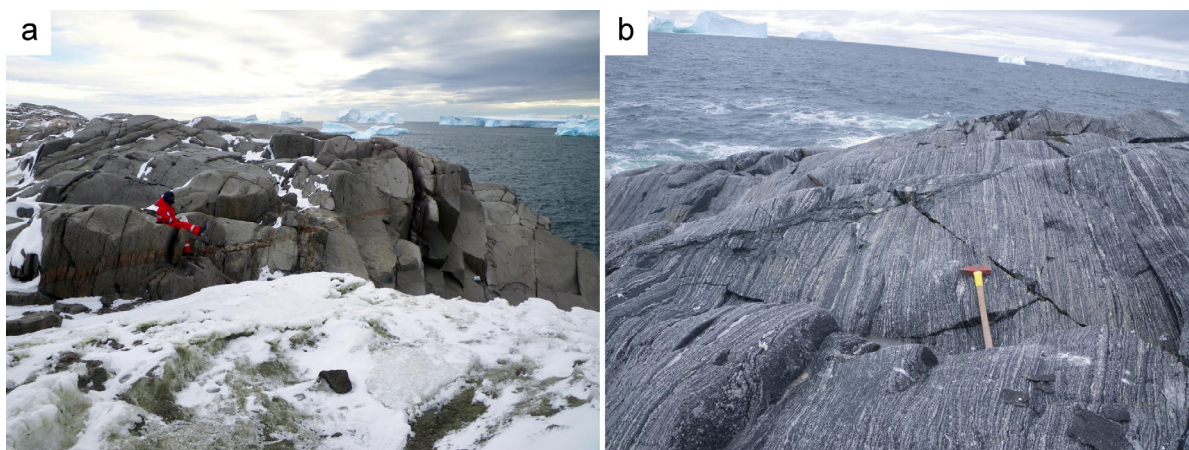


Fig. 8.2: a) Shallowly dipping rhyolitic dyke intruded granitic rocks on one of the Backer Islands, close to sample MZ17-14, view to the NW b) Banded orthogneiss forming some of the coastal outcrops of Clark Island, sample location MZ17-41, view to the E.

For cosmogenic exposure dating, 28 erratic block samples were taken from eleven islands (Fig. 8.1, Table 8.2). Sample locations on McKinzie, Dymont and Brownson Islands are characterized by glacial deposits of several tens of m² which comprised rounded boulders in varying compositions and sizes (Fig. 8.3a). At other localities individual erratic blocks were sitting on top of glacially eroded bedrock which locally showed well-defined glacial striations (Fig. 8.3b). E-W-striking stream-lined bedrock ridges were quite prominent on the Lindsey and Schaefer Islands and probably reflect glacial transport.

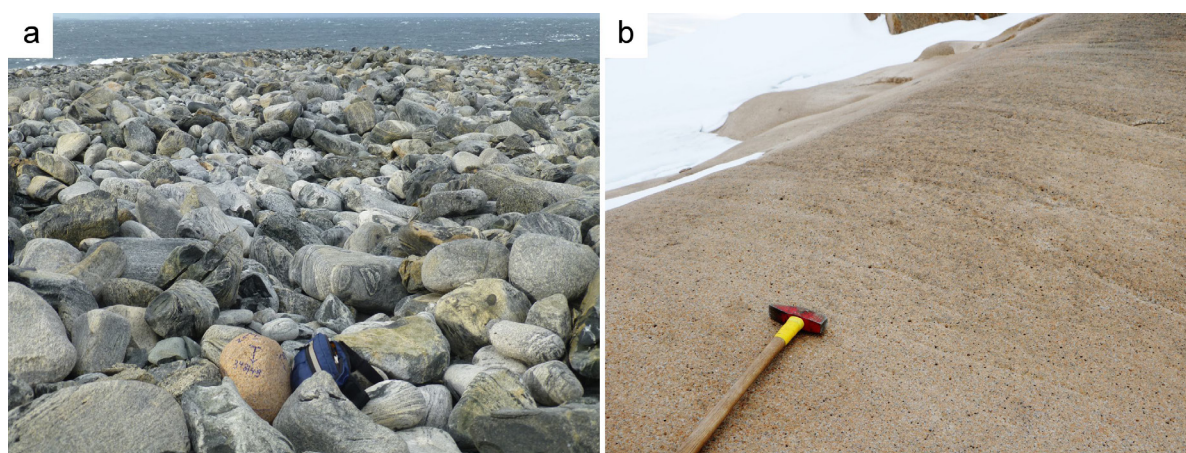


Fig. 8.3: a) Large rounded blocks form a glacial deposit on Dymont Island. The red granite block in the front was sampled (MZ17-58). View to the S. b) Glacial striations on a leucogranite from one of the Backer Islands, close to sample MZ17-18, view to the NW.

Martin Peninsula

Only one locality on Martin Peninsula was visited and sampled for thermochronology. This was the Siglin Rocks, a nunatak which rises ca. 50 m from the surrounding ice. The flat top yields many large angular blocks of the same composition which thus reflect the underlying geological unit: porphyritic hornblende- and biotite-bearing granite.

Detrital samples

Altogether nine detrital samples from seven box corer and two gravity corer sites were taken (Fig. 8.1). The samples were sieved in order to obtain the coarse clastic material >2 mm. At two locations the sand fraction was also sampled. Most of the box corers were rich in coarse-grained material, with single dropstones up to 20 cm in size. The samples generally yield a high proportion of plutonic rocks, mostly of granitic to granodioritic composition which reflect their high abundance in the source areas and the relative high erosional resistivity of quartz-bearing lithologies. Less abundant were rhyolitic to basaltic volcanic rocks and their sedimentary derivatives. Banded quartz-rich metamorphic rocks (gneisses and migmatites) were also present. Non-volcanic sedimentary rocks were generally absent.

Data management

All data and associated metadata will be stored in the Data Publisher for Earth & Environmental Science PANGAEA (www.pangaea.de).

Tab. 8.1: Samples collected for thermochronological, thin section and structural analyses. Detrital samples were collected by gravity (†) and box corer (‡).

No	ID	Lat. S	Long. W	elev. m	Locality	Region	Lithology
1	MZ17-01	-72.72	-103.45	0	Waite Island	KP	hbl-bt-granodiorite
2	MZ17-03	-74.51	-102.44	44	Backer Islands	PIB	porphyritic bt-granite
3	MZ17-07	-74.47	-102.30	3	Backer Islands	PIB	hbl-bt-granite
4	MZ17-09	-74.44	-102.55	13	Backer Islands	PIB	leucogranite
5	MZ17-11	-74.34	-102.81	10	Backer Islands	PIB	porphyritic hbl-bt-granite
6	MZ17-12	-74.34	-102.82	23	Backer Islands	PIB	porphyritic hbl-bt-granite
7	MZ17-13	-74.34	-102.81	7	Backer Islands	PIB	rhyolitic dike
8	MZ17-14	-74.34	-102.82	1	Backer Islands	PIB	cataclastic granite
9	MZ17-21	-74.45	-102.37	14	Backer Islands	PIB	Grt-ms-pegmatite
10	MZ17-22	-74.45	-102.37	15	Backer Islands	PIB	leucogranite
11	MZ17-23	-74.42	-102.44	10	Backer Islands	PIB	qz-rich bt-granite
12	MZ17-31	-74.34	-102.81	15	Backer Islands	PIB	rhyolitic dike
13	MZ17-34	-74.17	-103.64	24	Brownson Islands	PIB	bt-granite
14	MZ17-35	-74.05	-105.19	4	Clark Island	PIB	granitic/gneissic enclave
15	MZ17-36	-74.05	-105.19	4	Clark Island	PIB	felsic enclave
16	MZ17-37	-74.05	-105.19	4	Clark Island	PIB	porphyritic basalt
17	MZ17-39	-74.07	-105.15	5	Clark Island	PIB	hbl-bt-orthogneiss
18	MZ17-40	-74.09	-105.17	12	Clark Island	PIB	hbl-bt-orthogneiss
19	MZ17-41	-74.09	-105.17	12	Clark Island	PIB	hbl-bt-orthogneiss
20	MZ17-42	-73.97	-104.14	3	Jaynes Island	PIB	hbl-bt-granodiorite
21	MZ17-45	-73.60	-103.13	10	Lindsey Islands	CP	grey bt-granite
22	MZ17-47	-73.64	-103.23	5	Schaefer Islands	CP	grey bt-granite
23	MZ17-49	-73.64	-103.23	11	Schaefer Islands	CP	porphyritic basaltic dike
24	MZ17-50	-73.64	-103.23	11	Schaefer Islands	CP	felsic dike
25	MZ17-51	-73.64	-103.23	11	Schaefer Islands	CP	mafic dike
26	MZ17-52	-73.65	-103.22	1	Schaefer Islands	CP	bt-granite
27	MZ17-53	-73.66	-101.37	5	Molar Island	FB	hbl-bt-orthogneiss

8. Exhumation and Deglaciation of the Amundsen Sea Region

No	ID	Lat. S	Long. W	elev. m	Locality	Region	Lithology
28	MZ17-54	-73.66	-101.53	7	Early Islands	FB	hbl-bt-orthogneiss
29	MZ17-55	-72.70	-103.49	12	Waite Island	KP	hbl-bt-granodiorite
30	MZ17-56	-72.71	-103.43	15	Waite Islands	KP	hbl-bt-granodiorite
31	MZ17-57	-72.71	-103.43	15	Waite Islands	KP	hbl-bt-granodiorite
32	MZ17-60	-74.13	-101.93	3	Dyment Island	CB	layered bt-granite
33	MZ17-61	-74.38	-102.67	10	Backer Islands	PIB	porphyritic bt-granite
34	MZ17-62	-74.18	-115.10	143	Siglin Rocks	MP	hbl-bt-granite
35	PS104/001-2†	-71.88	-103.38	-745	Cosgrove-Abbot-Trough		grain-size >5mm, variable rock types
36	PS104/007-2‡	-74.87	-100.76	-698	SE Pine Island Ice Shelf front		coarse-grained magmatic dropstone
37	PS104/008-2†	-74.87	-100.71	-698	SE Pine Island Ice Shelf front		grain-size >5mm, variable rock types
38	PS104/012-1‡	-74.68	-101.62	-358	E Pine Island Bay		grain-size >20mm, variable rock types
39	PS104/022-3‡	-72.77	-107.09	-733	Pine Island Trough		grain-size >2 to >50mm, variable rock types
40	PS104/031-2‡	-73.08	-103.83	-577	Cosgrove-Abbot-Trough		grain-size <2 to >50mm, variable rock types
41	PS104/035-2‡	-74.56	-102.62	-336	NE Pine Island Bay		grain-size >2mm, variable rock types
42	PS104/036-1‡	-74.53	-102.62	-618	NE Pine Island Bay		grain-size >2mm, variable rock types
43	PS104/043-3‡	-73.30	-112.33	-482	Bear Ridge		grain-size <2 to >20mm, variable rock types,

BR-Bear Ridge; bt-biotite; CB-Cranton Bay; CP-Canisteo Peninsula; FB-Ferrero Bay; grt-garnet; hbl-hornblende; MP-Martin Peninsula; ms-muscovite; PIB-Pine Island Bay; qz- quartz

Tab. 8.2: Samples collected for cosmogenic exposure dating

No	ID	Lat. S	Long. W	elev. m	Locality	Region	Lithology
1	MZ17-02	-74.51	-102.44	44	Backer Islands	PIB	red AKfs-granite
2	MZ17-04	-74.51	-102.44	44	Backer Islands	PIB	red porphyritic bt-granite
3	MZ17-05	-74.51	-102.44	44	Backer Islands	PIB	qz-diorite
4	MZ17-06	-74.47	-102.30	21	Backer Islands	PIB	red porphyritic bt-granite
5	MZ17-08	-74.47	-102.30	3	Backer Islands	PIB	red AKfs-granite
6	MZ17-10	-74.51	-102.44	40	Backer Islands	PIB	red AKfs-granite
7	MZ17-15	-74.03	-101.75	1	McKinzie Islands	CB	red granite
8	MZ17-16	-74.03	-101.74	3	McKinzie Islands	CB	red granite
9	MZ17-17	-74.03	-101.75	1	McKinzie Islands	CB	red granite
10	MZ17-18	-74.45	-102.37	11	Backer Islands	PIB	leucogranite
11	MZ17-19	-74.45	-102.37	6	Backer Islands	PIB	qz-amphibolite
12	MZ17-20	-74.45	-102.37	6	Backer Islands	PIB	red bt-granite
13	MZ17-24	-74.14	-103.33	5	Brownson Islands	PIB	red AKfs-granite

No	ID	Lat. S	Long. W	elev. m	Locality	Region	Lithology
14	MZ17-25	-74.14	-103.33	3	Brownson Islands	PIB	grey hbl-bt-granite
15	MZ17-26	-74.14	-103.33	3	Brownson Islands	PIB	porphyritic bt-granite
16	MZ17-27	-74.14	-103.33	3	Brownson Islands	PIB	granite
17	MZ17-28	-74.14	-103.37	15	Brownson Islands	PIB	bt-granite
18	MZ17-29	-74.14	-103.37	15	Brownson Islands	PIB	bt-granite
19	MZ17-30	-74.51	-102.44	36	Backer Islands	PIB	red AKfs-granite
20	MZ17-32	-74.17	-103.64	24	Brownson Islands	PIB	grey bt-granite
21	MZ17-33	-74.17	-103.64	24	Brownson Islands	PIB	porphyritic bt-granite
22	MZ17-38	-74.07	-105.15	5	Clark Island	PIB	bt-granite
23	MZ17-43	-73.60	-103.12	4	Lindsey Islands	CP	pink bt-granite
24	MZ17-44	-73.60	-103.12	4	Lindsey Islands	CP	qz-hbl-diorite
25	MZ17-46	-73.64	-103.23	4	Schaefer Islands	CP	banded hbl-bt-gneiss
26	MZ17-48	-73.60	-103.13	18	Lindsey Islands	CP	red AKfs-granite
27	MZ17-58	-74.12	-101.93	10	Dyment Island	CB	red bt-granite
28	MZ17-59	-74.13	-101.93	4	Dyment Island	CB	porphyritic bt-granite

AKfs-Alkalifeldspar, bt-biotite; CB-Cranton Bay; CP-Canisteo Peninsula; FB-Ferrero Bay; hbl-hornblende; MP-Martin Peninsula; PIB-Pine Island Bay; qz- quartz

References

- Barker PF, Camerlenghi A (2002) Glacial history of the Antarctic Peninsula from Pacific margin sediments. Proceedings of the ocean drilling program, scientific results, 178, 1-40.
- Johnson JS, Bentley MJ, Gohl K (2008) First exposure ages from the Amundsen Sea Embayment, West Antarctica: the late quaternary context for recent thinning of Pine Island, Smith, and Pope Glaciers. *Geology*, 36, 223-226.
- Lindow J., Castex M, Wittmann H, Johnson JS, Lisker F, Gohl K, and Spiegel C (2014) Glacial retreat in the Amundsen Sea sector, West Antarctica—first cosmogenic evidence from central Pine Island Bay and the Kohler Range. *Quaternary Science Reviews*, 98, 166-173.
- Mukasa, SB, Dalziel IWD (2000) Marie Byrd Land, West Antarctica: Evolution of Gondwana's Pacific margin constrained by zircon U-Pb geochronology and feldspar common-Pb isotopic compositions. *Geological Society of America Bulletin*, 112(4), 611-627.
- Pankhurst RJ, Weaver SD, Bradshaw JD, Storey BC, Ireland TR (1998) Geochronology and geochemistry of pre-Jurassic superterranes in Marie Byrd Land, Antarctica. *Journal of Geophys. Res.: Solid Earth*, 103(B2), 2529-2547.
- Spiegel C, Lindow J, Kamp PJ, Meisel O, Mukasa S, Lisker F, Kuhn G, and Gohl G (2016) Tectonomorphic evolution of Marie Byrd Land – Implications for Cenozoic rifting activity and onset of West Antarctic glaciation. *Global and Planetary Change*, 145, 98-115.
- Wilson DS, Pollard D, DeConto RM, Jamieson SSR, Luyendyk BP (2013) Initiation of the West Antarctic Ice Sheet and estimates of total Antarctic ice volume in the earliest Oligocene. *Geophys. Res. Lett.*, 40(16), 4305-4309.

9. REPEATED GNSS MEASUREMENTS IN THE AMUNDSEN SEA REGION TO INVESTIGATE GLACIAL ISOSTATIC ADJUSTMENT AND ICE-SHELF DYNAMICS

Mirko Scheinert, Benjamin Ebermann

TU Dresden

Grant-No. AWI_PS104_03

Objectives

The current Antarctic ice-mass loss in the order of 100 Gt/a is greatly countered by the mass imbalance of the West Antarctic Ice Sheet (WAIS). The WAIS contribution is equivalent to a mean global (eustatic) sea-level change of approx. +0.4 mm/a. The most sensitive region is the Amundsen Sea Embayment with the large outlet glaciers Pine Island, Thwaites and Smith Glacier. In order to come up with reliable estimates of the ice-mass balance the geodetic methods of satellite gravimetry and satellite altimetry are being utilized. Their results have to be corrected for the effect of glacial isostatic adjustment (GIA). However, the GIA correction still forms a main source of uncertainty and, especially for satellite gravimetry, the largest error contribution. The GIA mass effect stays in the same order of magnitude as present ice-mass changes themselves (Groh et al., 2012, 2014). Models that are being used to predict the GIA effects still lack observational constraints as well as sufficient complexity in terms of ice-load history and rheology. Geodetic GNSS measurements on bedrock deliver independent data to validate GIA models (e.g. IJ05-R2 (Ivins et al., 2013) or W12a (Whitehouse et al., 2012)). Even more, geodetic GNSS provides the only tool to directly measure the GIA effect. The originally inferred height change includes the sum of the GIA effect and the elastic deformation due to present-day ice-mass changes. The latter can be determined by means of satellite altimetry and, hence, separated from the total deformation.

Already in 2006 and 2010 we realized GNSS measurements in the area of investigation. For three stations (PIG2, MANT and BEAR) vertical deformation rates from 14 to 22 mm/a were determined from these repeated GNSS observations (Groh et al., 2012). In 2010 it was not possible to realize measurements at the fourth site MURP, such that for this station a respective result cannot be given yet. However, due to a cooperation with BAS, the site MURP could be measured for about one week in the Antarctic season 2015/2016. Hence, further GNSS measurements are needed to improve the reliability and accuracy of the inferred results. The long time basis of ten years and the technologically identical setup enable us to reach an accuracy for the inferred linear trend comparable to that gained from continuous observations. Even more, it is our aim to discriminate areas of increased ice-mass loss as it would be expected e.g. for Smith Glacier.

A further goal of this project is to collect organic material (excrement, guano, lichens) which may, once dated, serve as a proxy for minimum ages of recent deglaciation and for recent sea level curves, respectively.

Furthermore, GNSS measurements on ice shelves (preferably Crosson and Dotson) shall complement the program to investigate tidal dynamics in the coastal areas, where satellite altimetry or classic tide gauge measurements are not feasible. In combination with geodetic

remote sensing techniques (feature tracking, SAR interferometry) the flow regime of the outlet glaciers and their adjacent ice shelves can be determined.

Work at sea

All locations to be investigated are situated on land. Hence, they could only be reached by helicopter. In order to stick with the regulations and to make optimal usage of helicopter operations, these land visits were coordinated and mainly realized together with the land geology group (see Chapter 7). Fig. 9.1 gives an overview on all sites where we realized GPS measurements and took samples.

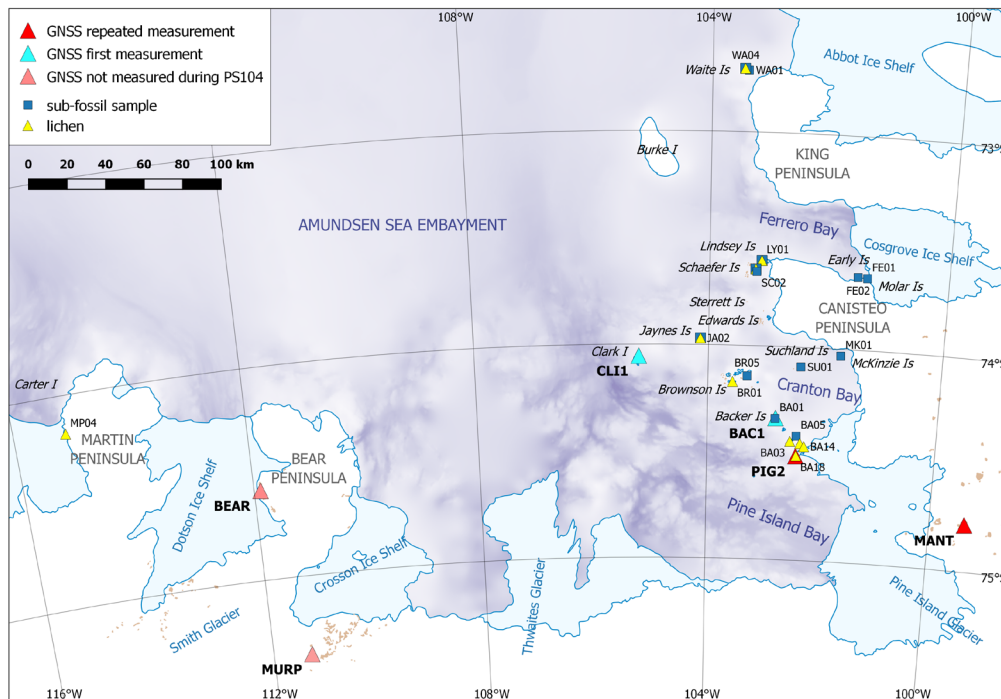


Fig. 9.1: Overview map with GNSS sites and locations of sub-fossil and lichen samples

Due to weather, ice conditions and time schedule it was not possible to reach the GPS sites MURP (Mt. Murphy) and BEAR (Bear Peninsula). At the sites MANT (Mt. Manthe) and PIG2 (southern Backer Islands, at the edge of the Northern Pine Island Ice Shelf) repeated GPS measurements could be carried out. Additionally, at two locations new GPS sites could be marked and measured for the first time, namely at northern Backer Islands (BAC1) and at Clark Island (CLI1). At each site, the power supply was realized by means of one 34Ah sealed battery and two 30W solar panels. The set-up of these four sites is illustrated by Fig. 9.2. The observation time of all GPS stations is given in Table 9.1.

At BAC1 the equipment was supplemented by a radio modem to broadcast correction data that could be received by a specially equipped receiver to be handled in the so-called RTK mode (real-time kinematic). The configuration included a special directional antenna and an enhanced power supply, see Fig. 9.2.

The RTK measurements were carried out using a geodetic GPS receiver in the so-called rover mode. For this, the receiver (powered by a small internal battery) is transported in a special bag, and the antenna is mounted on a special rod that enables to mark the location to be

measured, see Fig. 9.3. With receiving the correction signal the RTK rover can determine the position with an accuracy in the centimeter level within very short time (less than one minute). If the correction signal cannot be received the accuracy is only in the meter level and can possibly be improved by post-processing whenever other reference stations can be used. These RTK measurements should be used to determining the positions where sub-fossil and lichen samples were taken (for the days of observation see Table 9.1).

Tab. 9.1: Overview of GPS measurements

Site ID	MANT	PIG2	BAC1	CLI1	RTK
Receiver	Trimble R7	Trimble R7	Leica GR25	Leica GRX 1200+GNSS	Leica GS25
Antenna	Trimble Microcentd.	Trimble Microcentd.	Leica AR10	Leica AR10	Leica AX 1203 +GNSS
Obs Time					
February	13				
	14				
	15				
	16				
	17				
	18				
	19				
	20				
	21				
	22				
	23				
	24				
	25				
	26				
	27				
	28				
March	1				
	2				
	3				
	4				
	5				
<i>All times are UTC.</i>					
<i>Observation time less than 24 hours.</i>					
<i>Observation time 24 hours.</i>					
<i>RTK: Real Time Kinematic (Solutions in the cm-level were possible only when the reference station at BAC1 was running from 17 to 20 Feb 2017.)</i>					

As for the sites MURP and BEAR (see above) it was not possible to deploy any GPS equipment at one of the ice shelves (Northern Pine Island Glacier Ice Shelf, Crosson or Dotson Ice Shelf). Especially the weather conditions (low visibility and/or bad contrasts) prevented any helicopter landing at the ice shelf.

Furthermore, 20 samples of lichen as well as 32 samples of sub-fossil material (bones, guano, skin, teeth) were taken at numerous locations at the islands in Pine Island Bay, Cranton Bay, Ferrero Bay and surroundings, see Fig. 9.4 and Tables 9.2 and 9.3. Thereof, one lichen sample could be taken at a location visited at Martin Peninsula. Thus, it could be proven that lichens occur also under the harsh conditions of the coastal areas of Amundsen Sea Embayment.



Fig. 9.2: GPS sites on bedrock. Clockwise from upper left: Backer Islands North (BAC1), Mt. Manthe (MANT), Backer Islands South (PIG2), Clark Island (CLI1). The GPS antenna is always fixed directly to the bedrock by means of a special bolt. Solar panels provide power to charge the batteries, which are placed together with the GPS receiver within the Zarges aluminium box.



Fig. 9.3: GPS real-time kinematic (RTK). The antenna is mounted on a special rod of defined length that enables to marking the location to be measured. The receiver is carried in a special bag. Left: Suchland Islands (site SU01), right: Molar Islands (site FE01)

Preliminary results

The analysis of the GPS data will be done at the home institution in post-processing applying differential GPS (DGPS) strategies. For this, further reference stations of the International GNSS Service (IGS) in Antarctica and the surrounding continents will be used along with precise orbit and clock data. While for the sites PIG2 and MANT new vertical deformation results can be expected (through the combination with the 2006 and 2010 measurements), for the sites BAC1 and CLI1 we will get only the result of the first observation epoch.

Likewise, the RTK data will be examined, and especially in those cases where no correction signal could be received a DGPS analysis eventually will enable to strive for a better accuracy of the positioning.

The sub-fossil material will be analysed by cooperation with Mike Bentley, Durham University (UK), and the lichen samples by cooperation with Sieglinde Ott, University of Dusseldorf.



Fig. 9.4: Left: Lichen sample (Brownson Islands). Right: Digging in a pebble place of an abandoned penguin colony for sampling lowermost layers of guano (Waite Islands)

Tab. 9.2: Overview of sampled lichens

ISLAND	ID	Latitude	Longitude	Sample ID	Date	Note
		[°]	[°]			
Backer	BA14	-74,4651	-102,3021	#1	16.02.2017	crustose lichen
				#2-1	16.02.2017	yellow-orange, with crustose l., weathered surface
	#2-2					
	BA03	-74,4429	-102,5503	#3-1	16.02.2017	bigger crustose l., yellow-orange
				#3-2		
	BA18	-74,5097	-102,4344	#4-A	16.02.2017	crustose lichens
	BA06	-74,4508	-102,3736	#4	18.02.2017	crustose lichen
				#5		
#6				1m apart from #4/#5		
#7-1				bigger crustose lichen		
#7-2					--, same location	
#8				yellow lichen		
#8-Z	moss					
Brownson	BR01	-74,1708	-103,5772	#9	20.02.2017	numerous lichens (black and yellow)
				#10		
Jaynes	JA02	-73,9700	-104,1380	#11	23.02.2017	moss
Lindsey	LY01	-73,6009	-103,1361	#12	25.02.2017	sample with stone
Schaefer	SC01	-73,6410	-103,2328	#13	25.02.2017	large-surface lichens
Waite	WA04	-72,7048	-103,4915	#14	28.02.2017	yellow lichen
Martin Peninsula	MP04	-74,1813	-115,1031	#15	06.03.2017	black lichens, higher growth

Tab. 9.3: Overview of sampled sub-fossil material.

ISLAND	ID	Latitude	Longitude	Sample ID	Date	Remark
		[°]	[°]			
Molar	FE01	-73,6627	-101,3692	#B19	27.02.2017	deposits
				#B20	27.02.2017	deposits (brownish)
				#B21	27.02.2017	deposits (white)
Early	FE02	-73,6595	-101,5275	#B22	27.02.2017	deposits
				#B23	27.02.2017	Guano
				#B24	27.02.2017	Penguin sample
McKinzie	MK01	-74,0321	-101,7418	#B01	18.02.2017	bone
Suchland	SU01	-74,0919	-102,4126	#B08	20.02.2017	bone, +??
				#B09	20.02.2017	?? Guano
				#B26	28.02.2017	Guano (beneath pebbles)
Waite	WA01	-72,7126	-103,4317	#B27	28.02.2017	bone
				#B25	28.02.2017	feather parts (?)
Lindsey	LY01	-73,6009	-103,1361	#B12	25.02.2017	bones
				#B13-1	25.02.2017	bones
				#B13-2	25.02.2017	bones
				#B13-3	25.02.2017	bones
Schaefer	SC01	-73,6410	-103,2328	#B14	25.02.2017	bones
				#B15-1	25.02.2017	bones
				#B15-2	25.02.2017	bones
				#B16	25.02.2017	bones
				#B17	26.02.2017	many bones
	SC02	-73,6526	-103,2154	#B18	26.02.2017	bones
Brownson	BR05	-74,1429	-103,3302	#B04	19.02.2017	bones
				#B05	19.02.2017	skin
				#B06	19.02.2017	bones, 6cm depth below surface
Jaynes	JA02	-73,9700	-104,1380	#B10	23.02.2017	bone
				#B11	23.02.2017	layer of dry material
Backer	BA01	-74,3382	-102,8232	#B07-1	20.02.2017	bones (seal?)
				#B07-2	20.02.2017	bones (seal?)
				#B07-3	20.02.2017	skin
				#B02	18.02.2017	jaw with teeth
	BA05	-74,4171	-102,4430	#B03	18.02.2017	skin (penguin?)

Data management

The geodetic GPS data will be stored within the frame of the SCAR GPS Database which is maintained at TU Dresden. The long-term preservation of the data will be maintained also through the close cooperation within the SCAR Scientific Programme SERCE (Solid Earth Responses and Influences on Cryosphere Evolution). A common structure of the data holdings is ensured through the application of the same scientific software package utilized to analyze geodetic GNSS measurements at TU Dresden (i.e., the Bernese GPS Software). Further products and resulting models will be archived in the PANGAEA database at AWI.

References

- Groh A, Ewert H, Scheinert M, Fritsche M, Rülke A, Richter A, Rosenau R, Dietrich R (2012) An Investigation of Glacial Isostatic Adjustment over the Amundsen Sea sector, West Antarctica. *Global Planet. Change*, 98–99, pp. 45–53.
- Groh A, Ewert H, Rosenau R, Fagiolini E, Gruber C, Floricioiu D, Abdel Jaber W, Linow S, Flechtner F, Eineder M, Dierking W, Dietrich R (2014) Mass, volume and velocity of the Antarctic Ice Sheet: present-day changes and error effects. *Surveys in Geophysics*, doi: 10.1007/s10712-014-9286-y.
- Ivins ER, James TS, Wahr J, Schrama EJO, Landerer FW, Simon KM (2013) Antarctic contribution to sea level rise observed by GRACE with improved GIA correction. *Journal of Geophysical Research: Solid Earth*, 118 (6), 3126–3141.
- Whitehouse PL, Bentley MJ, Milne GA, King MA, Thomas ID (2012) A new glacial isostatic adjustment model for Antarctica: calibrated and tested using observations of relative sea-level change and present-day uplift rates. *Geophys. J. Int.*, 190.3, 1464–1482.

10. HELICOPTER-MAGNETIC SURVEYING TO DELINEATE BASEMENT TECTONICS

Florian Riefstahl¹, Ricarda Dziadek¹,
Thorsten Eggers¹, Karsten Gohl¹

¹AWI

Grant-No. AWI_PS104_01

Objectives

Major boundaries between suspected crustal blocks and volcanic zones in Pine Island Bay have been proposed by various researchers without available data to prove their existence. The glacier troughs and Pine Island Bay itself are thought to have developed along such tectonic boundaries. Helicopter-magnetic surveys in the Pine Island Bay area provide the necessary database to map these boundaries and to derive models that link tectonic lineaments to preferential sedimentary and ice stream transport paths. The magnetic anomaly grid allows calculating the Curie depth or the depth to the bottom of the magnetic source to derive trends in geothermal heat flux (see also Chapter 7). The objectives of the aeromagnetic surveys are:

- Linking the AWI helicopter-magnetic flight lines of ANT-XXIII/4 in 2006 and ANT-XXVI/3 in 2010 (Gohl et al., 2013) with the AGASEA (University of Texas-Austin and BAS) aeromagnetic surveys from 2005 (Holt et al., 2007) to improve the levelling of the magnetic anomaly data between all three datasets.
- Increasing the number of survey and tie lines from ANT-XXIII/4 and ANT-XXVI/3 in areas with only poor coverage.
- Collection of aeromagnetic data in areas where no data exist already (i.e., inner Pine Island Bay, Thwaites Glacier, King Peninsula, Canisteo Peninsula, Thurston Island).
- Improving and expanding magnetic anomaly grids of the Amundsen Sea Embayment for delineation of tectonic structures as well as deriving Curie depths for deriving geothermal heat flux.

Work at sea

The recording of aeromagnetic data was performed using the AWI's Scintrex caesium vapour (CS-3) magnetometer, which was towed in a 'bird' 30 m below the helicopter BO-105 to avoid magnetic disturbances. The magnetometer was connected to the AGIS system (Airborne Geophysical Information System, PICO ENVIROTEC INC.), MMS-4 data acquisition receiver, GPS receiver (Hemisphere Crescent R100 GPS receiver) and radio altimeter on-board of the helicopter. The MMS-4 receiver processes the signal of the Scintrex magnetic sensor, whereas the AGIS allows displaying the received data on the operator's navigation screen, and storage of the collected data on hard disk.

Daily flight planning was done using ArcGIS and PICO's PEIConvert software. The combination of both programmes improves the flexibility of the operator to change the flight plans on fast response, which is essential in an area like the Amundsen Sea where changing ice and

weather conditions meant that the ship's itinerary was often altered on short notice. Also short-termed changes in the cruise plan required very fast response of the flight plans. The AGIS system is intended for survey plans covering large areas. Since the potential working areas cover several UTM zones, it was decided to use a Lambert conical projection for the area of Amundsen Sea (standard parallels = 75°S and 71°S; centre of projection = 73°S and 110°W; false northing/easting = 0/0). In this projection, survey and tie lines are only negligibly distorted. The AGIS software in the helicopter was fed with pre-compiled project files before every flight. Fig. 10.1 shows the area of the helicopter-magnetic survey tracks.

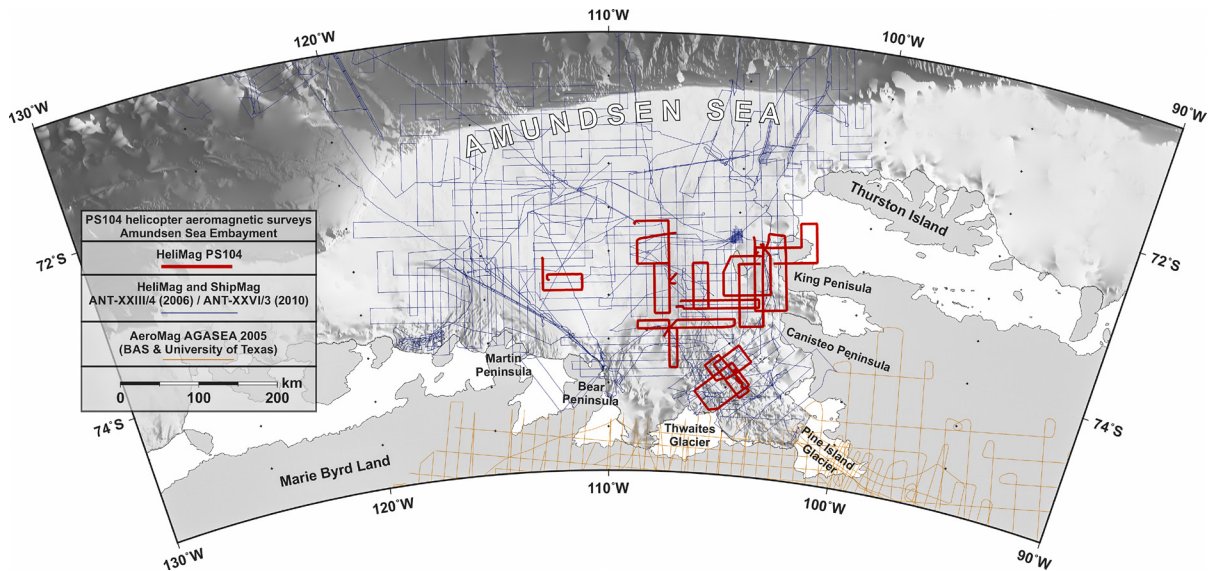


Fig. 10.1: Helicopter-magnetic survey tracks in the Amundsen Sea Embayment from this expedition (thick red lines) and previous expeditions from AWI (thin blue lines; Gohl et al., 2013) and BAS & University of Texas (thin orange coloured lines).

Data acquisition went smoothly most of the time. Known interactions of the magnetometer cable and HF communication with *Polarstern* were avoided by placing the magnetometer cable through the door on the right-hand side of the helicopter as far as possible away from the HF antenna. No interactions were observed during the flights radio communication with *Polarstern*. However, the “cold” start-up of the systems was often challenging which is likely related electrostatic charge of the helicopter, computers and / or the magnetometer in the bird. Several minutes after take-off from *Polarstern*, all computers worked normally and allowed continuous magnetic records along the planned flight tracks. From time to time flight tracks had to be re-planned during flight, especially during extended periods of local snowfall.

Flights in western direction (heading $270^\circ \pm 5^\circ$) were often associated with high-pitch noise in the magnetic signal. This noise is present if the magnetic sensor leaves the range of sensitivity and is most likely related to the setup of the magnetic sensor in the bird (47.5° angle), magnetic inclination in the area of Amundsen Sea and extensive movements of the bird during the flights. We tried to fly more north-south profile lines, if possible, to avoid these disturbances on east-west routes. However, this noise can be edited and filtered during post-processing of the magnetic field data.

An unexpected certification issue of the helicopter BO-105 delayed the beginning of the

magnetic surveys by more than one week, and alternating and unsteady weather conditions did not allow to take-off every day. It was possible to collect 2,876 km (1,552 nm) during 14 flights (and one test flight where no data were recorded). However, many flights had to be cancelled and some had to be reduced or even aborted due to weather conditions. Together with the magnetic field data collected during ANT-XXIII/4 in 2006 (20,900 km) and ANT-XXVI/3 in 2010 (15,300 km) (Gohl et al., 2013) the total distance of aeromagnetic flight lines in the Amundsen Sea Embayment was increased to 39,075 km.

Due to the delay of the survey, the important area of the southern Pine Island Bay could not be covered. Later, the weather conditions neither allowed to cross the aeromagnetic lines of the AGASEA project of University of Texas–Austin and BAS collected in 2005 (Holt et al., 2007) nor to cover the areas north of Bear Peninsula, Thwaites Glacier or the inner Pine Island Bay. Despite of the weather conditions, a first test flight over the Pine Island Trough (flight 000) did not yield usable data because of a mis-configuration of the GPS receiver, but it was possible to collect magnetic field data in the areas of the central Pine Island Trough (flights 001-004 and 012-013), between Canisteo and King Peninsula and Burke Island (flights 001 and 005-008) as well as in Pine Island Bay (flights 009-011). Additionally, the coverage of flight lines was extended up to 20 km farther east over King Peninsula (flights 007-008) (Flight details see Tab 10.1).

Tab. 10.1: Helicopter-magnetics flight details

Flight no.	Distance		Date	Time	Time rec.	File
	[nm]	[km]	[UTC]	[UTC]	[min]	
000	*	*	21/02/2017	*	*	test flight
001	118.4	219.4	22/02/2017	14:27	83	B7022220.P33
002	119.5	221.4	24/02/2017	18:14	84	B7022418.P15
003	100.9	187.1	25/02/2017	20:40	70	B7022520.P40
004	84.5	156.7	26/02/2017	21:44	59	B7022621.P44
005	124.8	231.4	27/02/2017	20:15	86	B7022720.P15
006	133.7	247.9	27/02/2017	22:39	92	B7022722.P40
007	130.8	242.5	28/02/2017	20:00	83	B7022819.P55
008	126.9	235.2	28/02/2017	22:32	87	B7022822.P32
009	109.2	202.4	03/03/2017	19:58	75	B7030319.P57
010	108.1	200.4	03/03/2017	21:51	77	B7030321.P56
011	60.1	111.4	04/03/2017	19:55	41	B7030419.P55
012	124.0	229.8	05/03/2017	15:48	81	B7030515.P46
013	121.3	224.9	05/03/2017	17:57	84	B7030517.P57
014	89.6	166.0	08/03/2017	22:11	59	B7030822.P12
Total	1552.1	2876.4	-	-	1061	-

Expected results

The first data processing was conducted after each flight, which included the conversion from

PEI binary format to ASCII format. After the expedition, the flight line data will be integrated into the existing magnetic database of this area to complement the magnetic anomaly grid. The refined grid will improve the analyses on the crustal type and characteristics of the crystalline basement in terms of its tectonic evolution.

Data management

All data will be uploaded into the AWI geophysical data archive as well as to the SCAR ADMAP database.

References

Gohl K, Denk A, Wobbe F, Eagles G (2013) Deciphering tectonic phases of the Amundsen Sea Embayment shelf, West Antarctica, from a magnetic anomaly grid, *Tectonophysics*, 585, 113-123, doi:10.1016/j.tecto.2012.06.036.

Holt JW, Blankenship DD, Ferraccioli F, Vaughan DG, Young DA, Kempf SD, Diehl TM (2007) New aeromagnetic results from the Thwaites Glacier catchment, West Antarctica: in *Antarctica: A Keystone in a Changing World – Online Proceedings of the 10th ISAES*, edited by Cooper, AK, Raymond, CR et al., USGS Open-File Report 2007-1047, Extended Abstract 153.

11. SATELLITE ICE RECONNAISSANCE BY NEAR REAL-TIME (NRT) SERVICE OF DLR

Karsten Gohl¹, Kathrin Höppner² (not on board),
Christine Wesche¹ (not on board)

¹AWI
²DLR

Objectives

Accurate sea-ice and iceberg reconnaissance was essential on this expedition, because the MeBo drilling operations required that *Polarstern* remained on station within a relatively small perimeter for 24 to 36 hours. In addition to radar and ice radar observations on the bridge and daily sea-ice concentration images from University of Bremen (<https://seaice.uni-bremen.de/sea-ice-concentration/>), high-resolution radar images help to identify areas of sea-ice cover and iceberg abundances, independent of cloud cover.

As part of a close cooperation between the Alfred Wegener Institute and the German Aerospace Center (DLR), *Polarstern* was supported by DLR on its cruise PS104 with high-resolution geo-coded radar images acquired by the German TerraSAR-X and TanDEM-X satellites. These current information on sea ice and iceberg conditions in the area of operation assisted *Polarstern's* sailing through ice-covered waters. The satellite data are received at DLR's German Antarctic Receiving Station (GARS) O'Higgins (northern Antarctic Peninsula) directly after the acquisition – in the best case within the same orbit, otherwise within the following one – and are locally processed in near real-time (NRT). Subsequently, just about 60 minutes after the raw data is acquired from the satellite, the information product is transferred via email from GARS O'Higgins to the ship. Such a product is generated up to two times a day.

The TerraSAR-X image acquisitions were provided through the DLR TerraSAR-X science project OCE3373.

Work at sea

For the NRT service to be useful, it was necessary that DLR received coordinates of targeted areas in which *Polarstern* was supposed to operate in the following two to four days. With such information, the appropriate image windows along particular orbits could be identified. Such NRT-processed TerraSAR-X or TanDEM-X images were received as geo-referenced PNG-formatted files on a daily basis for most days. Each image covers an area of about 100 x 150 km in size with a max. 18 m resolution. Depending on the satellite's orbit, images were available up to twice a day on some days. In cases of unfavourable orbits, a few days were lacking of images. As the planning for MeBo drill sites had to change quite frequently on short notice, it was not always possible to obtain the images of a particular area in time.

In general, the image coverage of the working area was quite sufficient and very useful for planning of the MeBo drill sites and the ship track (examples in Fig. 11.1). Although high concentrations of sea-ice was not a problem at the beginning of the working time spent on the Amundsen Sea Embayment shelf, it was the iceberg abundance at most planned drill sites that needed close attention. Many of the drill sites were chosen after assessing the TerraSAR-X/

TanDEM-X images for risks of icebergs and massive multi-year ice floes. The images were also used to help navigate the ship through belts of high iceberg abundances along the Bear Ridge between the eastern and western Amundsen Sea Embayment shelf.

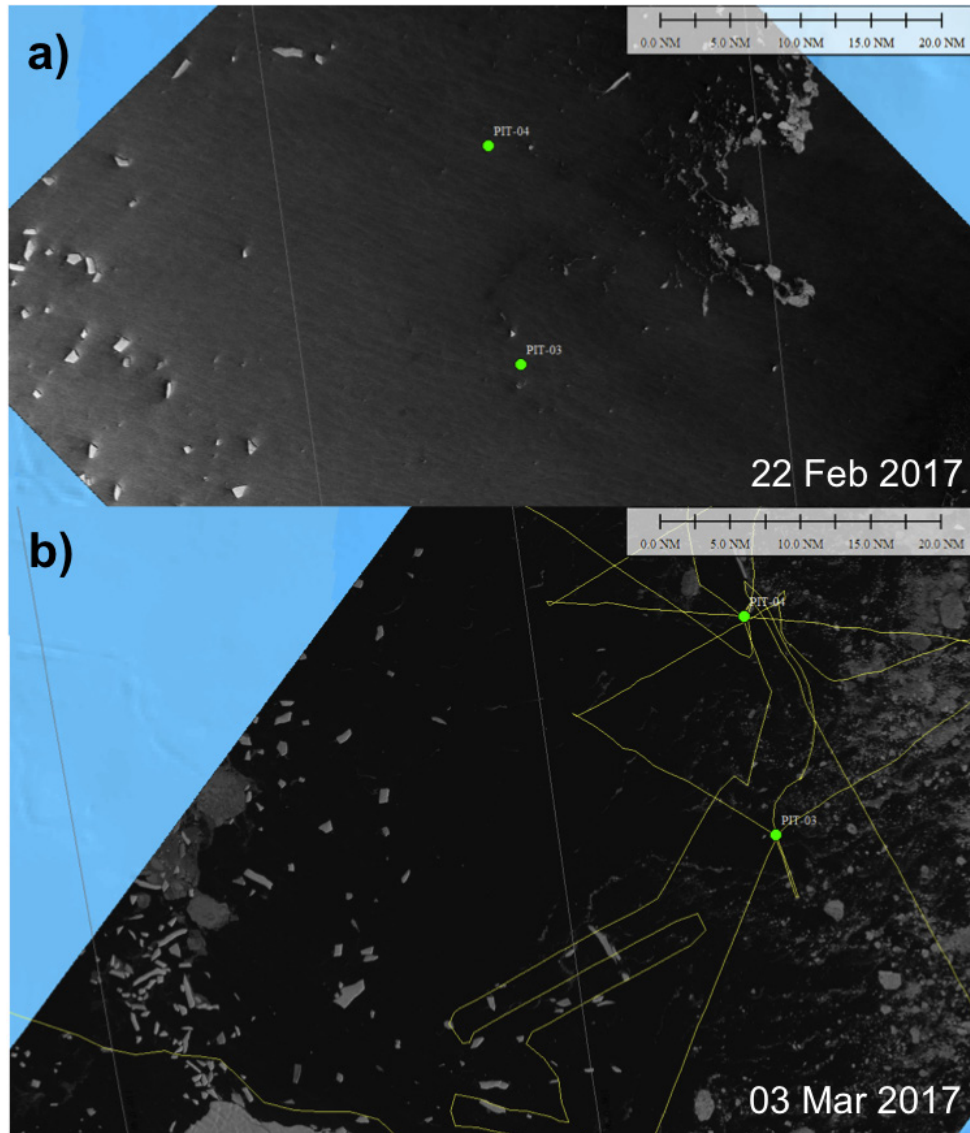


Fig. 11.1: Examples of TanDEM-X images (© DLR 2017) showing the distribution of icebergs and ice floe fields. (a) Image of 22 Feb 2017 was used to decide that MeBo drill sites PIT-03 and PIT-04 (yellow dots) have low risk of icebergs and sea-ice. Both sites were drilled between 22 and 25 Feb. (b) Image of 3 March 2017 shows that abundant icebergs and sea-ice drifted into the area, making further drilling operations near the existing two site too risky. Yellow lines mark the final ship track.

APPENDIX

A.1 PARTICIPATING INSTITUTIONS

A.2 CRUISE PARTICIPANTS

A.3 SHIP'S CREW

A.4 ACTION LOG / STATION LIST

A.1 TEILNEHMENDEINSTITUTE/PARTICIPATINGINSTITUTIONS

	Address
AWI	Alfred-Wegener-Institut Helmholtz-Zentrum für Polar- und Meeresforschung Am Alten Hafen 26 27568 Bremerhaven Germany
BAS	British Antarctic Survey High Cross, Madingley Road Cambridge, CB3 0ET UK
Bauer GmbH	Bauer Maschinen GmbH Bauer-Str. 1 86529 Schrobenhausen Germany
U Bremen	Universität Bremen Fachbereich Geowissenschaften Klagenfurter Str. 28359 Bremen Germany
TUD	Technische Universität Dresden Institut für Planetare Geodäsie 01062 Dresden Germany
DWD	Deutscher Wetterdienst Geschäftsbereich Wettervorhersage Seeschiffahrtsberatung Bernhard Nocht Str. 76 20359 Hamburg Germany
HeliService	Heli Service International GmbH Airport Emden Gorch-Fock-Str. 105 26721 Emden Germany

	Address
Imperial	Imperial College London Department of Earth Science & Engineering South Kensington Campus London SW7 2AZ UK
Lancaster U	Lancaster University Lancaster Environment Centre Lancaster LA1 4YQ UK
U Leipzig	Universität Leipzig Institut für Geophysik und Geologie Talstr. 35 04103 Leipzig Germany
MARUM	MARUM – Center for Marine Environmental Sciences Universität Bremen Leobener Str. 28359 Bremen Germany
Marybio	Marybio Malpú 871, 3 ^a 1006 ACK Capital Federal, Buenos Aires Argentina
U Southampton	University of Southampton National Oceanographic Centre Southampton European Way Southampton SO14 3ZH UK
VNII	VNII Okeangeologia 1, Angliysky Avenue St. Petersburg 190121 Russia

A.2 FAHRTTEILNEHMER / CRUISE PARTICIPANTS

Name/ Last name	Vorname/ First name	Institut/ Institute	Beruf/ Profession
Afanasyeva	Victoria	VNII	Geologist
Arevalo	Marcelo	AWI	Technician, geology
Arndt	Jan Erik	AWI	Geophysicist, bathymetry
Bergenthal	Markus	MARUM	Geologist/technician
Bickert	Torsten	MARUM	Geologist
Börner	Thomas	Bauer/MARUM	Technician, drilling
Bohaty	Steven	U Southampton	Geologist
Braakmann- Folgmann	Anne	AWI	Student, geodesy
Burkhardt	Elke	AWI	Biologist
Cammareri	Alejandro	Marybio	Biologist
Düßmann	Ralf	MARUM	Technician, drilling
Dziadek	Ricarda	AWI	PhD student, geophysics
Ebermann	Benjamin	TUD	Geodesist
Eggers	Thorsten	AWI	Technician, geophysics
Ehrmann	Werner	U Leipzig	Geologist
Esper	Oliver	AWI	Geologist
Flau	Michael	AWI	Technician, biology
Frederichs	Thomas	MARUM	Geophysicist
Freudenthal	Tim	MARUM	Geologist
Fröhlich	Siefke	MARUM	Technician, drilling
Gebhardt	Catalina	AWI	Geophysicist
Gohl	Karsten	AWI	Geophysicist / Chief-Scientist
Haupt	Tobias	AWI	Geodesist, bathymetry
Hillenbrand	Claus-Dieter	BAS	Geologist
Hochmuth	Katharina	AWI	Geophysicist
Kausche	Arne	MARUM	Technician, drilling
Klages	Johann	AWI	Geologist

Name/ Last name	Vorname/ First name	Institut/ Institute	Beruf/ Profession
Klein	Thorsten	MARUM	Technician, drilling
Küssner	Kevin	AWI	PhD student, geology
Larter	Robert	BAS	Geophysicist
Lensch	Norbert	AWI	Technician, geology
Najman	Yanina	Lancaster U	Geologist
Noorlander	Kees	MARUM	Technician, drilling
Pälike	Heiko	MARUM	Geologist
Reuter	Michael	MARUM	Technician, drilling
Riefstahl	Florian	AWI	PhD student, geophysics
Ronge	Thomas	AWI	Geologist
Scheinert	Mirko	TUD	Geodesist
Schüürman	Jan	AWI	Student, geology
Simoës Pereira	Patric	Imperial	PhD student, geology
Smith	James	BAS	Geologist
Uenzelmann- Neben	Gabriele	AWI	Geophysicist
van de Flierdt	Tina	Imperial	Geologist
Zundel	Max	U Bremen	PhD student, geology
Miller	Max	DWD	Meteorologist
Hempelt	Juliane	DWD	Technician, meteorology
Steffens	Martin	HeliService	Pilot, helicopter
Brauer	Jens	HeliService	Pilot, helicopter
Heckmann	Hans	HeliService	Technician, helicopter
Weißsohn	Jörn	HeliService	Technician, helicopter

A.3 SCHIFFSBESATZUNG / SHIP'S CREW

No.	Name	Rank
01.	Schwarze, Stefan	Master
02.	Grundmann, Uwe	1. Offc.
03.	Fallei, Holger	2. Offc.
04.	Hering, Igor	2. Offc.
05.	Langhinrichs, Moritz	2. Offc.
06.	Farysch, Bernd	Ch. Eng.
07.	Grafe, Jens	2. Eng.
08.	Krinfeld, Oleksandr	2. Eng.
09.	Holst, Wolfgang	3. Eng.
10.	Redmer, Jens	Elec. Eng.
11.	Christian, Boris	Comm. Offc.
12.	Frank, Gerhard	ELO
13.	Himmel, Frank	ELO
14.	Hüttebräucker, Olaf	ELO
15.	Nasis, Ilias	ELO
16.	Scholl, Thomas	Doctor
17.	Loidl, Reiner	Boatsw.
18.	Reise, Lutz	Carpenter
19.	Becker, Holger	A.B.
20.	Brück, Sebastian	A.B.
21.	Leisner, Karl-Heinz	A.B.
22.	Löscher, Steffen	A.B.
23.	Scheel, Sebastian	A.B.
24.	Bäcker, Andreas	A.B.
25.	Hagemann, Manfred	A.B.
26.	Wende, Uwe	A.B.
27.	Winkler, Michael	A.B.
28.	Preußner, Jörg	Storek.
29.	Lamm, Gerd	Mot-man
30.	Rhau, Lars-Peter	Mot-man
31.	Schünemann, Mario	Mot-man
32.	Schwarz, Uwe	Mot-man

No.	Name	Rank
33.	Teichert, Uwe	Mot-man
34.	Redmer, Klaus-Peter	Cook
35.	Martens, Michael	Cooksmate
36.	Silinski, Frank	Cooksmate
37.	Czyborra, Bärbel	1. Stwdess
38.	Wöckener, Martina	Stwdess/Nurse
39.	Chen, Dan Sheng	2. Steward
40.	Dibenau, Torsten	2. Steward
41.	Duka, Maribel	2. Stwdess
42.	Shi, Wubo	2. Steward
43.	Silinski, Carmen	2. Stwdess
44.	Sun, Yong Shen	2. Steward

A.4 STATIONSLISTE / STATION LIST PS104

Station	Date	Time	Latitude	Longitude	Depth (m)	Gear	Action	Comment
PS104_0_Underway-1	2017-02-03	11:56	-53,0206	-70,77243	67	WST	profile start	
PS104_0_Underway-2	2017-02-10	12:55	-57,04876	-80,11059	4742	ADCP_150	profile start	
PS104_0_Underway-2	2017-03-16	12:02	-55,39283	-78,80182	4387	ADCP_150	profile end	
PS104_0_Underway-3	2017-02-10	12:57	-57,04856	-80,11147	4741	TSG_KEEL	profile start	
PS104_0_Underway-3	2017-03-16	12:02	-55,39321	-78,80239	4387	TSG_KEEL	profile end	
PS104_0_Underway-4	2017-02-10	13:00	-57,05294	-80,11829	4711	GRAV	profile start	
PS104_0_Underway-4	2017-03-16	12:02	-55,39365	-78,80304	4387	GRAV	profile end	
PS104_0_Underway-5	2017-02-10	13:05	-57,06704	-80,13035	4803	MAG	profile start	
PS104_0_Underway-5	2017-03-16	12:02	-55,39445	-78,8042	4387	MAG	profile end	
PS104_0_Underway-6	2017-02-10	14:00	-57,21196	-80,29474	5129	HS	profile start	
PS104_0_Underway-6	2017-03-16	12:01	-55,39491	-78,80491	4387	HS	profile end	
PS104_0_Underway-7	2017-02-10	21:00	-58,36021	-81,69778	4576	PS	profile start	
PS104_0_Underway-7	2017-03-16	12:01	-55,39602	-78,80663	4387	PS	profile end	
PS104_0_Underway-8	2017-02-11	18:35	-61,83111	-86,28685	4855	FBOX	profile start	
PS104_0_Underway-8	2017-03-16	12:01	-55,39656	-78,80743	4387	FBOX	profile end	
PS104_0_Underway-9	2017-02-11	18:36	-61,83275	-86,28916	4863	PCO2_GO	profile start	
PS104_0_Underway-9	2017-03-16	12:00	-55,3971	-78,80824	4387	PCO2_GO	profile end	
PS104_0_Underway-10	2017-02-11	18:36	-61,83484	-86,29223	4842	PCO2_SUB	profile start	
PS104_0_Underway-10	2017-03-16	12:00	-55,39859	-78,81042	4386	PCO2_SUB	profile end	
PS104_1-1	2017-02-14	17:54	-71,87909	-103,38318	NA	TVMUC	station start	
PS104_1-1	2017-02-14	18:19	-71,87907	-103,38259	NA	TVMUC	at depth	
PS104_1-1	2017-02-14	18:39	-71,87878	-103,38326	NA	TVMUC	station end	
PS104_2-1	2017-02-14	19:47	-71,87894	-103,38386	NA	GC	station start	
PS104_2-1	2017-02-14	19:59	-71,87893	-103,38346	NA	GC	at depth	
PS104_2-1	2017-02-14	20:16	-71,87872	-103,38374	NA	GC	station end	
PS104_3-1	2017-02-15	15:36	-74,98356	-102,02104	904	MOOR	station start	
PS104_3-1	2017-02-15	16:28	-74,98243	-102,02238	925	MOOR	station end	

Station	Date	Time	Latitude	Longitude	Depth (m)	Gear	Action	Comment
PS104_4-1	2017-02-15	18:01	-74,95715	-101,82809	1041	CTDOZE	station start	
PS104_4-1	2017-02-15	18:34	-74,95791	-101,82918	1041	CTDOZE	at depth	
PS104_4-1	2017-02-15	19:06	-74,95793	-101,82886	1041	CTDOZE	station end	
PS104_4-2	2017-02-15	19:11	-74,95787	-101,82866	NA	GC	station start	
PS104_4-2	2017-02-15	19:28	-74,95775	-101,82856	NA	GC	at depth	
PS104_4-2	2017-02-15	19:48	-74,9577	-101,82888	NA	GC	station end	
PS104_4-3	2017-02-15	21:30	-74,95805	-101,826	NA	TVMUC	station start	
PS104_4-3	2017-02-15	21:57	-74,95807	-101,82555	NA	TVMUC	at depth	
PS104_4-3	2017-02-15	22:20	-74,95787	-101,82506	NA	TVMUC	station end	
PS104_5-1	2017-02-16	00:31	-74,95894	-101,8608	1026	refl	station start	
PS104_5-1	2017-02-16	02:31	-74,99213	-101,53348	1062	refl	profile start	
PS104_5-1	2017-02-16	15:07	-75,04366	-101,78681	922	refl	profile end	
PS104_5-1	2017-02-16	16:00	-75,06667	-101,91852	686	refl	station end	
PS104_6-1	2017-02-16	18:15	-74,96604	-101,74982	1050	GC	station start	
PS104_6-1	2017-02-16	18:33	-74,96593	-101,74856	NA	GC	at depth	
PS104_6-1	2017-02-16	19:01	-74,96609	-101,74937	NA	GC	station end	
PS104_6-2	2017-02-16	19:27	-74,96582	-101,74864	NA	MeBo70	station start	
PS104_6-2	2017-02-16	22:34	-74,96602	-101,74888	NA	MeBo70	at depth	
PS104_6-2	2017-02-17	17:18	-74,97492	-101,7611	NA	MeBo70	station end	
PS104_7-1	2017-02-17	20:54	-74,86548	-100,76078	698	CTDOZE	station start	
PS104_7-1	2017-02-17	21:21	-74,86609	-100,76011	698	CTDOZE	at depth	
PS104_7-1	2017-02-17	21:50	-74,86644	-100,76022	698	CTDOZE	station end	
PS104_7-2	2017-02-17	21:55	-74,86644	-100,76075	NA	BC	station start	
PS104_7-2	2017-02-17	22:10	-74,8664	-100,76096	NA	BC	at depth	
PS104_7-2	2017-02-17	22:23	-74,86669	-100,76087	NA	BC	station end	
PS104_8-1	2017-02-17	23:17	-74,8677	-100,71173	NA	BC	station start	
PS104_8-1	2017-02-17	23:32	-74,8672	-100,71096	NA	BC	at depth	
PS104_8-1	2017-02-17	23:49	-74,86686	-100,70963	NA	BC	station end	
PS104_8-2	2017-02-18	00:22	-74,86833	-100,71208	NA	GC	station start	
PS104_8-2	2017-02-18	00:33	-74,86845	-100,71148	NA	GC	at depth	
PS104_8-2	2017-02-18	00:58	-74,86817	-100,71184	NA	GC	station end	
PS104_9-1	2017-02-18	14:12	-74,98704	-101,86966	NA	GC	station start	
PS104_9-1	2017-02-18	14:28	-74,98688	-101,86893	NA	GC	at depth	
PS104_9-1	2017-02-18	14:56	-74,98727	-101,86986	NA	GC	station end	
PS104_9-2	2017-02-18	20:22	-74,98711	-101,87063	NA	MeBo70	station start	
PS104_9-2	2017-02-18	21:49	-74,98684	-101,86991	NA	MeBo70	at depth	
PS104_9-3	2017-02-19	08:36	-74,98665	-101,86784	NA	MeBo70	at depth	
PS104_9-3	2017-02-19	12:09	-74,98645	-101,86582	NA	MeBo70	station end	
PS104_10-1	2017-02-18	15:47	-75,03178	-101,94254	NA	HF	station start	
PS104_10-1	2017-02-18	16:09	-75,03091	-101,93866	NA	HF	at depth	
PS104_10-1	2017-02-18	16:41	-75,03112	-101,93839	NA	HF	station end	
PS104_11-1	2017-02-18	17:47	-74,9427	-102,29405	939	HF	station start	
PS104_11-1	2017-02-18	18:08	-74,94247	-102,29497	939	HF	at depth	

A.4 Stationsliste / Station List PS104

Station	Date	Time	Latitude	Longitude	Depth (m)	Gear	Action	Comment
PS104_11-1	2017-02-18	18:38	-74,94266	-102,29406	939	HF	station end	
PS104_12-1	2017-02-19	14:36	-74,68458	-101,62535	357	BC	station start	
PS104_12-1	2017-02-19	14:46	-74,68384	-101,62452	357	BC	at depth	
PS104_12-1	2017-02-19	14:56	-74,68371	-101,62681	357	BC	station end	
PS104_12-2	2017-02-19	15:36	-74,68372	-101,62268	NA	GC	station start	
PS104_12-2	2017-02-19	15:44	-74,68366	-101,62202	NA	GC	at depth	
PS104_12-2	2017-02-19	16:04	-74,68328	-101,62036	NA	GC	station end	
PS104_12-3	2017-02-19	17:32	-74,68385	-101,6247	NA	GC	station start	
PS104_12-3	2017-02-19	17:45	-74,68379	-101,62489	NA	GC	at depth	
PS104_12-3	2017-02-19	18:08	-74,68362	-101,62378	NA	GC	station end	
PS104_12-4	2017-02-19	18:53	-74,68364	-101,62416	NA	MUC	station start	
PS104_12-4	2017-02-19	19:04	-74,68355	-101,62378	NA	MUC	at depth	
PS104_12-4	2017-02-19	19:15	-74,6838	-101,62309	NA	MUC	station end	
PS104_13-1	2017-02-19	23:08	-74,83837	-101,0433	545	MUC	station start	
PS104_13-1	2017-02-19	23:25	-74,83802	-101,04381	545	MUC	at depth	
PS104_13-1	2017-02-19	23:39	-74,8379	-101,04388	545	MUC	station end	
PS104_13-2	2017-02-20	00:01	-74,83809	-101,0437	NA	GC	at depth	
PS104_13-2	2017-02-20	00:26	-74,83695	-101,04083	NA	GC	station end	
PS104_14-1	2017-02-20	04:44	-74,54944	-102,58605	599	GC	station start	
PS104_14-1	2017-02-20	04:58	-74,54898	-102,58599	599	GC	at depth	
PS104_14-1	2017-02-20	05:21	-74,54895	-102,58604	599	GC	station end	
PS104_14-2	2017-02-20	05:40	-74,54898	-102,58587	NA	MUC	station start	
PS104_14-2	2017-02-20	06:00	-74,549	-102,58568	NA	MUC	at depth	
PS104_14-2	2017-02-20	06:13	-74,54857	-102,58369	NA	MUC	station end	
PS104_14-3	2017-02-20	06:41	-74,54921	-102,58698	NA	GC	station start	
PS104_14-3	2017-02-20	06:51	-74,54896	-102,58678	NA	GC	at depth	
PS104_14-3	2017-02-20	07:06	-74,54876	-102,58403	NA	GC	station end	
PS104_15-1	2017-02-20	10:59	-74,80311	-102,34375	NA	HF	station start	
PS104_15-1	2017-02-20	11:18	-74,80301	-102,34366	NA	HF	at depth	
PS104_15-1	2017-02-20	11:48	-74,80352	-102,34368	NA	HF	station end	
PS104_16-1	2017-02-20	13:33	-74,98063	-102,02967	158	MOOR	station start	
PS104_16-1	2017-02-20	14:12	-74,9813	-102,03643	158	MOOR	station end	
PS104_17-1	2017-02-20	19:18	-74,35837	-104,74734	1395	CTDOZE	station start	
PS104_17-1	2017-02-20	19:54	-74,35941	-104,74736	1395	CTDOZE	at depth	
PS104_17-1	2017-02-20	20:33	-74,35905	-104,74748	1395	CTDOZE	station end	
PS104_17-2	2017-02-20	21:03	-74,35907	-104,74781	NA	MUC	station start	
PS104_17-2	2017-02-20	21:39	-74,35932	-104,74726	NA	MUC	at depth	
PS104_17-2	2017-02-20	22:01	-74,35954	-104,74877	NA	MUC	station end	
PS104_17-3	2017-02-20	22:36	-74,35931	-104,74708	1427	HF	station start	
PS104_17-3	2017-02-20	23:00	-74,35904	-104,74696	1427	HF	at depth	
PS104_17-3	2017-02-20	23:34	-74,3569	-104,75266	1427	HF	station end	
PS104_18-1	2017-02-20	23:50	-74,35536	-104,75794	1428	HF	station start	
PS104_18-1	2017-02-21	00:15	-74,35515	-104,75689	1428	HF	at depth	

Station	Date	Time	Latitude	Longitude	Depth (m)	Gear	Action	Comment
PS104_18-1	2017-02-21	00:45	-74,3555	-104,75932	1428	HF	station end	
PS104_19-1	2017-02-21	01:31	-74,36311	-105,14319	736	refl	station start	
PS104_19-1	2017-02-21	03:13	-74,35937	-104,71093	1381	refl	profile start	
PS104_19-1	2017-02-21	17:00	-73,42227	-106,89677	909	refl	profile end	
PS104_19-1	2017-02-21	17:42	-73,37882	-106,92795	904	refl	station end	
PS104_20-1	2017-02-21	22:41	-73,56835	-107,09249	946	GC	station start	
PS104_20-1	2017-02-21	22:54	-73,56814	-107,09278	946	GC	at depth	
PS104_20-1	2017-02-21	23:11	-73,56827	-107,09287	946	GC	station end	
PS104_20-2	2017-02-21	23:39	-73,5683	-107,0919	NA	MeBo70	station start	
PS104_20-2	2017-02-22	01:21	-73,56839	-107,09153	NA	MeBo70	at depth	
PS104_20-2	2017-02-23	03:51	-73,56835	-107,09394	NA	MeBo70	station end	
PS104_20-3	2017-02-23	04:04	-73,56824	-107,09356	947	GC	station start	
PS104_20-3	2017-02-23	04:18	-73,56818	-107,09367	947	GC	at depth	
PS104_20-3	2017-02-23	04:37	-73,56818	-107,09522	947	GC	station end	
PS104_21-1	2017-02-23	20:31	-73,30472	-107,11037	819	GC	station start	
PS104_21-1	2017-02-23	20:48	-73,30484	-107,10951	882	GC	at depth	
PS104_21-1	2017-02-23	21:09	-73,30482	-107,10998	NA	GC	station end	
PS104_21-2	2017-02-23	21:38	-73,30534	-107,10955	NA	MeBo70	station start	
PS104_21-2	2017-02-23	23:07	-73,30532	-107,10947	NA	MeBo70	at depth	
PS104_21-2	2017-02-24	07:42	-73,30525	-107,09843	NA	MeBo70	station end	
PS104_21-3	2017-02-25	02:35	-73,30552	-107,10765	NA	MeBo70	station start	
PS104_21-3	2017-02-25	03:53	-73,30551	-107,10688	NA	MeBo70	at depth	
PS104_21-3	2017-02-25	19:20	-73,30553	-107,10008	NA	MeBo70	station end	
PS104_22-1	2017-02-24	20:04	-72,76836	-107,09287	712	CTDOZE	station start	
PS104_22-1	2017-02-24	20:26	-72,76762	-107,09293	733	CTDOZE	at depth	
PS104_22-1	2017-02-24	20:50	-72,76774	-107,09314	733	CTDOZE	station end	
PS104_22-2	2017-02-24	21:03	-72,76782	-107,09264	732	GC	station start	
PS104_22-2	2017-02-24	21:14	-72,76781	-107,09242	733	GC	at depth	
PS104_22-2	2017-02-24	21:37	-72,76787	-107,09276	NA	GC	station end	
PS104_22-3	2017-02-24	21:51	-72,76791	-107,09242	NA	BC	station start	
PS104_22-3	2017-02-24	22:04	-72,76793	-107,09198	NA	BC	at depth	
PS104_22-3	2017-02-24	22:18	-72,76781	-107,09251	NA	BC	station end	
PS104_23-1	2017-02-25	20:15	-73,23233	-107,04895	834	refl	station start	
PS104_23-1	2017-02-25	22:27	-73,14853	-107,02004	792	refl	profile start	
PS104_23-1	2017-02-26	21:52	-73,37945	-106,83712	885	refl	profile end	
PS104_23-1	2017-02-26	22:34	-73,39352	-106,724	860	refl	station end	
PS104_24-1	2017-02-27	16:04	-72,99523	-103,83825	520	GC	station start	
PS104_24-1	2017-02-27	16:13	-72,99513	-103,83867	NA	GC	at depth	
PS104_24-1	2017-02-27	16:25	-72,99494	-103,83782	NA	GC	station end	
PS104_24-2	2017-02-27	16:44	-72,99515	-103,83756	NA	MeBo70	station start	
PS104_24-2	2017-02-27	17:47	-72,9952	-103,83716	NA	MeBo70	at depth	
PS104_24-2	2017-02-27	20:25	-72,99304	-103,84317	NA	MeBo70	station end	
PS104_25-1	2017-02-27	20:50	-72,9839	-103,90705	513	GC	station start	

A.4 Stationsliste / Station List PS104

Station	Date	Time	Latitude	Longitude	Depth (m)	Gear	Action	Comment
PS104_25-1	2017-02-27	20:59	-72,98336	-103,90729	530	GC	at depth	
PS104_25-1	2017-02-27	21:13	-72,98342	-103,90868	524	GC	station end	
PS104_26-1	2017-02-27	21:43	-72,96267	-103,9208	534	GC	station start	
PS104_26-1	2017-02-27	21:52	-72,96228	-103,92018	534	GC	at depth	
PS104_27-1	2017-02-27	22:41	-72,92103	-104,03034	515	GC	station start	
PS104_27-1	2017-02-27	22:51	-72,92092	-104,03004	515	GC	at depth	
PS104_27-1	2017-02-27	23:04	-72,92103	-104,03089	516	GC	station end	
PS104_28-1	2017-02-27	23:32	-72,89164	-104,09929	518	GC	station start	
PS104_28-1	2017-02-27	23:41	-72,89164	-104,09933	518	GC	at depth	
PS104_28-1	2017-02-27	23:55	-72,89189	-104,09967	518	GC	station end	
PS104_29-1	2017-02-28	01:36	-72,71925	-104,28612	539	GC	station start	
PS104_29-1	2017-02-28	01:45	-72,71952	-104,28431	535	GC	at depth	
PS104_29-1	2017-02-28	01:58	-72,71989	-104,28448	538	GC	station end	
PS104_30-1	2017-02-28	04:06	-72,90224	-104,19788	488	GC	station start	
PS104_30-1	2017-02-28	04:15	-72,90223	-104,19827	NA	GC	at depth	
PS104_30-1	2017-02-28	04:28	-72,90263	-104,19844	NA	GC	station end	
PS104_31-1	2017-02-28	05:54	-73,07652	-103,82902	561	GC	station start	
PS104_31-1	2017-02-28	06:06	-73,07669	-103,82917	NA	GC	at depth	
PS104_31-1	2017-02-28	06:19	-73,07628	-103,82824	NA	GC	station end	
PS104_31-2	2017-02-28	06:34	-73,077	-103,8275	NA	BC	station start	
PS104_31-2	2017-02-28	06:47	-73,07625	-103,82696	NA	BC	at depth	
PS104_31-2	2017-02-28	07:02	-73,07636	-103,82754	NA	BC	station end	
PS104_32-1	2017-02-28	15:27	-73,19654	-103,90868	667	refl	profile start	
PS104_32-1	2017-03-01	08:22	-73,1778	-104,08551	568	refl	profile end	
PS104_33-1	2017-03-01	15:25	-72,8913	-104,09926	NA	HF	station start	
PS104_33-1	2017-03-01	15:38	-72,89122	-104,0989	NA	HF	at depth	
PS104_33-1	2017-03-01	16:00	-72,89119	-104,09901	NA	HF	station end	
PS104_34-1	2017-03-02	06:13	-74,41617	-102,99146	769	GC	station start	
PS104_34-1	2017-03-02	06:27	-74,41607	-102,99122	NA	GC	at depth	
PS104_34-1	2017-03-02	06:46	-74,41576	-102,99097	NA	GC	station end	
PS104_34-2	2017-03-02	07:43	-74,41571	-102,99035	NA	HF	station start	
PS104_34-2	2017-03-02	08:12	-74,41554	-102,99027	NA	HF	at depth	
PS104_34-2	2017-03-02	08:38	-74,41591	-102,99114	NA	HF	station end	
PS104_34-3	2017-03-02	09:15	-74,41752	-103,00479	NA	HF	station start	
PS104_34-3	2017-03-02	09:32	-74,41725	-103,00534	NA	HF	at depth	
PS104_34-3	2017-03-02	09:58	-74,41729	-103,00562	NA	HF	station end	
PS104_34-4	2017-03-02	10:25	-74,41566	-103,00009	NA	HF	station start	
PS104_34-4	2017-03-02	10:42	-74,41589	-103,00096	NA	HF	at depth	
PS104_34-4	2017-03-02	11:11	-74,41549	-102,99972	NA	HF	station end	
PS104_34-5	2017-03-02	12:20	-74,41494	-102,99869	NA	HF	station start	
PS104_34-5	2017-03-02	12:38	-74,41494	-102,99765	NA	HF	at depth	
PS104_34-5	2017-03-02	12:59	-74,41447	-102,99551	NA	HF	station end	
PS104_34-6	2017-03-02	13:21	-74,41403	-102,99467	NA	HF	station start	

Station	Date	Time	Latitude	Longitude	Depth (m)	Gear	Action	Comment
PS104_34-6	2017-03-02	13:34	-74,414	-102,99461	NA	HF	at depth	
PS104_34-6	2017-03-02	13:55	-74,41402	-102,99519	NA	HF	station end	
PS104_34-7	2017-03-02	14:05	-74,41309	-102,99171	NA	HF	station start	
PS104_34-7	2017-03-02	14:16	-74,41306	-102,99157	NA	HF	at depth	
PS104_34-7	2017-03-02	14:53	-74,41319	-102,99179	NA	HF	station end	
PS104_34-8	2017-03-02	15:00	-74,41201	-102,98785	NA	HF	station start	
PS104_34-8	2017-03-02	15:11	-74,41215	-102,98831	NA	HF	at depth	
PS104_34-8	2017-03-02	15:32	-74,4122	-102,9883	NA	HF	station end	
PS104_34-9	2017-03-02	16:00	-74,41604	-102,98566	NA	HF	station start	
PS104_34-9	2017-03-02	16:14	-74,41608	-102,98653	NA	HF	at depth	
PS104_34-9	2017-03-02	16:39	-74,41619	-102,98578	NA	HF	station end	
PS104_34-10	2017-03-02	17:11	-74,41579	-102,99104	NA	GC	station start	
PS104_34-10	2017-03-02	17:25	-74,41588	-102,99118	NA	GC	at depth	
PS104_34-10	2017-03-02	17:42	-74,41671	-102,99212	NA	GC	station end	
PS104_35-1	2017-03-02	19:43	-74,56418	-102,62301	324	GC	station start	
PS104_35-1	2017-03-02	19:50	-74,5639	-102,6234	NA	GC	at depth	
PS104_35-1	2017-03-02	20:02	-74,56414	-102,62309	NA	GC	station end	
PS104_35-2	2017-03-02	20:15	-74,56382	-102,62342	NA	BC	station start	
PS104_35-2	2017-03-02	20:23	-74,56357	-102,62337	NA	BC	at depth	
PS104_35-2	2017-03-02	20:33	-74,56363	-102,62454	NA	BC	station end	
PS104_36-1	2017-03-02	20:59	-74,5334	-102,617	618	BC	station start	
PS104_36-1	2017-03-02	21:12	-74,53348	-102,61867	NA	BC	at depth	
PS104_36-1	2017-03-02	21:25	-74,5331	-102,6184	NA	BC	station end	
PS104_36-2	2017-03-02	21:51	-74,53288	-102,61989	NA	GC	station start	
PS104_36-2	2017-03-02	22:03	-74,53306	-102,62051	NA	GC	at depth	
PS104_36-2	2017-03-02	22:19	-74,53305	-102,62107	NA	GC	station end	
PS104_37-1	2017-03-03	05:07	-74,32988	-104,82188	NA	HF	station start	
PS104_37-1	2017-03-03	05:31	-74,32998	-104,82239	NA	HF	at depth	
PS104_37-2	2017-03-03	06:16	-74,33088	-104,81939	NA	HF	station start	
PS104_37-2	2017-03-03	06:36	-74,33091	-104,8194	NA	HF	at depth	
PS104_37-2	2017-03-03	07:07	-74,33126	-104,82117	NA	HF	station end	
PS104_37-3	2017-03-03	07:37	-74,33898	-104,79906	NA	HF	station start	
PS104_37-3	2017-03-03	07:58	-74,33898	-104,79917	NA	HF	at depth	
PS104_37-3	2017-03-03	08:28	-74,33966	-104,80117	NA	HF	station end	
PS104_37-4	2017-03-03	08:56	-74,34934	-104,72155	NA	HF	station start	
PS104_37-4	2017-03-03	09:15	-74,34947	-104,72133	NA	HF	at depth	
PS104_37-5	2017-03-03	10:18	-74,35519	-104,76041	NA	HF	station start	
PS104_37-5	2017-03-03	10:33	-74,35463	-104,75971	NA	HF	at depth	
PS104_37-5	2017-03-03	11:01	-74,35445	-104,75874	NA	HF	station end	
PS104_38-1	2017-03-03	12:23	-74,3497	-104,73958	NA	MeBo70	station start	
PS104_38-1	2017-03-03	14:16	-74,34937	-104,73938	NA	MeBo70	at depth	

A.4 Stationsliste / Station List PS104

Station	Date	Time	Latitude	Longitude	Depth (m)	Gear	Action	Comment
PS104_38-1	2017-03-04	22:45	-74,34954	-104,73652	NA	MeBo70	station end	
PS104_38-2	2017-03-04	23:06	-74,34934	-104,73818	NA	HF	station start	
PS104_38-2	2017-03-04	23:22	-74,34935	-104,73725	NA	HF	at depth	
PS104_38-2	2017-03-04	23:50	-74,34937	-104,73771	NA	HF	station end	
PS104_38-3	2017-03-05	00:07	-74,34949	-104,7366	NA	GC	station start	
PS104_38-3	2017-03-05	00:26	-74,34924	-104,73828	NA	GC	at depth	
PS104_38-3	2017-03-05	00:50	-74,34931	-104,73612	NA	GC	station end	
PS104_39-1	2017-03-05	01:20	-74,34429	-104,73326	1306	refl	station start	
PS104_39-1	2017-03-05	02:15	-74,31398	-104,6818	1024	refl	profile start	
PS104_39-1	2017-03-05	06:18	-74,31016	-105,06862	1133	refl	profile end	
PS104_40-1	2017-03-06	16:26	-73,29817	-112,32472	482	GC	station start	
PS104_40-1	2017-03-06	16:39	-73,29848	-112,32276	NA	GC	at depth	
PS104_40-1	2017-03-06	16:52	-73,29852	-112,32293	NA	GC	station end	
PS104_40-2	2017-03-06	17:43	-73,29693	-112,32401	483	MeBo70	station start	
PS104_40-2	2017-03-06	18:56	-73,2974	-112,32147	483	MeBo70	at depth	
PS104_40-2	2017-03-07	01:29	-73,2965	-112,33755	NA	MeBo70	station end	
PS104_40-3	2017-03-08	20:03	-73,29725	-112,32447	483	MeBo70	station start	
PS104_40-3	2017-03-08	20:59	-73,29655	-112,32294	NA	MeBo70	at depth	
PS104_40-3	2017-03-09	23:33	-73,29759	-112,32189	NA	MeBo70	station end	
PS104_41-1	2017-03-07	04:27	-73,05307	-111,96473	NA	MeBo70	station start	
PS104_41-1	2017-03-07	05:08	-73,05309	-111,96473	NA	MeBo70	at depth	
PS104_41-1	2017-03-07	14:50	-73,05311	-111,96401	NA	MeBo70	station end	
PS104_42-1	2017-03-07	19:03	-73,3315	-111,57856	NA	MeBo70	station start	
PS104_42-1	2017-03-07	20:30	-73,33152	-111,5783	NA	MeBo70	at depth	
PS104_42-1	2017-03-08	14:20	-73,33166	-111,5806	NA	MeBo70	station end	
PS104_43-1	2017-03-08	19:25	-73,29708	-112,33334	479	GC	station start	
PS104_43-1	2017-03-08	19:37	-73,29712	-112,33154	481	GC	at depth	
PS104_43-1	2017-03-08	19:50	-73,2972	-112,33007	NA	GC	station end	
PS104_43-2	2017-03-10	00:46	-73,2968	-112,33199	477	CTDOZE	station start	
PS104_43-2	2017-03-10	01:04	-73,29703	-112,32847	482	CTDOZE	at depth	
PS104_43-2	2017-03-10	01:30	-73,29644	-112,32844	482	CTDOZE	station end	
PS104_43-3	2017-03-10	01:41	-73,29693	-112,32943	482	BC	station start	
PS104_43-3	2017-03-10	01:48	-73,29717	-112,32921	482	BC	at depth	
PS104_43-3	2017-03-10	01:59	-73,29713	-112,32949	482	BC	station end	
PS104_43-4	2017-03-10	02:19	-73,29704	-112,33051	483	HF	station start	
PS104_43-4	2017-03-10	02:29	-73,29706	-112,33014	483	HF	at depth	
PS104_43-4	2017-03-10	02:45	-73,29682	-112,33164	481	HF	station end	
PS104_44-1	2017-03-11	02:19	-72,15485	-112,16325	520	refl	profile end	
PS104_45-1	2017-03-11	06:22	-71,94692	-110,67506	559	GC	station start	
PS104_45-1	2017-03-11	06:34	-71,94716	-110,67636	559	GC	at depth	
PS104_45-1	2017-03-11	06:49	-71,94731	-110,67395	550	GC	station end	

Gear abbreviations

Gear

ADCP_150	Vessel mounted Acoustic Doppler Current Profiler 150 kHz
BC	Box Corer
CTDOZE	CTD AWI-OZE
FBOX	FerryBox
GC	Gravity Corer
GRAV	Sea Gravimeter
HF	Heat Flow Probe
HS	Hydrosweep
MAG	Magnetometer
MOOR	Mooring
MUC	Multi Corer
MeBo70	Meeresboden-Bohrgeraet MARUM
PCO2_GO	pCO2 GO
PCO2_SUB	pCO2 Subctech
PS	Parasound
TSG_KEEL	Thermosalinograph Keel
TVMUC	Video Multi Corer
WST	Weatherstation
refl	Seismic reflection

Die **Berichte zur Polar- und Meeresforschung** (ISSN 1866-3192) werden beginnend mit dem Band 569 (2008) als Open-Access-Publikation herausgegeben. Ein Verzeichnis aller Bände einschließlich der Druckausgaben (ISSN 1618-3193, Band 377-568, von 2000 bis 2008) sowie der früheren **Berichte zur Polarforschung** (ISSN 0176-5027, Band 1-376, von 1981 bis 2000) befindet sich im electronic Publication Information Center (**ePIC**) des Alfred-Wegener-Instituts, Helmholtz-Zentrum für Polar- und Meeresforschung (AWI); see <http://epic.awi.de>. Durch Auswahl "Reports on Polar- and Marine Research" (via "browse"/"type") wird eine Liste der Publikationen, sortiert nach Bandnummer, innerhalb der absteigenden chronologischen Reihenfolge der Jahrgänge mit Verweis auf das jeweilige pdf-Symbol zum Herunterladen angezeigt.

The **Reports on Polar and Marine Research** (ISSN 1866-3192) are available as open access publications since 2008. A table of all volumes including the printed issues (ISSN 1618-3193, Vol. 377-568, from 2000 until 2008), as well as the earlier **Reports on Polar Research** (ISSN 0176-5027, Vol. 1-376, from 1981 until 2000) is provided by the electronic Publication Information Center (**ePIC**) of the Alfred Wegener Institute, Helmholtz Centre for Polar and Marine Research (AWI); see URL <http://epic.awi.de>. To generate a list of all Reports, use the URL <http://epic.awi.de> and select "browse"/"type" to browse "Reports on Polar and Marine Research". A chronological list in declining order will be presented, and pdf-icons displayed for downloading.

Zuletzt erschienene Ausgaben:

Recently published issues:

712 (2017) The Expedition PS104 of the Research Vessel POLARSTERN to the Amundsen Sea in 2017, by Karsten Gohl

711 (2017) Mid-Range forecasting of the German Waterways streamflow based on hydrologic, atmospheric and oceanic data, by Monica Ionita

710 (2017) The Expedition PS103 of the Research Vessel POLARSTERN to the Weddell Sea in 2016/2017, edited by Olaf Boebel

709 (2017) Russian-German Cooperation: Expeditions to Siberia in 2016, edited by Pier Paul Overduin, Franziska Blender, Dmitry Y. Bolshiyarov, Mikhail N. Grigoriev, Anne Morgenstern, Hanno Meyer

708 (2017) The role of atmospheric circulation patterns on the variability of ice core constituents in coastal Dronning Maud Land, Antarctica, by Kerstin Schmidt

707 (2017) Distribution patterns and migratory behavior of Antarctic blue whales, by Karolin Thomisch

706 (2017) The Expedition PS101 of the Research Vessel POLARSTERN to the Arctic Ocean in 2016, edited by Antje Boetius and Autun Purser

705 (2017) The Expedition PS100 of the Research Vessel POLARSTERN to the Fram Strait in 2016, edited by Torsten Kanzow

704 (2016) The Expeditions PS99.1 and PS99.2 of the Research Vessel POLARSTERN to the Fram Strait in 2016, edited by Thomas Soltwedel

703 (2016) The Expedition PS94 of the Research Vessel POLARSTERN to the central Arctic Ocean in 2015, edited by Ursula Schauer

702 (2016) The Expeditions PS95.1 and PS95.2 of the Research Vessel POLARSTERN to the Atlantic Ocean in 2015, edited by Rainer Knust and Karin Lochte

701 (2016) The Expedition PS97 of the Research Vessel POLARSTERN to the Drake Passage in 2016, edited by Frank Lamy



ALFRED-WEGENER-INSTITUT
HELMHOLTZ-ZENTRUM FÜR POLAR-
UND MEERESFORSCHUNG

BREMERHAVEN

Am Handelshafen 12
27570 Bremerhaven
Telefon 0471 4831-0
Telefax 0471 4831-1149
www.awi.de

